Population and ecophysiological modelling of the cultured mussel *Perna perna*: towards the development of a carrying capacity model

Felipe Matarazzo Suplicy, M.Sc.

Submitted in fulfillment of the requirements for the Degree of
Doctor of Philosophy in Aquaculture

University of Tasmania
(October, 2004)

Statement

This thesis contains no material which has been accepted for a degree or diploma by the University or any other institution, except by way of background information and duly acknowledge in the thesis. To the best of my knowledge and belief it contains no material previously published or written by another person except where due acknowledgments is made in the text.

Felipe Matarazzo Suplicy

This thesis may be made available for loan
and limited copying in accordance with the
Copyright act 1968.

I dedicate this thesis to my wife Liana and to my kids Mateus and Luana, born during these four years.

Acknowledgements

The present work was realized with the support of CNPq, a Brazilian governmental agency for the scientific and technologic development. The author acknowledge with grateful thanks:

Dr. Peter A. Thompson, for his contribution in many discussions, excellent supervision in the first year of this study and for his strong support while I was in Australia and also when I was doing my experiments in Brazil. Special thanks for the friendship and support always offered to me and to my family during all our period in Australia.

Dr. Natalie Moltschaniwskyj, for kindly accepting to substitute Dr. Peter Thompson in the supervision on my thesis and to her excellent work helping me on data analysis, scientific writing, and especially for her patience in reviewing my English.

Dr. Jaime F. Ferreira from Marine Mollusk Culture Laboratory (LCMM - UFSC) for providing the facilities and field transport during the experimental period in Brazil.

Dr. Jarbas Bonetti and Dr. Davide Franco for the support with workforce and equipments during the experiments and Brazil.

I also grateful acknowledge my colleagues Ross Daglish, Louise Ward, Justin Ho, James Harris, Ed Smith, Jean Schmith, Guilherme Rupp to name a few, for the enthusiasm and friendship that made this four years more enjoyable at each day. Grateful thanks are also extended to the fantastic staff from both University of Tasmania (Greg Kent, Paul Cassidy, Murray, Annabel Tyson, Jo, Shahin and Carol) and Universidade Federal de Santa Catarina (Itamar, Nelson Silveira, Mariza Canozi, Adriana Oliveira, Claudio Blacher, and Zero) for their support and assistance.

Acknowledgment is also made to various anonymous reviewers for their valuable criticism and comments of the manuscripts submitted for publication.

List of Tables

List of Figures

Index

Thesis Abstract

The overall aim of this thesis was to integrate the ecophysiology and population dynamics of the mussel *Perna perna* in Southern Brazil into a model that can ultimately be used for carrying capacity analysis in a tropical environment. The first chapter quantified and modelled the filter-feeding behavior of mussels feeding on natural seston. Models were generated that described each step of the feeding process and produced a predictive model of rates of food uptake. Feeding experiments using the biodeposition approach were conducted with mussels ranging in shell height from 3.94 to 9.22 cm of three sites, including turbid and clear water environments. Among the feeding steps characterized and modelled were filtration rate, rejection rate, organic selection efficiency, the organic content of ingested matter, absorption efficiency, and absorption rate. The coupling of the equations that described filter-feeding processes produced a robust model with relatively low complexity and specificity. The model can predict the *P. perna* feeding behavior in turbid or clear water and can be used with different species if the correct coefficients are used.

In the second chapter, growth and mortality rates using size frequency distributions of *P. perna* in suspended culture in two locations were studied. Growth rates were used as forcing functions in a model to predict size class distributions on one meter mussel ropes. Settlement of new individuals was included in the model using the unique settlement rate observed in each location. Mortality rates were estimated at 0.06 $year^{-1}$ in the populations at both locations. The integration of growth and mortality data

in a predictive model resulted in good predictions of size frequency distributions at two locations in Brazil.

The third chapter coupled the feeding model developed earlier with a model of energy balance and scope for growth. This model was divided in four sectors to facilitate description and explanation of the functions controlling feeding and metabolic responses to varying food availability and seawater temperature. The seston sector included characteristics of seston likely to influence food and energy acquisition in mussels. It also included relationships that estimated the energy content of phytoplankton and detritus, the main components of mussel diet. The feeding sector described suspension-feeding behavior using natural seston as described in the first chapter. In the energy allocation sector, absorbed matter was transformed to absorbed energy using estimates of energy content of food provided in the seston sector. After accounting for the maintenance requirements of the mussels (heat loss, excretion, and mucus production), the scope for growth was directed to the growth sector. The growth sector included byssus, organic shell, and soft tissue production based on energy partitioning estimated from monthly measurements of tissue (somatic and reproductive) and shell growth. The model successfully predicted mussel shell length and dry tissue weight during the simulation period and estimated the response of mussels to food acquisition, energy expenditure, and allocation to growth.

In the fourth and last chapter, mussel population dynamics and ecophysiology were coupled to model feedbacks from the bivalve population to the environment. These

feedbacks included population level estimates of the rates of filtration, excretion, and biodeposition. Seston (TPM, POM and CHL a) dynamics were investigated in three temporal scales: biweekly for four years, weekly for eight months, and tidally (neap and spring tides). Characterization of the study area enabled an estimation of bivalve standing sock, total surface area, and volume of the area. Measurements of water level across tides allowed estimates of tidal water renewal inside the area. Some aspects of interest for carrying capacity analysis presented in the last chapter were the water mass residence time for the area, bivalve clearance time (the time needed for the total bivalve biomass to filter a volume of water equivalent to the system volume), and phytoplankton production time (the time it takes for the primary production within the system to replace the phytoplankton biomass within the system).

Among the important aspects for carrying capacity studies not included in this model are the spatial resolution of hydrodynamics processes and physical/biological processes related to seston dynamics like sedimentation, resuspension, and mineralization of organic compounds, interacting together with the population ecophysiology to predict the exploitation carrying capacity for this system. Although there was good agreement of the model prediction with the observed mussel growth data, the model needs to be tested with an independent set of data before it is can be used as a management tool. Therefore, it appears that the integration of whole animal models with population models can be used in carrying capacity analysis for shellfish culture areas in Brazil.

Chapter 1

Development of ecophysiological models for carrying capacity analysis in shellfish culture: a case study in Southern Brazil.

1.1. Introduction

Aquaculture production is growing at more than 10% per year, compared with 3% for terrestrial livestock and 1.5% for capture fisheries (GESAMP, 2001). Similarly, the culture of marine bivalve mollusks has markedly increased in the past two decades. Available areas for shellfish farming are becoming limited by access, pollution, operational logistics, habitat suitability, and competition by other recreational or commercial use (Smaal, 1991). As available culture space becomes occupied, the growth rates of individual bivalves may slow and mortality rates increase due to disease outbreaks associated with overcrowding (Grant *et al.*, 1993). Reduction in growth rates and longer times to reach commercial size due to overstocking has already been reported for Hiroshima and Marennes-Oléron bays (Héral, 1993). As the aquaculture industry grows there is pressure from government authorities, the general public, and other sea users to minimize environmental impacts and develop sustainable practices.

1. 2. The concept of carrying capacity for bivalve aquaculture

The sustainable level of shellfish farming is referred to as carrying capacity and is generally estimated for an inlet, cove, or bay. There are many definitions of carrying capacity based either on ecological and/or economic considerations. To be cost-effective estimates of environmental carrying capacity should consider aspects of environmental impact likely to occur in a given situation. In principle, it need only be applied to the aspect of the environment that becomes limiting first (GESAMP, 2001). The main

environmental impacts caused by suspended mussel culture are depletion of phytoplankton and accumulation of biodeposits beneath the farms, the second of which produces an anoxic environment and impoverishment of fauna (Rodhouse & Roden, 1987, Kaiser *et al.*, 1998). At acceptable levels of farming density, zooplankton grazing and associated processes, i.e. excretion of ammonia and deposition of faecal pellets, are widely spread in the system. Furthermore, mussel farms influence the organic and inorganic nitrogen pools (both on sediment and water column) within a farming area (Kaspar *et al.*, 1985).

Despite these environmental considerations, most carrying capacity analysis for shellfish culture is approached from an economic perspective, based on the effect of stock size on bivalve growth rate and its resultant yield. For example, carrying capacity has been defined as "the total biomass supported by a given ecosystem as a function of the water residence time, primary production time and bivalve clearance time." Dame & Prins (1998). Carver & Mallet (1990) and James & Ross (1996) define it as the stock density at which production levels are maximized without negatively affecting growth rates. Smaal *et al.* (1998) notes that increased stocking rates may both result in low individual growth rate and maximal production, however, with undersized individuals. It is desirable that whatever the definition used, it should encompass economic as well as environmental considerations (Fréchette, 1991). Héral (1993), using the exploitation carrying capacity defined above, found that in Marennes-Oléron Bay the stock size that gives the maximum yield of a marketable cohort is determined by an asymptotic equation of the same type as the one used for the growth of the populations, like the Von

Bertalanffy equation. Regardless of the definition used it is commonly accepted that an inverse relationship between stocking density and individual growth rates has resulted in the need to reliably assess the carrying capacity of aquaculture sites (Incze *et al.*, 1981; Carver & Mallet, 1990; Raillard & Ménesguen, 1994; Dowd, 1997).

1.3. Carrying capacity models

The aim of this Ph.D. thesis was to describe and model some aspects of *Perna perna* feeding behavior and physiology, and describe temporal changes, at a range of scales, of main seston characteristics allowing an analysis of the response of bivalves to dynamic environments. These models are used to develop a larger model that predicts the main feedbacks between mussel culture and the environment for mussel culture in a subtropical environment like Southern Brazil. The clarification of ecophysiological processes of *P. perna* and their interaction with the culture environment is of significant value for the evaluation of exploitable and sustainable levels of mussel farming in subtropical regions like Southern Brazil. The approach of this thesis was to focus on bivalve population physiological responses coupled with less detailed model of water renewal. Although this model runs the risk of becoming too complex to be practicable in the management of the industry, this study attempted to describe and model the main physiological interactions that occur under culture for the mussel *P. perna* in Southern Brazil.

More complex models should describe more accurately the response of a real system. However, as more parameters are included in a model the level of uncertainty increases. This is because field parameters estimations are never free of errors and these errors are carried through into the model contributing to its uncertainty (Jørgensen 1994). There is a fine line between generating a simple versus a complex model and what is known about the system. As a result modellers usually have to trade-off between knowing much about little or little about much about a biological situation.

The components involved in carrying capacity analysis for mussel culture selected for this study were: *i*) feeding behavior; *ii*) individual energetic physiology and scope for growth, *iii*) population dynamics, *iv*) relationships between mussel population ecophysiology, primary production and seston availability. These components were selected considering the limited information available about *P. Perna* ecophysiology and population dynamics in Southern Brazil. In the following sections a brief overview of each component considered as the minimum requirements for modelling carrying capacity and their associated difficulties will be presented. The first three of these four components form the basis of this thesis, the fourth component is outside of the scope of the thesis, but has been included for completeness. Details about each of these model components will be provided latter on the related chapters of this study.

1.4. Mussel physiology (Chapters 2 and 4)

Most studies of carrying capacity use models of scope for growth of individuals (SFG) based on flows of energy or material (Grant, 1993). Scope for growth in bivalves is generally a function of food consumed, faeces and pseudofaeces produced, respiration and excretion:

$$SFG = FR - (PF + F + R + U)$$

where: FR = consumption, PF = pseudofaeces, F = faeces, R = respiration, and U = excretion. Variations of this equation are found in the literature, depending on the level of the detail of the model. Some studies do not include pseudofaeces and/or excretion, while other models partition SFG for somatic and reproductive tissues in their analysis.

It is necessary to identify which variables SFG is most sensitive to allow methods measuring these variables to be refined allowing accuracy in estimates (Fréchette, 1991). SFG will include non-linear components such as allometry and temperature responses. Although these terms are related to environmental conditions their sum total in a SFG model may not be related in the same way to the same variables (Grant, 1996). Among factors that have the greatest impact on bivalve energy budgets, food and temperature are considered the most important (Grant, 1996). A simple set of differential equations was used by Dowd (1997) to reproduce a generic bivalve physiological model, as a submodel in a carrying capacity analysis. He noted that uncertainty in estimates of physiological parameters strongly influenced the prediction of allowable stocking density. This was

because the carrying capacity model was highly sensitive to variations in the physiological sub-model.

Differences in maximum sustainable stocks sizes among species have been explained as a function of interspecific differences in the rates of physiological processes. For example, the higher energetic demand of *Crassostrea gigas* compared with *C. angulata* in Marennes-Olerón Bay results in a 60% difference in maximum stocking rates (Héral, 1993). This finding reinforces the need to determine which bioenergetic relationships can be used across species boundaries if the objective is to apply a growth model to a wide variety of species and culture situations (Grant, 1996). Therefore, development of models that describe how bivalves control feeding behavior in relation to food availability, and how this response affects scope for growth, allows comparisons between species, and the identification of similar responses to seston quantity and quality. If the model reproduces the main energetic relationships, it can be used for different species by replacing the equation coefficients with coefficients measured for each species.

Some more detailed SFG models partition the allocation of material into somatic tissues, reproductive tissues, and shell (Brylinsky & Sephton, 1991; Scholten & Smaal, 1998; Pouvreau *et al.*, 2000). These models assume that energy surplus to maintenance (respiration and excretion in Pouvreau's model and respiration, excretion and mucus production in Scholten's model) was partitioned between body tissues and organic shell. However, the rules specifying the bivalve priorities for resources partitioning of surplus

energy to somatic and reproductive tissues tissue and organic shell poorly understood (Pouvreau *et al.*, 2000; Scholten & Small, 1998). These detailed SFG models differ in the rules controlling the partitioning of assimilated material to different body parts and shell and mechanisms controlling the excretion rate.

Furthermore, an important aspect of SFG models is that the use of food and the assimilation in the tissues involves several steps which need to be successively simplified in the model. Although these simplifications may violate some biological features, they are necessary to assist building a model that synthesizes and apply this information in a meaningful way (Pouvreau *et al.*, 2000; Brylinsky & Sephton, 1991).

1.5. Population dynamics (Chapter 3)

Population dynamics of the targeted cultivated species have to be described in different areas to compare results given by the growth rate model and observations (Héral, 1993). However, most carrying capacity models emphasize ingestion and energetics of individuals, rather than population dynamics Grant (1993). Consequently, several aspects of population ecology, e.g. recruitment and differential mortality among size classes, are neglected. This will directly affect predictions of the feedbacks between bivalve populations to the environment, e.g. filtration, excretion, and biodeposition rates.

1.6. Hydrodynamics and Seston Characterization

For hydrodynamic data, simultaneous records of tidal levels as well as precise and recent bathymetry are necessary. This information is used to calculate water residence time inside the water body, which is the simplest analysis, employed for water and associated food renewal. Further increase in details is possible with the formulation of one and two-dimensional models. The one-dimensional models include advection and diffusion movements of water and suspended particles between adjacent boxes or sections of a bay. In contrast the two-dimensional approach includes sedimentation of biodeposits, phytoplankton, zooplankton and detritus, as well as resuspension from the bottom. Long time series of current velocity and direction are also necessary as current speed and wind are the dominant factors controlling energy flow in bivalve systems by their action on processes such as advection, diffusion, and resuspension (Fréchette, 1993; Héral, 1993). Continuous records of salinity and turbidity are also useful to validate models of advection and transport processes (Héral, 1993). The temporal and spatial scales at which information about physical and biological processes are obtained is important as they ultimately have to be linked in one model (Fréchette, 1993; Héral, 1993; Grant 1993).

Most of the hydrodynamics models developed for carrying capacity analysis use the box model concept, whereby the coastal inlet is divided into distinct regions or sectors. Exchange of suspended particles between adjacent boxes is assumed to be proportional to spatial differences in their respective concentrations, scaled by an

exchange coefficient (e.g. Dowd, 1997). Density, differential sinking, and advection rates of organic (phytoplankton and detritus) and inorganic (resuspended silt) fractions must be known to estimate rates of transport (Scholten *et al.*, 1990). This will allow transport rates for the different fractions based on measured vertical gradients of inorganic sediment, detritus and phytoplankton.

Carrying capacity predictions must be temporally and spatial specific otherwise estimates can be very misleading (Doering & Oviatt, 1986). Sampling strategies depend on the precision needed and the time scale of the model (Héral, 1993). Although food is usually estimated using mass measurements like TPM, PIM, and POM, together with Chlorophyll a, recent findings suggest that volumetric measurements of food may explain the control of food acquisition by some bivalves (Hawkins *et al.*, 2001). Additional measurements of particulate organic carbon (POC) and nitrogen (PON) also enable conversions from POM to POC and PON, which in turn are necessary to calculate carbon and nitrogen intake by bivalves. Although some studies use conversion factors obtained for other areas and times, it is likely that these conversion factors vary spatially and temporally. Measurements of primary production are also desirable as absolute values of instantaneous measurements of chlorophyll a do not predict the total food pool. Probably because of the limits on the number of variables, most carrying capacity models do not include a sub-model of primary production in their analysis.

Despite an urgent need from the aquaculture industry, environmental agencies, and other users to develop sustainable use of this common resource, there are no tools that can be immediately applied to a range of environments and species. This study aims

to contribute towards the development of a carrying capacity model through research about a bivalve species intensively farmed in Brazil. This was achieved through delivering new information about the ecophysiology of *Perna perna* in suspended culture in Santa Catarina.

Chapter 2

Modelling of filter-feeding behavior in the brown mussel *Perna perna* (L.), exposed to natural variations of seston availability in Santa Catarina, Brazil.

2.1. Abstract

The aim of this study was to quantify and model the filter-feeding behavior of the mussel *Perna perna* feeding on natural seston. Models were generated that described each step of the feeding process and produced a predictive model of rates of food uptake by *P. perna* in culture areas from Southern Brazil. Feeding experiments using the biodeposition approach were conducted with mussels ranging in shell height from 3.94 to 9.22 cm of three sites, including turbid and clear water environments. Organic content of the seston (OCS, fraction) decreased as total particulate matter (TPM, mg L^{-1}) increased. The maximum filtration rate (FR, mg L^{-1}) measured for an individual mussel was 156.7 mg h^{-1} and was recorded when TPM was 33.9 mg L^{-1} and OCS was 0.18. Rejection rate of particles had a strong positive relationship with TPM, and an inverse relationship with OCS. Maximum rejection rate recorded was 124.1 mg h^{-1} and was measured under the same seston conditions as maximum filtration rate. Net organic selection efficiency by mussels (NOSE, fraction) was related to the amount of particulate organic matter (POM, mg L^{-1}) and particulate inorganic matter (PIM, mg L^{-1}) available in the water. NOSE was positive below PIM values of 2 mg L^{-1}, but had negative values when POM was above 3 mg L^{-1} and PIM between 2 and 15 mg L^{-1}, and positive values when POM was below 3 mg L^{-1} and PIM above 15 mg L^{-1}. Maximum NOSE was 1.71, when PIM was 1.02 mg L^{-1} and POM was 0.67 mg L^{-1}. Organic content of ingested matter (OCI, fraction) had a positive relationship with NOSE and TPM. Maximum OCI was 1.24 and was measured when TPM was 33.9 mg L^{-1}, OCS was 0.18, FR was 151.30 mg h^{-1}, and NOSE was 1.30. The net absorption efficiency of ingested organics (NAEIO) increased with increasing OCI in a hyperbolic relationship. The net organic absorption rate (NOAR, mg h^{-1}) increased with

both FR and OCI. The coupling of the equations that described filter-feeding processes for *P. perna* in the STELLA software environment produced a robust model with relatively low complexity and specificity. The model can predict the *P. perna* feeding behavior in turbid or clear water and can be used with different species if the correct coefficients are used. The coupling of this feeding model with future models of energy budget, population dynamics, seston hydrodynamics, and primary production will be valuable for the evaluation of shellfish carrying capacity.

2.2. Introduction

Assessing carrying capacity, the environmental capacity for shellfish culture, is generally approached using ecophysiological modelling (e.g.; Brylinsky & Sephton, 1991; Newell & Campbell, 1998; Schölten & Smaal, 1998). The inclusion of processes relative to rates of selectivity, rejection, and absorption by mollusk filter feeders is of primary importance for both ecosystem and local scales models (Smaal *et al.*, 1998). Sessile suspension-feeders obtain energy by selectively feeding on seston, which includes a variable mixture of algae, detritus, and silt. Not only does the seston have a small fraction with nutritional value (Smaal & Haas, 1997), but the composition changes on time scales of minute to months (Grant, 1993). The available organic content of the seston ranges from 5 to 80% (Bayne & Hawkins, 1990). Such nutritional variability in the seston forces sessile organisms like mussels to maximize their energy intake, and ultimately their net energy balance, by varying rates of feeding and digestion in response to seston concentration and organic content (Bayne *et al.*, 1993).

The literature describing bivalve rates of filter-feeding and digestion is extensive (see reviews by Bayne & Newell, 1983; Griffiths & Griffiths, 1987; Bayne, 1993). However, recent findings suggest that previous studies have limited application because they used artificial diets and it is unclear to what extent artificial diets provide a realistic representation of "in situ" feeding behavior (Bayne & Hawkins, 1990). Normal feeding

processes and behavior are better measured in experiments where the animals are allowed to feed on natural seston (Hawkins *et al.*, 1996; Wong & Cheung, 2001; Gardner, 2002).

Most research on the ecophysiological processes in shellfish has focused on temperate species (e.g.. *Mytilus edulis*), and there has been limited work on tropical species and their environments (Hawkins *et al.*, 1998a; Wong & Cheung, 2001). Although bivalves use the same general selective mechanisms for food acquisition (Hawkins *et al.*, 1998b), there are both intra- and inter-specific differences in feeding rates (Navarro *et al.*, 1991). Describing the physiological responses characteristic of each species is needed, rather than extrapolating data from other species (Gardner & Thompson, 2001; James *et al.*, 2001). There are likely to be a number of significant differences in tropical environments. Our understanding of the feeding physiology of *Perna perna* (Linnaeus, 1758) (Berry & Schleyer, 1983; Bayne *et al.*, 1984; van Erkon Schurink & Griffiths, 1992) is limited to laboratory experiments using microalgae monocultures or a mix of microalgae species and silt. Furthermore, these studies were carried out in South Africa where cold south Atlantic currents are predominant; in contrast, the Brazilian coast has warm waters brought by central Atlantic currents. Such differences in temperature and productivity, and consequently in food availability and its organic content, will be reflected in ecophysiological differences of these filter feeders.

The aim of this study was to generate a model to predict food uptake by *P. perna* in culture areas of Southern Brazil, based on measurements of the filter -feeding process using natural seston. The model reproduce the sequential passage of food through the

feeding steps of filtration, selection, rejection, ingestion and absorption, and the calculation of each step is based on relationships either with quantity and quality of seston or with some of the preceding steps on the food processing sequence. Mussel aquaculture is a fast growing industry in Brazil and problems regarding the environmental capacity of this industry may occur in the near future. This research will have the capability to deliver information that can be incorporated into models of energy budget and growth as a function of stocking density, for use in planning and managing strategies of growing areas.

2.3. Methods

Feeding experiments were conducted at three sites within mussel farms in Southern Brazil; Brito Cove (48° 37' W, 27° 46' S), Porto Belo (48° 33' W, 27° 8' S), and Armação de Itapocoroi (48° 38' W, 26° 58' S). Rope-cultured *P. perna* were collected from mussel farms at each site immediately before the experiments. All experiments were done on one to three occasions at each site and were exposed to natural differences in concentration and organic content of seston at each site and time (Table 2.1). Each site was arbitrarily classified as turbid or clear, based on total particulate matter (TPM). The clear site had TPM < 5 mg L^{-1} (Porto Belo), while the turbid sites had TPM between 10 - 40 mg L^{-1} (Brito Cove and Armação do Itapocoroi). The use of multiple seston conditions was not intended to make comparisons of the mussel's feeding response at these sites, but rather, to characterize their feeding response across a variety of different environments and provide an equation that could be broadly used in carrying capacity studies.

UNIVERSITY OF TAS LIBRARY

The experiments were conducted on a raft containing a tray with ten individual 350 mL plastic chambers. Eight individual mussels, cleared of epibiotic growth, were

Table 2.1. Summary of environmental parameters and mussel size range for each day the experiments were run. Data of environmental characteristics are the mean ± SD. TPM: total dry particulate mass; POM: total particulate organic matter; OCS=organic content of TPM; ND= no data.

		Environmental characteristics n=12					Mussels	
Experiment days	Location	TPM ($mg\ L^{-1}$)	POM ($mg\ L^{-1}$)	OCS (fraction)	Temperature (°C)	Turbidity (NTU)	Shell length (cm)	Dry weight (g)
14/03/01	Brito Cove	29.6 ± 11.9	4.7 ± 3.7	0.15 ± 0.05	25.7 ± 0.5	ND	5.05 – 8.90	0.398 – 3.522
14/04/01	Brito Cove	12.4 ± 3.0	1.2 ± 0.3	0.10 ± 0.02	25.5 ± 0.5	7.7 ± 1.7	5.70 – 8.16	0.485 – 2.034
05/06/01	Brito Cove	9.8 ± 3.1	1.0 ± 0.1	0.11 ± 0.03	22.2 ± 0.3	4.5 ± 1.6	5.72 – 8.27	0.628 – 2.517
07/02/01	Porto Belo	1.7 ± 0.3	0.7 ± 0.3	0.41 ± 0.17	29.0 ± 0.4	0.5 ± 0.2	5.74 – 8.28	1.177 – 3.257
31/03/01	Porto Belo	1.6 ± 0.4	0.3 ± 0.1	0.20 ± 0.08	26.5 ± 0.4	1.0 ± 0.1	5.05 – 9.22	0.618 – 3.103
07/07/01	Porto Belo	1.2 ± 0.3	0.4 ± 0.1	0.36 ± 0.09	18.3 ± 0.0	0.3 ± 0.1	4.11 – 8.22	0.343 – 2.757
26/05/01	A. Itapocoroi	4.6 ± 0.7	2.3 ± 0.4	0.10 ± 0.08	21.3 ± 0.2	2.8 ± 0.8	6.00 – 8.49	0.857 – 3.087

placed in separate chambers, with two chambers left empty to act as blanks. Seawater was pumped into the chambers with flow rates in each compartment between 150 and 200 mL min^{-1}, these were adjusted at the beginning of the experiment. A baffle between the mussel and the inflow water provided a homogeneous distribution of water flow inside the feeding chambers (Fig. 2.1). The mussels were initially left undisturbed for one hour to acclimate, after which time all biodeposits on the bottom of the chambers were removed. Once the experiment started the mussels were allowed to feed for four hours, during which time all faeces and pseudofaeces for each mussel were separately collected using a pipette immediately after being released. For each individual mussel the faeces and pseudofaeces collected in each hour were stored in separate test tubes on ice. A 2 L sample of inflow seawater was collected every 20 minutes for the determination of seston concentration and organic content. Water temperature and salinity were monitored every hour during the experiment.

After five hours of feeding the experiment was terminated and the mussels and samples were transported back to the laboratory on ice. Biodeposit samples were homogenized by repeat-pipetting and filtered onto pre-ashed and weighed Whatman GFC filters (25 mm or 47 mm diameter). The samples were rinsed with 15 mL distilled water to remove salts and dried at 60°C for 48 hours before re-weighing and calculation of the total sample dry weight. Each sample was then ashed at 450°C for 4 h prior to final weighing, allowing calculation of both of the ash (inorganic) and ash-free (organic) mass of each filtered sample. To account for settled material in the chamber, the mean organic and inorganic weight of sediment material collected from the blank chambers was

Figure 2.1. Schematic diagram of the feeding tray used in the biodeposition experiments.

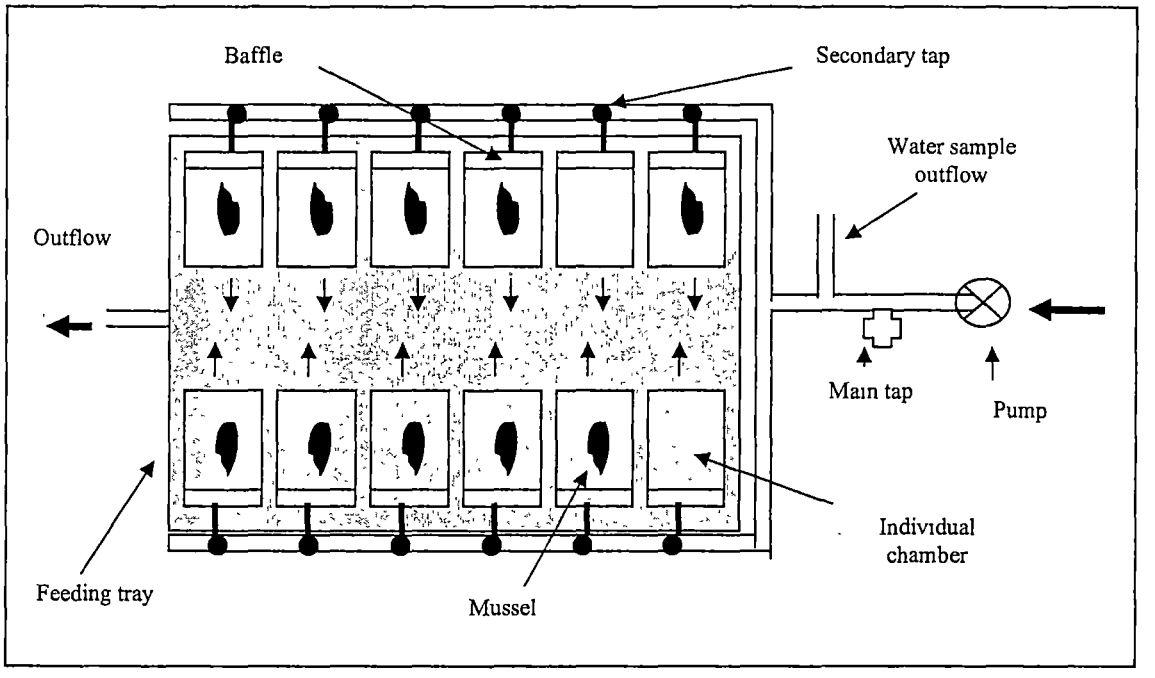

subtracted from the mean organic and inorganic weight of the collected faeces and pseudofaeces. To determine seston concentration and organic content, three 300 - 400 mL samples from the 2 L of inflow seawater collected were filtered onto pre-ashed and weighed Whatman GFC filters (25 mm diameter) and dried, ashed, and weighed in the same way as the biodeposit samples. The mean of the three values was calculated. The seston concentration and organic content for each hour was calculated as an average of the three 2 L samples taken during that hour.

To determine the lag time between when food was consumed by the mussels and when faeces and pseudofaeces production occurs mussels starved for one day in the laboratory were fed green microalgae. Green faeces were observed within an hour of feeding therefore we assumed the gut transit time to be 1 hour. Green pseudofaeces were seen within minutes of the microalgae being added. Therefore, in the analysis of the field data the quantity and content of the faeces was correlated with seston concentration and organic content in the preceding hour. No time lag was assumed in correlation with pseudofaeces production. Feeding and absorption parameters were defined and calculated (Table 2.2) using procedures outlined in Hawkins *et al.* (1996, 1998b), and using the mean of the hourly feeding rate obtained for each mussel throughout the experiment. Similarly, all abbreviations and terms used in the feeding behavior description came directly from his work. For the regression analysis, seston concentration and organic content were the means of the hourly values obtained during each experimental run.

From each mussel used in the experiments, total length was measured and soft tissue removed, dried at 60° C for 48 hours, and weighed. To standardize findings and

Table 2.2. Definitions and descriptions of the calculations used in each component of feeding behavior.

Parameter	Acronym	Units	Calculation
Particulate Inorganic Matter	PIM	mg L^{-1}	Ash free dry weight of TPM
Particulate Organic Matter	POM	mg L^{-1}	TPM -PIM
Organic Content of Seston	OCS	fraction	POM/TPM
Clearance Rate	CR	l h^{-1}	(mg inorganic matter egested both as true faeces and pseudofaeces h^{-1}) – (mg inorganic matter available l^{-1} seawater)
Total Filtration Rate	FR	mg h^{-1}	(mg inorganic matter egested both as true faeces and pseudofaeces h^{-1}) ÷ (1-OCF)
Organic Filtration Rate	OFR	mg h^{-1}	CR x mg total particulate organic matter l^{-1} seawater
Inorganic Filtration Rate	IFR	mg h^{-1}	CR x mg total particulate inorganic matter l^{-1} seawater
Organic Content of Filtered matter	OCF	fraction	OFR ÷ FR
Rejection Rate	RR	mg h^{-1}	mg total pseudofaeces egested h^{-1}
Inorganic Rejection Rate	IRR	mg h^{-1}	RR – ash free mg total pseudofaeces egested h^{-1}
Organic Rejection Rate	ORR	mg h^{-1}	RR - IRR
Net Organic Selection Efficiency	NOSE	fraction	[1-(organic fraction within pseudofaeces) ÷ (OCS)]
Ingestion Rate	IR	mg h^{-1}	FR – RR
Organic Ingestion Rate	OIR	mg h^{-1}	OFR – ORR

Inorganic Ingestion Rate	IIR	mg h^{-1}	IFR – IRR
Net Organic Ingestion Rate	NOIR	mg h^{-1}	[FR x (OCS)] – [RR x (organic fraction within pseudofaeces)]
Organic Content of Ingested matter	OCI	fraction	NOIR ÷ (FR-RR)
Net Absorption Efficiency from Ingested Organics	NAEIO	fraction	NOAR ÷ NOIR
Net Organic Absorption Rate	NOAR	mg h^{-1}	NOIR – [(mg total true faeces egested h^{-1}) x (organic fraction within true faeces)]

feeding behavior to allow comparison of results with other studies, feeding responses were expressed per 1 g dry weight using $Y_s = (W_s/W_e)^{b} * Y_e$, where Y_s is the corrected parameter, W_s is the standard weight (1 g), W_e is the weight or length of the experimental animal, Y_e is the uncorrected parameter, and b is the average size exponent (Hawkins *et al.*, 2001). However, given the absence of spawning synchronicity (Marques *et al.*, 1991), there is high variability in mussel dry weight within the same population in every time of the year. Therefore, we used the shell length equivalent of 1 g dry weight (6.26 cm) and the power exponent that scales the feeding rates with shell length ($b \approx 1.85$). The power exponent has previously been used for *Mytilus galloprovincialis* (Pérez Camacho & Gonzáles 1984; Navarro *et al.*, 1996) and for *P. perna* (Berry & Schleyer, 1983).

All statistical analysis was done using SPSS for Windows, Version 10 (SPSS Inc.) and Sigma Plot. Multiple regression models were fitted using the step-wise technique, entering the most significant independent variable at the first step and then adding or deleting independent variables until no further variables could be added to improve the overall fit. The coupling of the equations to produce an integrated feeding model and the posterior sensitivity analysis was done using STELLA research software (High Performance Systems, Inc.).

2.4. Results

Organic content of seston (OCS) decreased as TPM increased (Fig. 2.2., Table 2.3). Clearance rate of mussels decreased from 10 to 5 L h^{-1} as TPM increased from

<5 to 30 mg L^{-1} and OCS increased from < 0.15 to 0.40. The parabolic relationship (Fig. 2.3.A), suggests that *P. perna* pumps more water under low TPM (<10 mg L^{-1}) and OCS (<0.20) conditions.

Filtration rate (FR, mg h^{-1}), rejection rate (RR, mg h^{-1}), ingestion rate (IR, mg h^{-1}), and net organic absorption rate (NOAR, mg h^{-1}) were all related to TPM and OCS (Table 2.3., Fig. 2.3.B, C, D and E). The maximum filtration rate measured was 156.7 mg h^{-1} when TPM was 33.9 mg L^{-1} and OCS was 0.18. Rejection rate had strong positive relationship with TPM and inverse relationships with OCS. The maximum rejection rate recorded was 124.1 mg h^{-1}, which represented 83% of filtered matter, and was measured under the same seston conditions as the maximum filtration rate. Pseudofaeces production was observed when TPM levels were as low as 2 mg L^{-1}, suggesting a very low threshold for pseudofaeces production in this species.

Net organic selection efficiency (NOSE, fraction) was controlled by the proportion of particulate organic and inorganic matter in the water (POM, mg L^{-1} and PIM, mg L^{-1} respectively). Higher NOSE values were observed on the lower and higher extremes of PIM. Negative NOSE values, a minimum of -0.56, were recorded at intermediate values of PIM and POM, and positive values were recorded when POM was below 3 mg L^{-1} and PIM above 15 mg L^{-1}. Maximum NOSE was 1.71 when PIM was 1.02 mg L^{-1} and POM was 0.67 mg L^{-1} (Fig. 2.3.F, Table 2.3). Organic content of ingested matter (OCI, fraction) had a positive relationship with NOSE and it was not strongly affected by TPM. Maximum OCI was 1.24 when TPM was 33.9 mg L^{-1}, OCS was 0.18,

Figure 2.2. The relationship between average organic content (OCS, fraction) and average total particulate mass (TPM, mg L^{-1}) of seston in the experimental feeding conditions. Data are the mean of three replicate determinations per condition. Refer to Table 2.3 for equation.

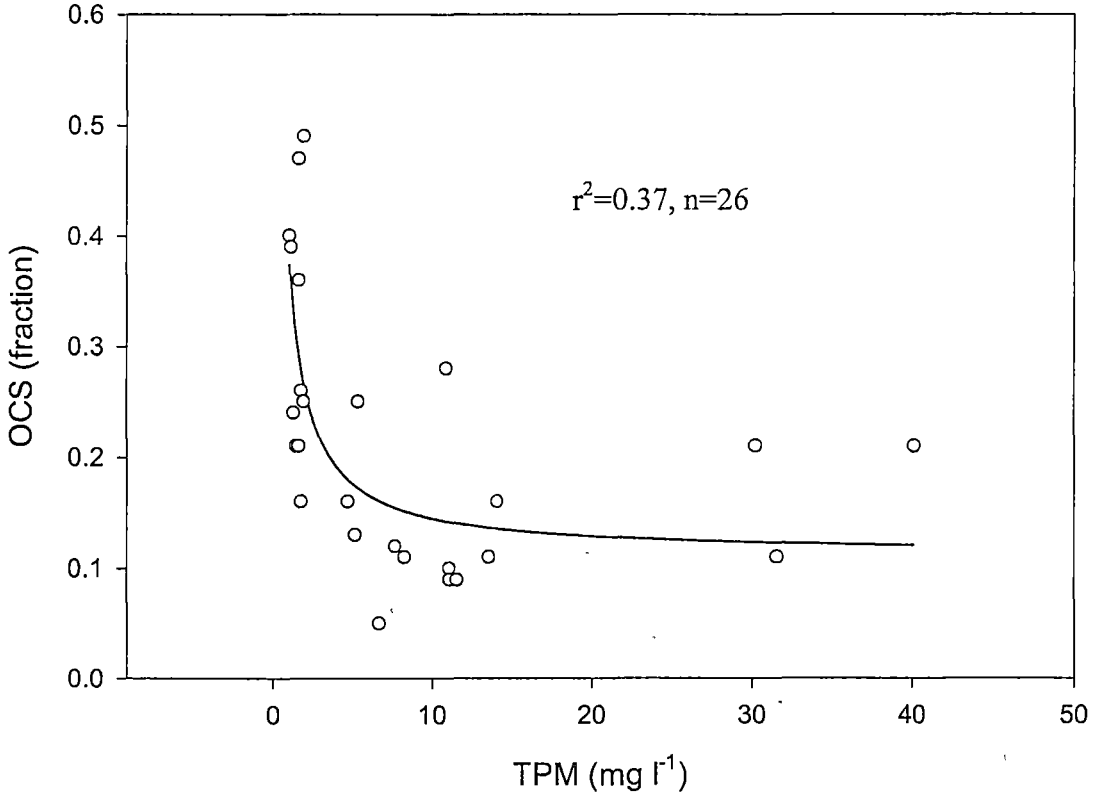

Figure 2.3. The relationship between total particulate matter (TPM, mg L^{-1}) and organic content of seston (OCS, fraction) and (A) clearance rates (CR l h^{-1}), (B) filtration rate (FR, mg h^{-1}), (C) rejection rate (RR, mg h^{-1}), (D) Ingestion rate (IR, mg h^{-1}), (E) net organic absorption rate (NOAR, mg h^{-1}). Net organic selection efficiency is plotted against particulate organic and inorganic matter (PIM and POM, mg L^{-1}). Refer to Table 2.3 for equations and statistics.

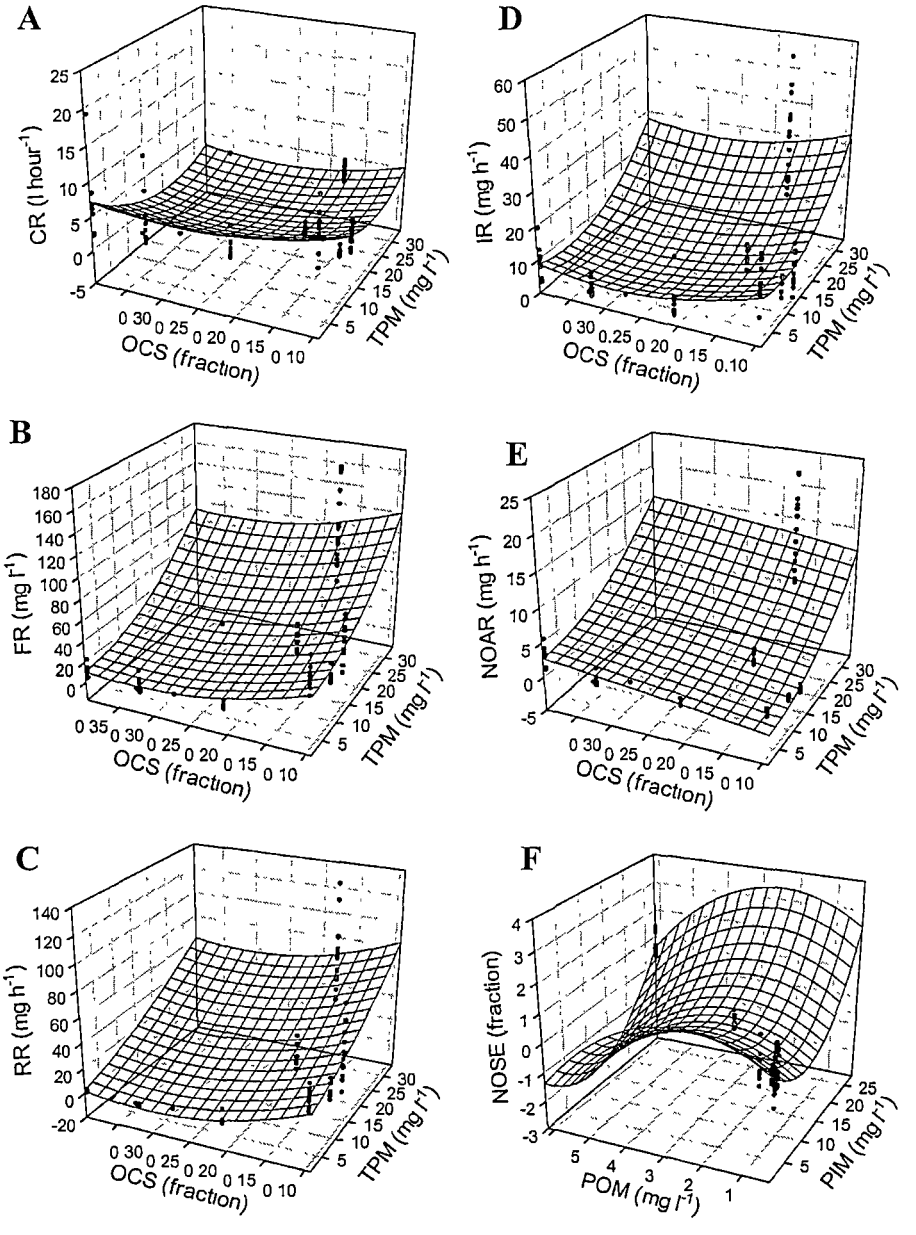

FR was 151.3 mg h^{-1}, and NOSE was 1.30 (Fig. 2.4.A, Table 2.3). The net organic ingestion rate (NOIR, fraction) was below 10 mg h^{-1} when mussels were feeding on TPM levels below 5 mg L^{-1}, but this increased to 25 mg h^{-1} when TPM was above 30 mg L^{-1} and ingestion rate was ca. 50 mg h^{-1} (Fig. 2.4.B, Table 2.3).

Both the net absorption efficiency of ingested organics (NAEIO, fraction) and the net organic absorption rate (NOAR, mg h^{-1}) had a hyperbolic relationship with the organic content of ingested matter (Fig. 2.4.C and 2.5., Table 2.3). NOAR was essentially controlled by quantity (filtration rate) and quality (OCI) of food passing through the digestive system (Fig. 2.4.C, Table 2.3). The absorption rate across the experiments varied from 21.84 mg h^{-1} (TPM 33.18 mg L^{-1}, OCS 0.18) to -0.69 mg h^{-1} (TPM 10.09 mg L^{-1}, OCS 0.10).

The differential equations, logical functions, and starting values of the state variables used to couple the equations describing the filter-feeding processes for *P. perna* in STELLA are listed on Table 2.4. We produced a robust model with relatively low complexity and specificity. Figure 6A depicts the conceptual diagram of the *P. perna* feeding process as a function of TPM and OCS. The sub-model inserted inside the "ingested matter" variable (Fig. 2.6B) reproduces the absorption of organic matter and the passage of inorganic matter as inert material through the gut. As the model was based on natural seston in both turbid and clear environments and feeding rates measured in these environments, we believe that it has incorporated feeding adaptations by *P. perna* for both kinds of environments. Model predictions and observed data of FR, RR, IR,

Figure 2.4. The relationship between (A) net organic selection efficiency (NOSE, fraction), total particulate matter (TPM, mg L^{-1}) and organic content of ingested (OCI, fraction); (B) ingestion rate (IR, mg h^{-1}), TPM and net organic ingestion rate (NOIR, mg h^{-1}); (C) net organic absorption rate (NOAR, mg h^{-1}), filtration rate (mg h^{-1}) and OCI. Refer to Table 2.3 for equations and statistics.

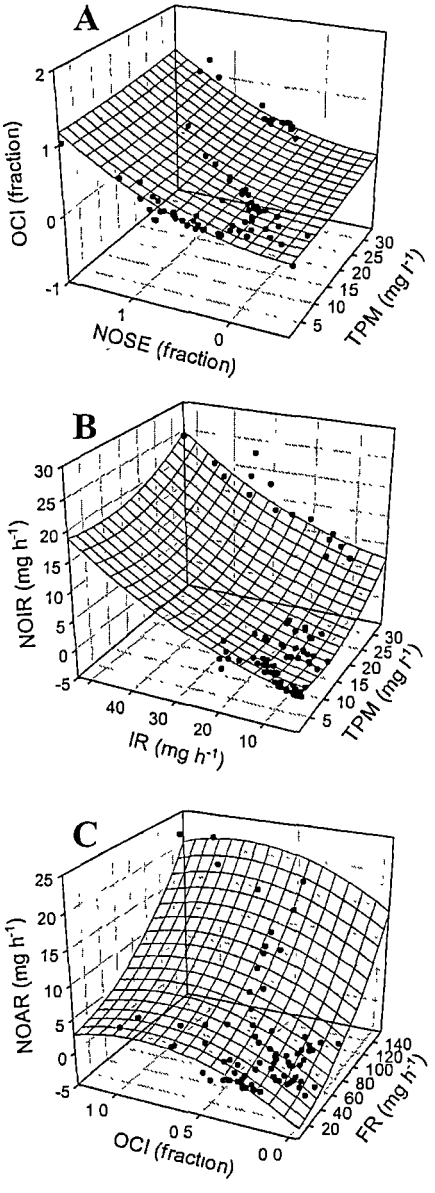

Table 2.3. Equations describing the relationships between the different steps of the filter-feeding mechanism in *P. perna* and the environmental variables TPM (mg L^{-1}) and OCS (fraction). Refer to Table 2.2 for acronyms and rate calculations.

Variables	Equation	Equation	Statistical information
OCS, TPM	$OCS=1/(2.55+0\ 47 \times TPM)$	(1)	$r^2 = 0.37$, F=14.85,df=1,25, P<0.001
CR, TPM and OCS	$CR=13\ 83(\pm2.91) - 0.65(\pm0.17) \times TPM - 47.85(\pm 22.82) \times OCS+0.011(\pm 0.004)\ TPM^2+83.8(\pm 43.02)\ OCS^2$	(2)	$r^2 = 0.27$, F=7.57, df=4,80, P<0.0001
FR, TPM and OCS	$FR=68.77(\pm21.45) - 0\ 12(\pm1.28) \times TPM - 370.10(\pm 167.72) \times OCS+0.07(\pm 0.03)\ TPM^2+565.8(\pm 330\ 89)\ OCS^2$	(3)	$r^2 = 0.70$, F=45.85, df=4,80, P<0.0001
RR, TPM and OCS	$RR=52.43(\pm14.90) - 0.97(\pm0.89) \times TPM - 362.47(\pm 116.54) \times OCS+0.02(\pm 0.02)\ TPM^2+589.79(\pm 229.92)\ OCS^2$	(4)	$r^2 = 0.72$, F=52.16, df=4,80, P<0.0001
IR, TPM and OCS	$IR=24.14(\pm6\ 96) - 0.62(\pm0.41) \times TPM - 117.37(\pm 54.46) \times OCS+0.03(\pm 0.01)\ TPM^2+203.97(\pm 107.45)\ OCS^2$	(5)	$r^2 = 0.54$, F=23.83, df=4,80, P<0 0001
AR, TPM and OCS	$AR=-1\ 93(\pm2.42) - 0\ 006(\pm0.14) \times TPM - 13.35(\pm 18.97) \times OCS+0.01\ (\pm 0.003)\ TPM^2-3\ 62(\pm 37.44)\ OCS^2$	(6)	$r^2 = 0.79$, F=75 85, df=4,80, P<0.0001
NOSE, PIM and POM	$NOSE=0.30(\pm0.08) - 0.21(\pm0.05) \times PIM + 1.03(\pm 0.24) \times POM+0.01(\pm 0\ 004)\ PIM^2-0.20(\pm 0.08)\ POM^2$	(7)	$r^2 = 0\ 40$, F=13.41, df=4,80, P<0.0001
OCI, TPM and NOSE	$OCI=0\ 13\ (\pm0.03) - 0.001(\pm0.005) \times TPM+ 0.27(\pm 0.06) \times NOSE+0.0002(\pm 0.0001)\ TPM^2+0.19(\pm0.05)\ NOSE^2$	(8)	$r^2 = 0.75$, F=62.58, df=4,80, P<0.0001
NOIR, TPM and IR	$NOIR=1.37\ (\pm0\ 50) - 0.23(\pm0.06) \times TPM+ 0.11(\pm 0.06) \times IR+0\ 01(\pm 0.001)\ TPM^2+0.004(\pm0.001)\ IR^2$	(9)	$r^2 = 0.92$, F=223 74, df=4,80, P<0.0001
NOAR, OCI and FR	$NOAR=-2\ 62\ (\pm0.55) - 0.012(\pm0.011) \times FR+ 15.73(\pm 0.06) \times OCI+0.0006(\pm 0.0001)\ FR^2-9.22(\pm1.93)\ OCI^2$	(10)	$r^2 = 0.90$, F=196.31, df=4,80, P<0.0001
NAEIO, OCI	$NAEIO=2.08(\pm0\ 33)\ OCI/\ (1+0.22\ (\pm0.26)\ OCI)$	(11)	$r^2 = 0.42$, F=57.64, df=4,80, P<0.0001

Table 2.4. Equations used in the formulation of feeding physiology model in STELLA.

TPM = GRAPH (time-series)
OCS = 1/(2.55 + 0.47 × TPM)
PIM = 0.22 + 0.81× TPM
POM = TPM-PIM
FR = 68.77 - 0.12 × TPM - 370.10 × OCS + 0.07 × TPM^2 + 565.80 × OCS^2
Filtered matter (t) = Filtered matter (t - dt) + (FR - RR - IR) × dt
INIT Filtered matter = 219.81
RR = 52.43 + 0.97 × TPM - 362.47 × OCS + 0.02 × TPM^2 + 589.79 × OCS^2
Pseudofaeces (t) = pseudofaeces (t - dt) + (rejection) × dt
IR = filtration-rejection
Ingested (t) = ingested (t - dt) + (ingestion' - NIIR - NOIR) × dt
INIT ingested = 36.46
NOIR = 1.37-0.23 × TPM + 0.11× IR + 0.01× TPM^2 + 0.004 × IR^2
NIIR = ingested-NOIR
Inorganic (t) = inorganic (t - dt) + (NIIR – IM on gut) × dt
Organic (t) = organic (t - dt) + (NOIR – OM on gut) × dt
OM on gut = organic
IM on gut = inorganic
INIT organic = 13.17
INIT inorganic = 23.29
Ingested matter = food on gut + organic + ingested + inorganic
Food on gut (t) = food on gut (t - dt) + (OM on gut + IM on gut - absorption' - egestion') × dt INIT food on gut = 0
NOSE = 0.30-0.21× PIM + 1.03 × POM + 0.01 × PIM^2 - 0.20 × POM^2
OCI = 0.13-0.001× TPM+ 0.27 × NOSE + 0.0002 × TPM^2 + 0.19 × $NOSE^2$
NOAR = -2.62 + 0.012 × FR + 15.73 × OCI + 0.0001 × FR^2 - 9.22 × OCI^2
Absorption' = NOAR
Absorption = absorption'
Absorbed matter (t) = absorbed matter (t - dt) + (absorption) × dt
INIT absorbed matter = 0
Egestion' = IM on gut + (NOIR-NOAR)
Egestion = egestion'
Faeces (t) = faeces (t - dt) + (egestion) × dt

Figure 2.5. The relationship between the organic content of ingested (OCI, fraction) and the net absorption efficiency from ingested organics (NAEIO, fraction). Refer to Table 2.3 for equations and statistic.

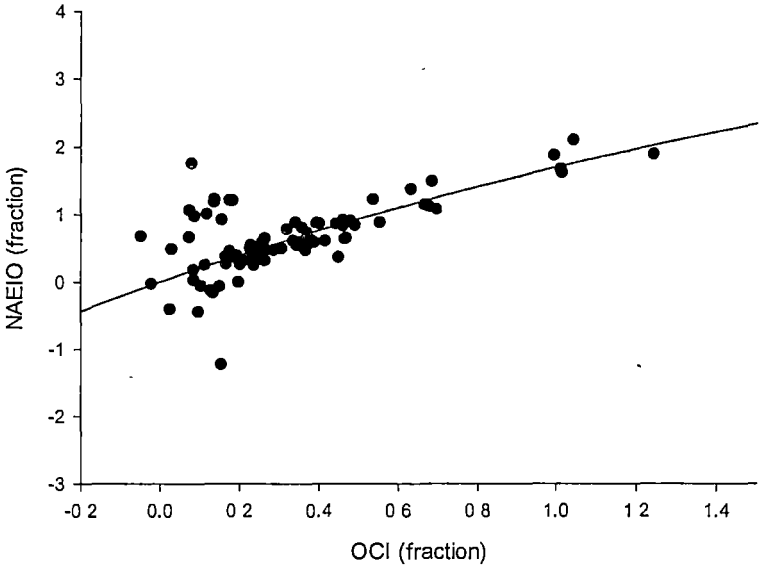

Figure 2. 6. (**A**) Diagram of the feeding processes of a general filter-feeding bivalve, used on the modelling of *P. perna* feeding physiology. (**B**) Diagram of the sub-model of a mussel gut showing the absorption of organic matter and faeces production. Refer to Tables 2.2 and Table 2.3 for variables and acronyms and Table 2.4 for logical and differential equations.

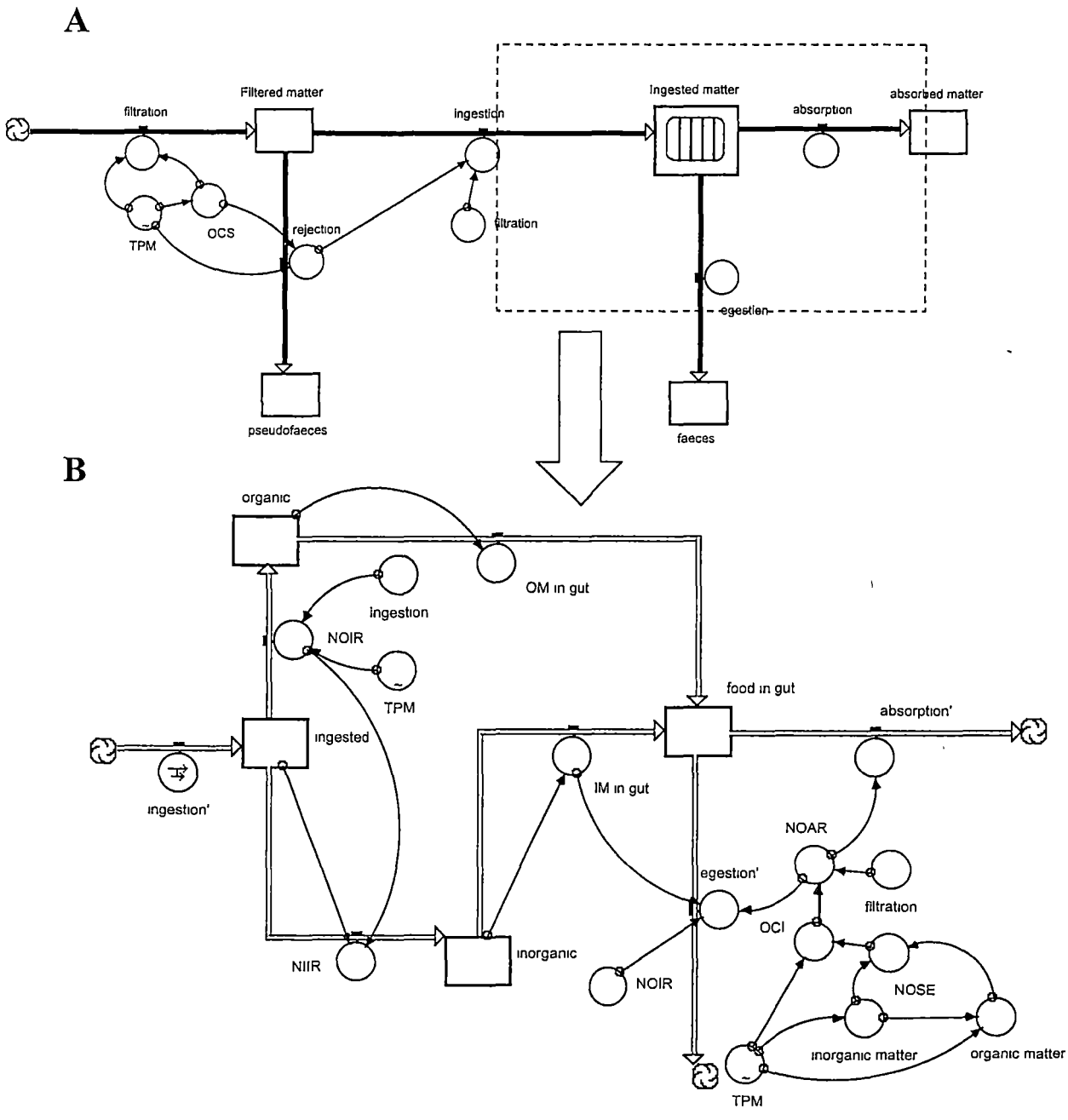

NOSE, OCI, and AR of mussels in a range of TPM between 2 and 40 mg L^{-1}, are shown in Fig. 2.7A, B, C, D, E and F respectively, showing that predicted values satisfactorily reproduce the main trends of feeding behavior observed in *P. perna*.

Bivalve feeding behavior is mainly controlled by concentration and organic content of seston (Hawkins *et al.*, 1998b). Therefore, it is likely that this model is sensitive to these forcing functions (TPM and OCS). In order to verify the model sensitivity to changes in the coefficients of the equation that predicts OCS as a function of TPM, we ran the model three times, varying the coefficients values. Each coefficient (equation (1), Table 2.3, Fig. 2.2) was varied by ± 10% from its standard value, and the sensitivity was measured by the following equation:

$$S = [\partial x/x]/[\partial P/P] \qquad \text{(Equation 1)}$$

where (S) is a measure of sensitivity, x refers to model outputs at the end of the integration period in the standard model, and ∂x is the change in the value of x brought about by varying the model coefficient. Similarly, the denominator measures the variation in the coefficient of interest divided by its standard value. This equation compares the percentage change in the model outputs with a given percentage change in one of the model parameters. The value of (S) was averaged for positive and negative variations and the results of the model outputs (absorbed matter, pseudofaeces and faeces produced) for the coefficients relating TPM and OCS are shown in Table 2.5. The output most sensitive to variation in the relationship between seston TPM and OCS was pseudofaeces production, as a result of increased or decreased rejection rate.

Figure 2.7. Predictions of the *P. perna* filter-feeding model produced on STELLA. (A) filtration rate (FR, mg h^{-1}), (B) rejection rate (RR, mg h^{-1}), (C) ingestion rate (IR, mg h^{-1}), (D) selection efficiency (NOSE, fraction), (E) organic content of ingested matter (OCI, fraction), and (F) net organic absorption rate (NOAR, mg h^{-1}), in the range of total particulate matter (TPM, mg L^{-1}) observed in this study.

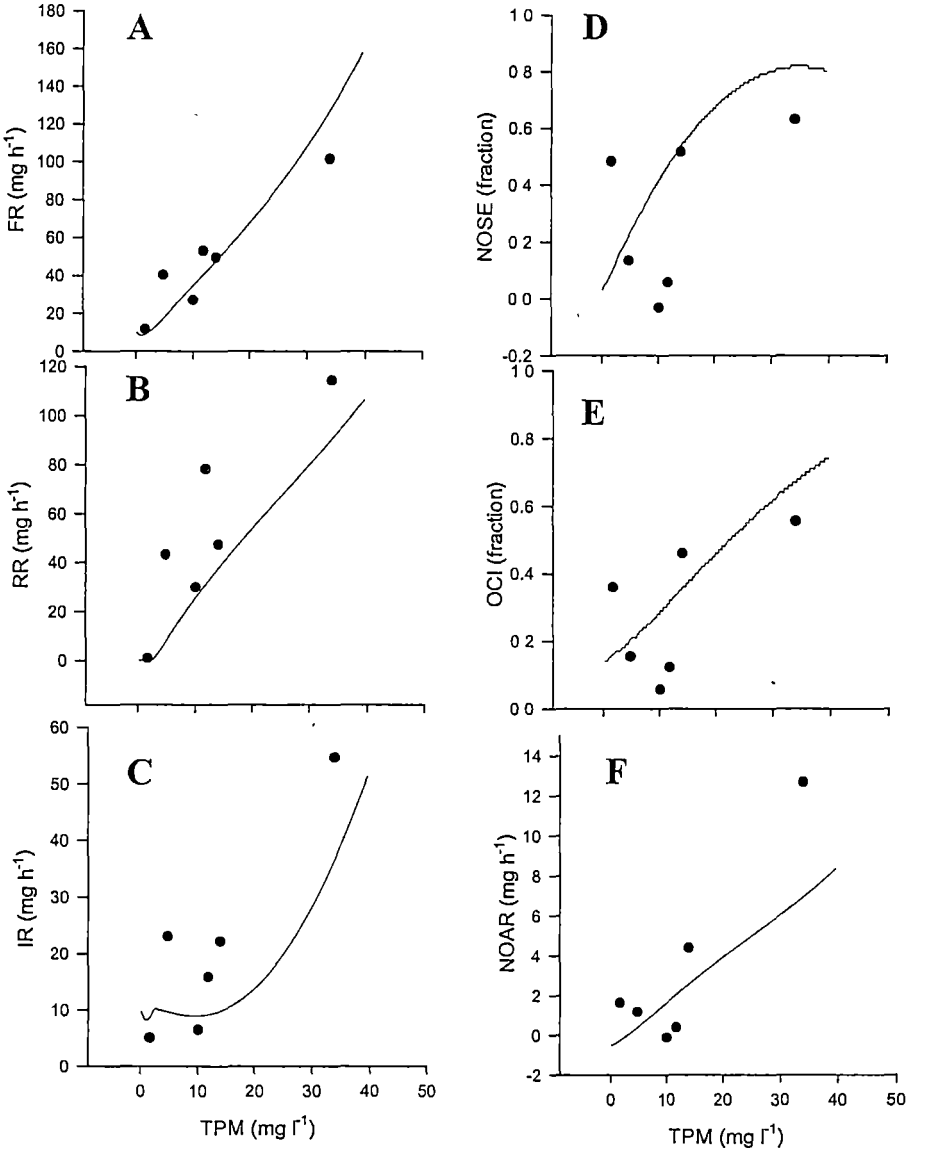

Table 2.5. Sensitivity analysis of absorbed matter, pseudofaeces and faeces production for the coefficients a and b in the equation OCS = 1/ (a + b*TPM).

	Absorbed matter	Pseudofaeces	Faeces
a	0.202	0.637	0.118
b	0.232	0.734	0.136

2.5. Discussion

This study showed that *P. perna*, like other mussels, controlled its feeding mechanisms to achieve an optimum organic absorption rate independent of fluctuations in seston concentration and quality. It is important to note that the range of TPM recorded were within normal values during the year for other bivalve aquaculture locations in Southern Brazil (Suplicy, unpub. data). Therefore, the TPM range experienced in the experiments and included in the model are directly applicable to Brazilian shellfish farms conditions. Although seasonal changes in feeding physiology were not examined in this study time series data of TPM, POM, and OCS from 1998 to 2002 do not suggest strong seasonal changes in food availability in the sub-tropical waters of Santa Catarina, (Chapter 5). Similarly, the condition index of *P. perna* does not follow a seasonal trend, as seen in *Mytilus edulis* (Navarro & Iglesias, 1995), because spawning occurs throughout the year with small peaks in summer, autumn and spring (Marques *et al.*, 1991). Therefore, we believe that the findings reported here can be used to predict feeding physiology throughout the year.

Food availability (TPM and OCS) was the main forcing function of the models produced, therefore characterizing the available seston is of primary importance to

generate a model to predict food uptake by *P. perna*. Data for Southern Brazil showed that the organic content of available food decreased as TPM increased, a common pattern in many estuaries and sheltered bays both in temperate and tropical waters (Hawkins *et al.*, 1996, 1998b). This reduction of the organic proportion is a function of the dilution of organic particles when resuspended silt increases particulate inorganic matter on the water column (Fréchette & Grant, 1991; Widdows *et al.*, 1979)

The methods used in this study to estimate clearance rates of filter feeders were less accurate than the methodology proposed by Hawkins *et al.*, (1998b; 1999) for measurements using natural seston. The most appropriate method to accurately measure clearance rates by bivalves is controversial (Cranford, 2001; Riisgård, 2001; Widdows, 2001). As new methods are being developed, new models about how these animals control their food uptake are being produced. It is agreed that mussels do not always filter at their maximal rate in their natural environment (Riisgård, 2001; Widdows, 2001). This may be due to a regulation of feeding processes in response to changes in quantity and quality of suspended particles, salinity, temperature and the presence of pollutants in the water (Widdows, 2001). This study was only able to explain 27% of the variation in clearance rates of mussels using TPM and OCS as independent variables, and POM did not explain a significant proportion of the remaining variance in clearance rate. However, in their experiments, Hawkins *et al.* (1999), increased the amount of the variability in clearance rate explained from 13% to 53% when they included Chl a and TPM as independent variables instead of only POM. Although all precautions proposed by Iglesias *et al.* (1998) in the use of the biodeposition method for suspension-feeding measurements were taken in this study, it seems that the new methodology proposed by Hawkins *et al.* (1998b; 1999) is more appropriate for studies using natural seston. It appears that

qualitative features of seston may be just as important as availability of food in mediating feeding responses (Hawkins *et al.*, 1998b). However, the general trend for decreasing clearance rates as seston concentrations increase is seen in other studies (Hawkins *et al.*, 1999; 1998b; Wong & Cheung, 2001). There are many methods to quantify concentration and organic content of seston in feeding experiments. Most use mass measurements of total particulate matter available in the seston (TPM, mg L^{-1}), particulate organic matter available in the seston (POM, mg L^{-1}), and the ratio between these two variables, which is the organic content of seston (OCS, fraction). Recent findings suggest that clearance rate is primarily dependent upon seston availability measured in terms of total volume, rather than mass. This helps to explain the confusing variation in clearance rate reported by many studies and stresses a need to consider volumetric constrains in bivalve feeding studies (Hawkins *et al.*, 2001). More detail about the seston organic fraction can be obtained if the carbon:nitrogen ratio is measured, which can vary from < 4 to > 26 (Bayne & Hawkins, 1990). The measurement of the biologically available organic carbon and nitrogen in the water and in associated biodeposits can provide, not only more accurate measurements of the clearance rate, but also important information about the absorption of these elements by filter feeders.

The biodeposition approach demands that the gut residence time is correctly calculated to generate accurate physiological feeding rates. As starved animals were used to estimate gut passage time this may have over-estimated the normal passage time. However, our estimates are comparable to those from other biodeposition studies using *Perna canaliculus*, in which the gut passage time for non-starved mussels was 80 minutes, and no delay time was assumed for *Perna viridis* (Hawkins *et al.*, 1998a).

Perna perna appeared to selectively enrich the organic content of ingested matter by rejecting particles of higher inorganic content before ingestion. This selection efficiency was a function both of filtration rate and the proportion between inorganic and organic particulate matter available in the water. The increase in selection efficiency at higher filtration rates is important, because this helps to maintain nutrient acquisition independent of fluctuations in seston organic content (Hawkins *et al.*, 1998a). Extreme values of net organic selection efficiency measured in this study (NOSE >1 or <0) must be considered with caution as they are probably measurement errors associated inadvertently with collecting settled sediment when collecting biodeposits. This would effectively alter the organic ratio of pseudofaeces. Extreme values were observed in 15% of measurements. Nevertheless, NOSE values recorded in this study (>0.7) suggest that *P. perna* is extremely efficient in selecting organic particles available in the seston. Hawkins *et al.* (1996) recorded NOSE values of up to 0.5 in *M. edulis*, and Hawkins *et al.* (1998) report maximum NOSE of 0.7 for *P. viridis*.

Maximum net organic ingestion rate (NOIR) recorded for *P. perna* was 24.05 mg h^{-1} and occurred when TPM was 33.93 mg L^{-1} and OCS was 0.18. This is similar to values obtained for *P. canaliculus* in New Zealand, which showed maximum organic ingestions rate of 27.3 ± 6.3 mg h^{-1} (Hawkins *et al.*, 1999), and for *P. viridis* in Malaysia with a recorded rate of 24.8 ± 3.6 mg h^{-1} (Hawkins *et al.*, 1998a). However, these rates are considerably higher than the maximum organic ingestion rate of 6.5 mg h^{-1} reported for *M. edulis* (Hawkins *et al.*, 1997). The growth rates of *P. perna* in Southern Brazil are among the fastest reported for mussels in the *Perna* genus, reaching commercial size (80 mm) in 8-10 months (Chapter 3). This rapid growth is probably related to higher weight-specific

rates of energy acquisition and higher water temperatures in the sub-tropical waters of Southern Brazil.

Data from this study suggested that *P. perna* takes advantage of the abundant organically rich seston available in Brazilian waters throughout the year by maintaining high ingestion rates. There is evidence that when ingestion rate is high absorption efficiency is high and gut residence time is short (Bayne *et al.*, 1988). Furthermore, the proportion of gut volume occupied by ingesta may vary, thereby facilitating an increase in absorption efficiency with little change in the gut passage time (Bayne *et al.*, 1987). Widdows *et al.* (1979) report that absorption efficiency declines as ingestion rate increases and food progresses from the digestive gland to the intestine. However, this pattern may be counterbalanced by elevated organic content of ingested matter due to selection processes (this study; Hawkins *et al.*, 1999) that positively increase the absorption efficiency and ultimately the absorption rate. Similarly to the considerations raised for NOSE values, negative absorption rate values are not biologically meaningful and must be considered with caution as these could be caused by collection of inorganic sediment together with mussel faeces. Negative absorption rates were measured in 7% of measurements.

The integration of all equations from Table 2.4 with STELLA software resulted in a reductive and deterministic non-linear model that reproduces the feeding processes of *P. perna* in both clear and turbid environments. The general conceptualization of the diagram was based on the description of the bivalve filter-feeding process provided at the TROPHEE workshop (Bayne, 1998; Hawkins *et al.*, 1998b), and final equations were based on intensive measurements that enabled calibration of the outputs. This feeding

model may not be a perfect reproduction of the bivalve feeding process, but the objective was to provide a useful tool to understand and predict feeding processes of this species. The model includes a complete sequence of steps in the feeding process that may cause an accumulation of predictive error (Grant & Bacher, 1998). However, its value lies in the ability to provide an understanding of the interaction between a mussel farm and the environment, for example the amount and organic content of biodeposits released into the water column and sediment beneath the farm.

Sensitivity analysis indicated that model predictions of absorbed matter and faeces production were less affected by changes in the relationship between TPM and OCS than models prediction of pseudofaeces production. This suggests that predicted absorption would stay reasonably invariable if the model is applied to environments with different seston concentration and organic content. Therefore, mussels maintain a reasonably constant organic ingestion rate in varying seston conditions by compensating for low organic content of the seston through adjusting selection efficiency and rejection of inorganic matter as pseudofaeces.

This feeding model can be used as an important tool for the understanding of how *P. perna* interact with the culture environment. Current studies are under way to integrate this feeding model with energy budget and population dynamics of *P. perna*. Further coupling of the *P. perna* biological models with physical models of seston hydrodynamics and models of primary production are also planned, and this approach will allow the development of carrying capacity analysis for suspended mussel culture in sub-tropical environments like the southern Brazilian coast.

Chapter 3

Modelling growth and population dynamics of the brown mussel *Perna perna* (L.) in suspended culture in Santa Catarina, Brazil.

3.1. Abstract

Growth and mortality rates using size frequency distributions of the brown mussel *Perna perna* in suspended culture in two locations were studied in Santa Catarina, southeast Brazil. Shell length data were fit to a Von Bertalanffy growth function, with L_∞ = 8.3 cm and k = 0.34 for Brito Cove, and L_∞ = 8.8 cm and k = 0.28 for Porto Belo. Increase in wet weight was plotted on a Gompertz growth curve with W_∞ = 61.6 g and $\underline{k}$ = 3.4 for Brito Cove, and W_∞ = 39.6 g and k = 1.8 for Porto Belo. In Brito Cove the size (shell length) frequency distribution of the population after eight months was 66.4 % harvestable (>7.5 cm), 21.1% large (5.5 – 7.49 cm) and 10.18 % medium (3.5–5.49 cm). In Porto Belo this distribution after seven months was 39.8%, 51.8% and 8.4% respectively. Attachment rates of new seeds after the installation of the ropes in both locations were higher in summer months; 10% of rope population in Brito Cove and close to 1% in Porto Belo. Mortality rates were estimated at 0.06 $year^{-1}$ in the populations at both locations. The integration of growth and mortality data in a predictive model using STELLA® software resulted in good predictions of size frequency distribution for both Brito Cove and Porto Belo. This model already has practical applications, but its full potential in applied ecology will be increased once it has been integrated with models for scope for growth, primary production, and hydrodynamics resulting in a model of carrying capacity analysis for mussel farming.

3.2. Introduction

Growth rates of individuals in a population directly affect predictions of survivorship, mortality, and production when dynamic population models are used. Therefore, estimates of growth parameters occupy a central role in estimating harvest from a stock assessment when using dynamic models (Tomalin, 1995). Although mussel growth rates in suspended culture conditions have been previously reported (e.g. Marques *et al.*, 1998), most of the available knowledge about mussel population dynamics is derived from natural mussel beds (e.g. Hickman, 1979; Stillman *et al.*, 2000; Hicks *et al.*, 2001). The development of aquaculture population models based on growth models is desirable both for economic and environmental reasons. Particularly as optimum yield and water filtration rates, based on culture densities, can be obtained as outputs from such models, and this information can be directly applied to carrying capacity analysis of shellfish farms.

Once estimations of growth, mortality, and production are available they can be integrated in a dynamic population model useful for fisheries and aquaculture stock management. Even when mussel seed of homogeneous size are used in a mussel farm, genetic differences among individual mussels often result in differences in growth rates. Therefore, realistically mussel farmers will not be able to harvest the entire crop at once. Population dynamic models based on growth rates can be used to predict the percentage of mussels in each size class after a given period of growout (Stillman et. al, 2000). This allows for more accurate estimates of production and the timing of production to better meet market demand, as well as better planning of reseeding, labor needs, and purchase of equipment associated with the growout phase.

The culture of the brown mussel *Perna perna* (Linnaeus, 1758) is a rapidly growing industry in Brazil (Suplicy, 2001). As the industry grows the requirement to minimize environmental impacts and develop sustainable practices has come from authorities, the general public, and other resource users. This paper aims to describe growth and population dynamics of *P. perna* on commercial culture systems in Southern Brazil. These data are then used to develop a model that predicts size frequency distribution and growth in economic and environmental modelling studies. Advances in computer sciences have led to the development of new versatile and easy-to-use modelling software like STELLA® (Costanza *et al.*, 1998). This software enables the use of models to understand a natural system and learn about it by visualizing the dynamics between its main components rather than simply coding the observed behavior and representing it using differential equations (Costanza *et al.*, 1998). Although STELLA® has been previously used to model copepod population dynamics (Marin, 1997), this study is the first to use this software to model mussel population dynamics in commercial aquaculture.

3.3. Methods

Two mussel farm areas of Santa Catarina, Southern Brazil were selected for this study; Brito Cove (48° 37' W, 27° 46' S) and Porto Belo (48° 33' W, 27° 8' S) (Fig. 3.1). Brito Cove, with a total area of 3.7 km^2, is an intensively farmed area where 43 growers have a total standing crop of 1,370 tones in 16.2 ha of culture leases. In contrast, Porto Belo, in the sheltered side of João Cunha Island is less intensively farmed with four growers maintaining a standing crop of 20 tones in 2.4 ha.

Fig. 3.1. The Santa Catarina State coast line indicating the position of Brito Cove and Porto Belo, and the location of the study locations.

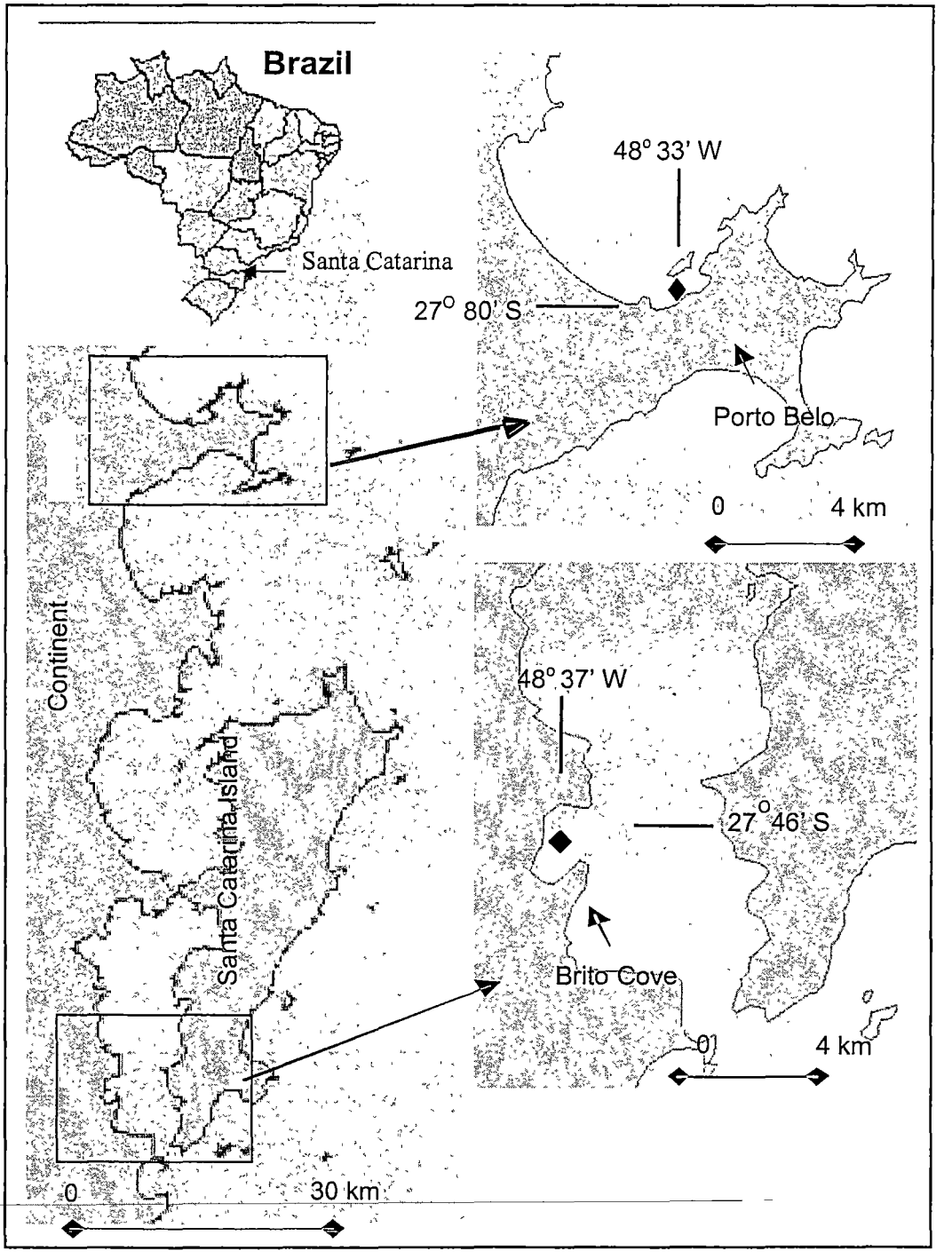

3.3.1 Growth, mortality, and production

Over a 7 month period (November 2000 to May 2001) growth rates, mortality rates, generated from size frequency distributions were obtained monthly from mussel ropes at both locations. At each location, 24 one-meter long mussel ropes were seeded with 200 small mussels (3.5 - 4.5 cm shell length). All mussels used were obtained from natural seed recruitment on collectors previously installed in a third mussel farming area, in an attempt to minimize the effect of different genetic stocks in the assessment of growth rates. There were 45 long lines in the Brito Cove study area and there was a possibility that estimates of growth rates may be affected by the position of mussel ropes within the lease. Therefore, eight mussel ropes were randomly allocated at each of the three positions within the growing lease; inside – on the first long line facing the shoreline, centre – in the middle of the farm, and outside – on the last long line facing the cove entrance. At Porto Belo there were no more than ten long-lines and variability among the long-lines was not considered to be a problem in obtaining estimates of growth rates and mortality, therefore all mussel ropes were installed in a single long-line in the middle of the farm.

Once a month three mussel ropes from each location (in Brito Cove one rope from each position) were randomly selected and their total wet weight was measured before removing and counting all the mussels. The shell length of each mussel was measured with calipers (0.01 cm) and the whole wet weight of 12 random individuals. Shell length data was put into size classes based on categories used by the industry, small (<1-3.49 cm), medium (3.5-5.49 cm), large (5.5-7.49 cm), and harvestable (>7.5 cm). These size classes were chosen because of their significance for commercial mussel culture.

Growth rates were estimated by plotting the modal shell length of the mussels from each of three ropes obtained each month and fitting a Von Bertalanffy model (Equation 1) over the seven months of available data (Tomalin, 1995).

$$L_t = L_\infty [1\text{-}e^{-k(t\text{-}t_0)}] \quad (1)$$

where L_t is length at time t, L_∞ is a estimate of the asymptotic length, k a constant representing the rate at which the asymptotic length is approached, and t_0 a third constant representing time when $L_t = 0$. The parameters were estimated by minimizing the residual sums of squares.

Mussel wet weight growth curves using 12 individuals sampled in each month were fitted using a Gompertz function (Equation 2)

$$W_t = W_\infty \times e\,[-e^{(-(t\text{-}t_0)/k)}] \quad (2)$$

where W_t is weight at time t, W_∞ is a constant representing the asymptotic weight, k a constant representing the rate at which the asymptotic weight is approached, and t_0 a third constant representing time when $W_t = 0$. The parameters were estimated by minimizing the residual sums of squares.

To separate the initial cohort of mussels placed on the ropes from those individuals that attached during the study (i.e. second cohort), we assumed that the size of all mussels from the initial cohort in Brito Cove would lie within a size range defined by the mean length predicted by Equation (1) ± 1.73*SE (giving 90% confidence limits, n=22). The same procedure was used to separate the cohorts in Porto Belo, however multiplying the standard errors by 1.75 (n=18). When estimating average survivorship, mussels that

attached after the study commenced were excluded from the count. Mussel rope standing crop (kg m^{-1}) was estimated by multiplying the number of surviving mussels by the mean wet weight in the corresponding month. Production in each consecutive month was the cumulative increase in biomass through time. Instantaneous mortality (Z), which included mussels that fell off, were predated, or died naturally over the period, was estimated as per (Crisp, 1984) by plotting $\log_{10}$ density (N) against time (Equation 3):

$$Z = 2.303 \times d(\log_{10}N)/dt \quad (3)$$

where $d(\log_{10}N)/dt$ is the slope of $\log_{10}$ density (N) against time, and annual mortality rate is equal $1\text{-}e^{-Z}$.

3.3.2. Model development

The relative growth rate using wet weight (Equation 2) was used as the main forcing function of a population dynamics model, developed using the software STELLA® Research (High Performance Systems Inc, Hanover, USA.). STELLA® facilitated the modelling process as it enabled the construction of a conceptual diagram with building blocks, allowing the visualization of material flows (mass or individuals) between state variables (population mass or size classes), and parameter behavior. An initial conceptual diagram and an underlying set of differential equations were developed based on practical farm experience and preliminary observations (unpublished). The initial model was then calibrated with data on rates of growth, seed attachment, and mortality measured in Brito Cove. This model was then validated with data from Porto Belo.

Sensitivity of model parameters, e.g. rates of mortality, seed attachment, and growth, was determined by running the model three times, changing the parameter values by ± 10% from its standard value. The sensitivity was calculated using Equation 4 (Jørgensen, 1994):

$$S = [\partial x/x]/[\partial P/P] \quad (4)$$

where (S) is a measure of sensitivity, x refers to model outputs at the end of the integration period in the standard model, and ∂x is the change in the value of x brought about by changing the model coefficient. Similarly, the denominator measures the variation in the coefficient of interest divided by its standard value. This equation compares the percentage change in the model outputs (percent frequency of individuals in each size-class) with a given percentage change in one of the model parameters.

3.3. Results

3.3.1. Growth, mortality, and production

At Brito Cove, using pooled data from the three ropes, after 7 months 66.4% of the seeded mussels reached commercial size (> 7.5 cm), 21.1% were in the large size class, and 10.2 % were on the medium size class (Fig. 3.2.A). New mussel seed (<1.5 cm) was observed in all months of the study with highest numbers in December, January, and February. The month with highest seed attachment was January, when 19 individuals represented 3.3 % of the rope population. At Porto Belo, 6 months of sampling was carried out because the mussel ropes went missing in the last month. At 6 months the size

frequency distribution at Porto Belo was not significantly different from Brito Cove (χ^2=1.65, df=2, P=0.438), with 8.4% of mussels in the medium size class, 51.83% were in the large size class and 39.8% greater than commercial size (Fig. 3.2.B). The mussel ropes in Porto Belo also had new individuals attached in almost all months of the study, although in lower numbers per rope. Highest settlement occurred in January and February with 3 and 4 new individuals respectively, which represented 0.7% of the rope population.

Equation 1 predicted average mussel shell lengths of 7.9 cm in Brito Cove after 7 months ($F_{regression}$=147.79, df=2, 20, P<0.001) (Fig. 3A) and 8.2 cm in Porto Belo after 6 months ($F_{regression}$=463.23 df=2, 16, P<0.001) (Fig. 3B). As the 95 % confidence limits of the growth curves overlapped, we assumed no significant difference in growth rates between Brito Cove and Porto Belo. Equation 2 predicted that on average mussels would reach 47. 9 g after 7 months in Brito Cove (Fig. 3C) ($F_{regression}$=257.91, df=2, 88, P<0.001) and 36.6 g after 6 months in Porto Belo (Fig. 3D) ($F_{regression}$=125.11, df=2, 69, P<0.001).

Despite the initial uniformity in seed shell length (4 ± 0.5 cm) we observed increasing variability in shell length of individuals within ropes. Variability in shell length within each rope was greater in Brito Cove than in Porto Belo (t=3.32, df=21, P=0.003), with variances as much as 40 % of the mean (Fig. 4).

Standing crop, survivorship, and mussel biomass increased at both locations (Table 1). The weight of mussels after 6 months was greater in Brito Cove than in Porto Belo (t=2.26, df=11, P=0.04), resulting in a greater monthly standing crop and production over the culture period. The mortality rate (Z) was 0.04 during 7 months at Brito Cove and

0.03 in the 6 months at Porto Belo (Fig. 3.5), which correspond to 0.06 $year^{-1}$ at both locations.

Fig. 3.2. Size class percent frequency distribution of *Perna perna* under suspended culture in Brito Cove (A) and Porto Belo (B). Small (<1-3.49 cm), medium (3.5-5.49 cm), large (5.5-7.49 cm), and harvestable (>7.5 cm). Data are from the three ropes pooled.

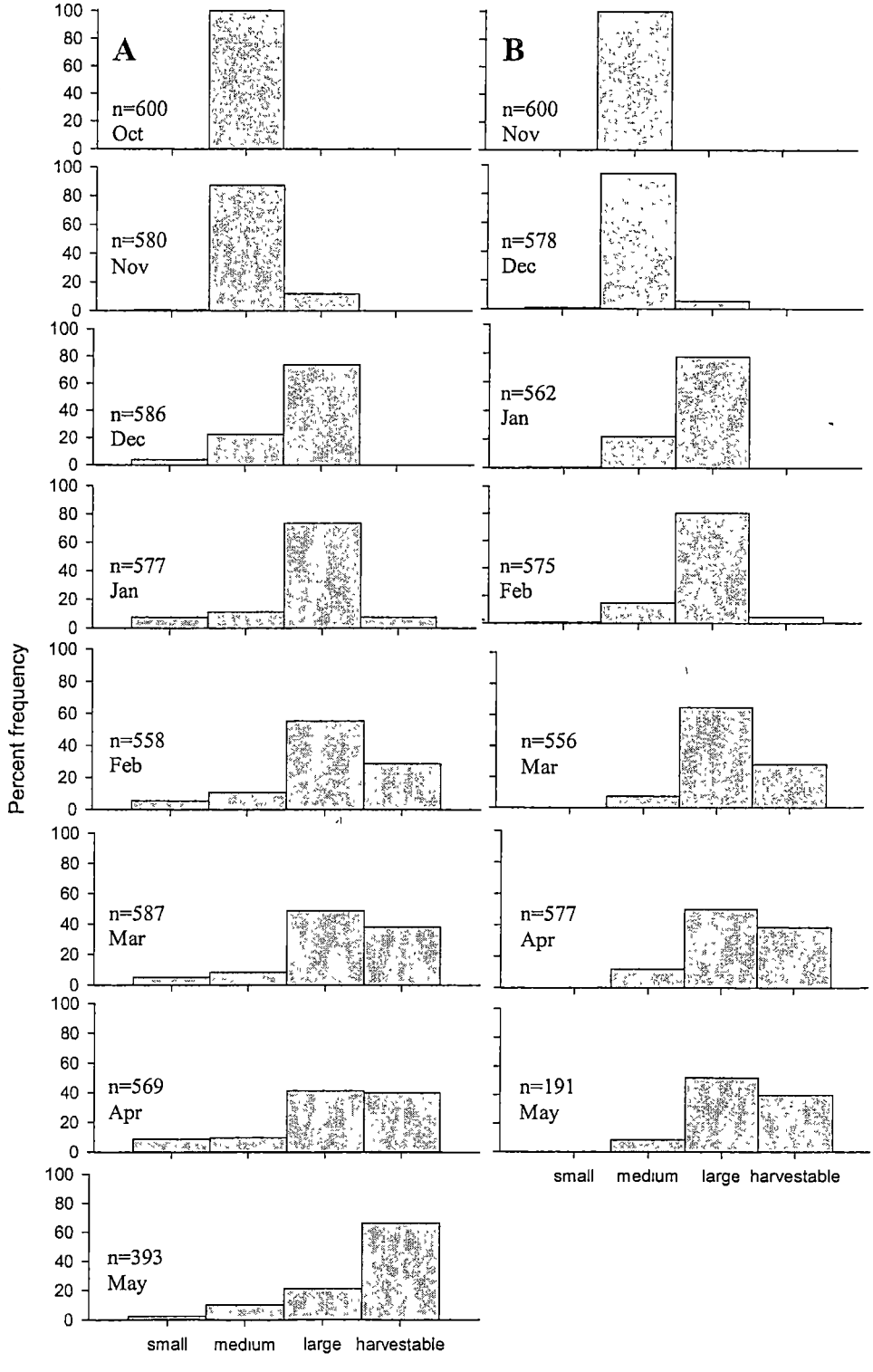

Fig. 3.3. Von Bertalanffy growth curves of shell length (cm) for Brito Cove (A) and Porto Belo (B). Gompertz growth curves of wet weight (g) for Brito Cove (C) and Porto Belo (D).

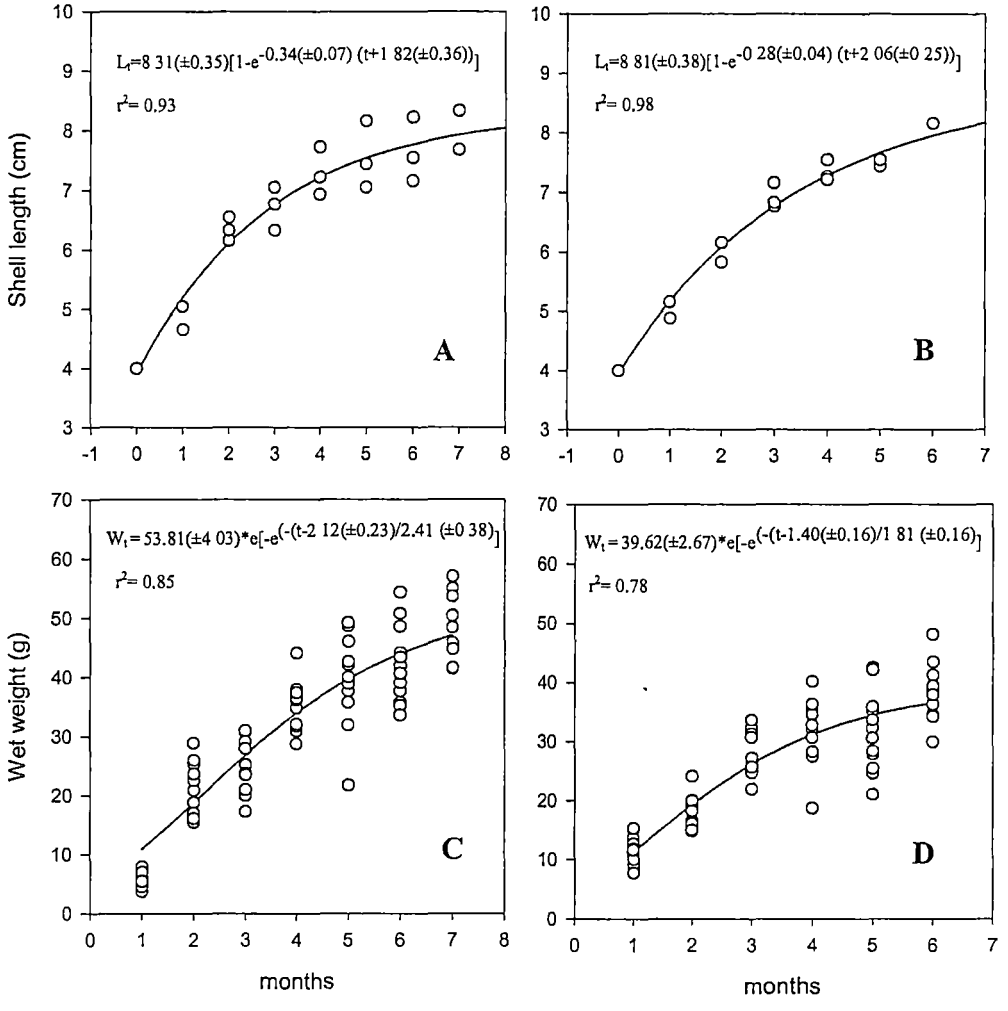

Fig. 3.4. Shell length coefficient of variation for mussels within a single farming rope at Brito Cove (A) and Porto Belo (B), during the study period. Symbols are superimposed in the first month in (A), and on the last month, one rope went missing at Brito Cove and two went missing at Porto Belo.

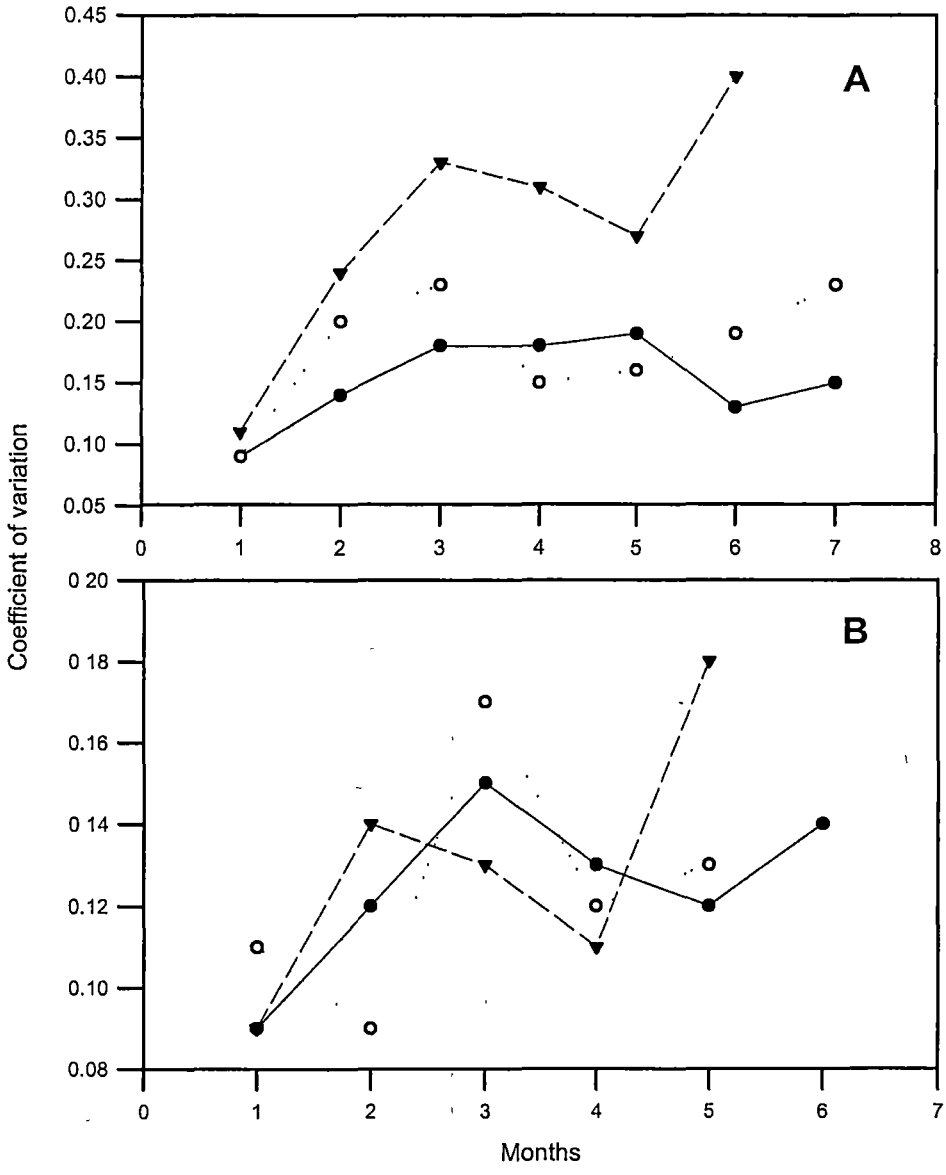

Table 3.1. Growth, survivorship, and production of *P. perna* mussels under suspended culture in two locations in Southern Brazil, Brito Cove (A), and Porto Belo (B) with attachments subsequent to the first cohort removed. Table adapted from Crisp, (1984).

A

Months after seeding	Shell length mode (cm) n = 3	Mean individual wet weight (g) n = 12	Average population density ($N\,m^{-1}$)	Standing crop (kg m^{-1})	Average value of $N\,m^{-1}$ over period	Average individual wet weight over period (g)	Decrease in population per rope ($-\Delta N$)	Increase in weight per mussel (g) (Δw)	Increase in production per rope (kg) (ΔP=N Δw)	Production throughout the study period (kg m^{-1}) $\sum_{0}^{t} \Delta P$
0	4.08 (± 0.08)	8.35 (± 1.72)	200	1.67	---	---	---	---	---	---
1	4.92 (± 0.22)	13.20 (± 3.07)	181	2.39	190.5	10.78	19	4.85	0.92	0.92
2	6.34 (± 0.19)	21.97 (± 4.30)	175	3.84	178	17.59	6	8.77	1.56	2.48
3	6.71 (± 0.36)	25.33 (± 4.62)	169	4.28	172	23.65	6	3.36	0.58	3.06
4	7.29 (± 0.39)	34.46 (± 4.26)	159	5.48	164	29.90	10	9.13	1.50	4.56
5	7.55 (± 0.55)	39.52 (± 7.58)	157	6.20	158	36.99	2	5.06	0.80	5.36
6	7.64 (± 0.65)	42.12 (± 6.51)	151	6.36	154	40.82	6	2.60	0.40	5.76
7	8.00 (± 0.67)	48.73 (± 5.07)	150	7.31	150.5	45.43	1	6.61	0.99	6.75

B

Months after seeding	Shell length mode (cm) n = 3	Mean individual weight (g) n = 12	Population density ($N\,m^{-1}$)	Standing crop (kg m^{-1})	Average value of $N\,m^{-1}$ over period	Average individual wet weight over period (g)	Decrease in population per rope ($-\Delta N$)	Increase in weight per mussel (g) (Δw)	Increase in production per rope (kg) (ΔP=N Δw)	Production throughout the study period (kg m^{-1}) $\sum_{0}^{t} \Delta P$
0	4.05 (± 0.06)	8.12 (± 1.80)	200	1.62	----	---	---	---	---	---
1	5.06 (± 0.16)	11.62 (± 2.41)	191	2.22	195.5	9.87	9	3.50	0.68	0.68
2	6.05 (± 0.19)	17.95 (± 2.60)	180	3.23	185.5	14.79	11	6.33	1.17	1.85
3	6.92 (± 0.21)	28.09 (± 3.67)	169	4.75	174.5	23.02	11	10.14	1.77	3.62
4	7.34 (± 0.17)	31.43 (± 5.74)	167	5.25	168	29.76	2	3.34	0.56	4.18
5	7.47 (± 0.06)	31.63 (± 6.72)	164	5.19	165.5	31.53	3	0.20	0.03	4.22
6	8.16	38.29 (± 4.93)	163	6.24	163.5	34.96	1	6.66	1.09	5.31

3.4.2. Model structure

In the population dynamics model (Table 3.2, Fig. 3.6) attachment of new individuals was set at 10% of the rope population at Brito Cove and at 1% at Porto Belo, based on measurements in this study. Attachment events by new individuals were controlled by a simple pulse function with attachment first occurring in month three and with an interval of two months between further attachments. This function was used to produce two or three peaks of spat settlement during the growth period, which is a common pattern in *P. perna* reproduction (Rojas, 1969; Lasiak and Barnard, 1995). Given the model calculation time step of half a day, our estimates of mortality rates were converted to $1x10^{-4}$ half-day^{-1}, and this value was used in the small, medium, and large size classes.

Relative growth rates as a function of animal mass were incorporated as a forcing function into a mass conservative population dynamics model. As different size classes used different portions of the relative growth rate curve, the coefficients that controlled growth rates were different between individuals in small, medium and large size classes (Table. 3.2). In the model, the increase in biomass in any size class was controlled by multiplying the relative growth rate by the number of individuals in that size class. Individuals moved to the next size class when the average weight of individuals, i.e. the total biomass in the size class divided by its population number, reached a target value (medium=7 g, large=17 g and harvestable = 50 g). These weight targets were calculated using the weight growth curves at the time when the individuals reached shell length commercial size-classes in the length growth curve.

Fig.3.5. Log survivorship curves for estimation of mussel mortality rates at Brito Cove and Porto Belo.

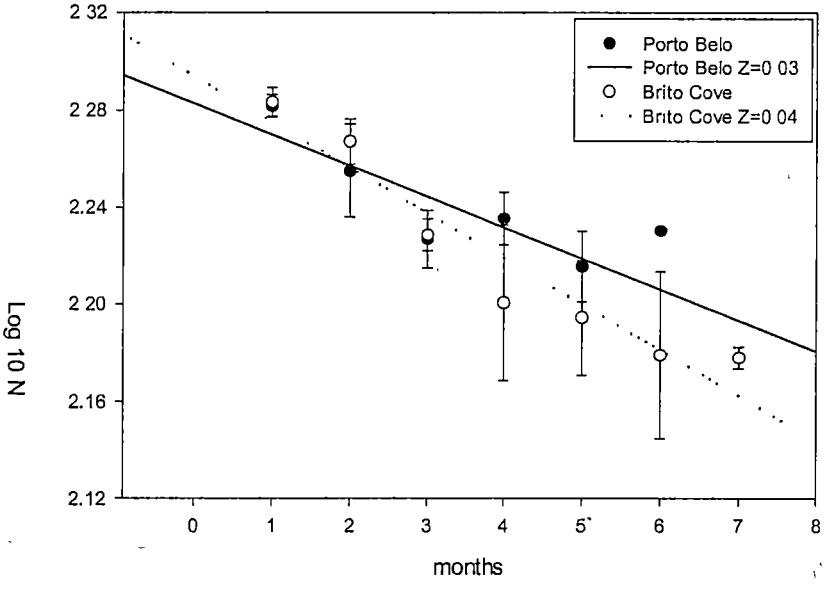

Table 3.2. Initial values of state variables, differential equations, functions and parameters of the population dynamics model developed for *P. perna* under suspended culture.

Initial values of state variables
Small mussel population (S) = 0
Small mussels mass = 0
Medium mussel population (M) = 200
Mass of medium population = 1400
Large mussel population (L) = 0
Mass of large population = 0
Harvested population = 0
Mass of harvested population = 0
Differential equations
Small Population (t) = Small Population (t - dt) + (adding small ones – graduating to medium population – mortality small) × dt
Mass of Small Population (t) = Mass of Small Population (t - dt) + (adding small mass + growing – moving mass to medium population – mass loss small) × dt
Medium Population (t) = Medium Population (t - dt) + (graduating to medium population – graduating to large population – mortality medium) × dt
Mass of Medium Population (t) = Mass of Medium Population (t - dt) + (moving mass to medium population + growing M – moving mass to large – mass loss medium) × dt
Large Population (t) = Large Population (t - dt) + (graduating to large population - harvesting – mortality large) × dt
Mass of large Population (t) = Mass of large Population (t - dt) + (moving mass to large + growing L – moving mass to harvested – mass loss large) × dt
Harvested Population (t) = Harvested Population (t - dt) + (harvesting) × dt
Mass of harvested population (t) = Mass of harvested population (t - dt) + (moving mass to harvested) × dt
Functions and parameters
Adding small ones = PULSE (((10 × whole population)/100), 90, 60)
Adding small mass = adding small ones × average mass per small one
Average mass per small one = 1.5
Growing S = if (Small Population >1and graduation fraction <0.02) then (individual growth S × Small Population) else (0)
Individual growth S = ((average mass of small population × growth rate for small population) + average mass of small population)
Growth rate for small population = if (Small Population>1 and graduation fraction<0.02) then (0.0095 × exp (-0.0519 × average mass of small population) + 0.0059 × exp (0.0519 × average mass of small population)) else (0)
Graduation fraction = GRAPH (average mass of small population) (3.50, 0.0102), (3.85, 0.011), (4.20, 0.0117), (4.55, 0.0128), (4.90, 0.0138), (5.25, 0.0152), (5.60, 0.0164), (5.95, 0.0172), (6.30, 0.0184), (6.65, 0.0191), (7.00, 0.02)
Average mass of small population = if (Small Population>1) then (Mass of Small

Population/Small Population) else (0)
Mass loss small = mortality small × 3
Mortality small = Small Population × mortality rate S
Mortality rate S = 0.0001
Graduating to medium population = if (average mass of small population >=7) then (Small Population × graduation fraction) else (0)
Moving mass to medium population = graduating to medium population × average mass of small population
Growing M = if (graduation fraction M <0.03) then (individual growth M × Medium Population) else (0)
Graduation fraction M = GRAPH (average mass of medium population)
(7.00, 0.0001), (8.00, 0.0039), (9.00, 0.006), (10.0, 0.0081), (11.0, 0.0117), (12.0, 0.0153), (13.0, 0.0178), (14.0, 0.0204), (15.0, 0.0217), (16.0, 0.0241), (17.0, 0.03)
Individual growth M = ((growth rate for medium population × average mass of medium population) + average mass of medium population)
Growth rate for medium population = if (Medium Population >1and graduation fraction M <0.03) then (0.0517 × exp (-0.0515 × average mass of medium population)- 0.0366 × exp (-0.0515 × average mass of medium population)) else (0)
Average mass of medium population = if (Medium Population>1) then (Mass of Medium Population/Medium Population) else (0)
Mass loss medium = mortality medium × 7
Mortality medium = Medium Population × mortality rate M
Mortality rate M = 0.0001
Graduating to large population = if (average mass of medium population >=17) then (Medium Population × graduation fraction M) else (0)
Average mass of large population = if (Large Population >1) then (Mass of large Population/Large Population) else (0)
Individual growth L = ((average mass of large population × growth rate for large population) + average mass of large population)
Growth rate for large population = if (Large Population>1 and graduation fraction L<0.01) then (0.0115 × exp (-0.0552 × average mass of large population) + 0.0058 × exp (-0.0552 × average mass of large population)) else (0)
Growing L = if (Large Population >1 and graduation fraction L <0.01) then (individual growth L × Large Population) else (0)
Moving mass to large = graduating to large population × average mass of medium population
Graduation fraction L = GRAPH (average mass of large population)
(21.0, 0.00), (23.9, 0.0003), (26.8, 0.00115), (29.7, 0.00235), (32.6, 0.00375), (35.5, 0.0047), (38.4, 0.00605), (41.3, 0.00705), (44.2, 0.00795), (47.1, 0.00915), (50.0, 0.01)
Mortality large = Large Population x mortality rate L
Mass loss large = mortality large × 30.6
Mortality rate L = 0.0001
Harvesting = if (average mass of large population>=50) then (Large Population × graduation fraction L) else (0)
Moving mass to harvested = harvesting × average mass of large population

Fig. 3.6. Schematic diagram of the mass conservative population dynamics model developed for *Perna perna* on STELLA® software.

Transparent bi-directional flows in the centre of the diagram represent the link between population and biomass.

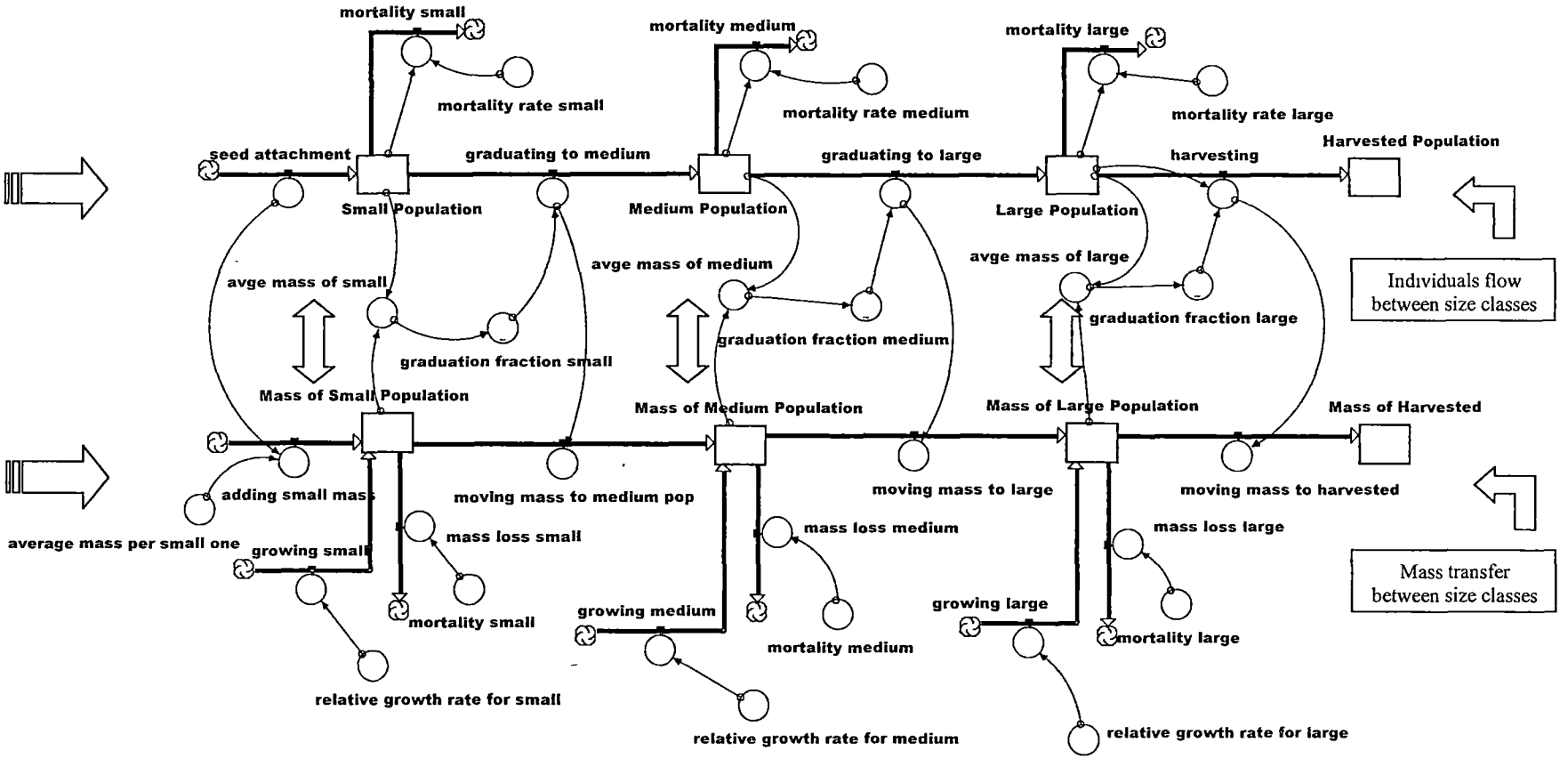

curves at the time when the individuals reached shell length commercial size-classes in the length growth curve.

The transition of individuals into the next size class continued until all mussels reached harvestable weight. Mortality rates, acted not only on the population size, but also on the loss of mass associated with mortality in each population. To achieve this mortality rates were multiplied by the weights 3, 7, and 30 g that were representative of mussels in small, medium, and large size classes respectively. To avoid all mussels being transferred to the next size class at the same time a graduation factor was included, which, reproduced a normal growth pattern observed on mussel leases. The graduation factor was the proportion of individuals in any size-class that will actually move to the next size-class in each time step of the model. This graduation factor was obtained from observed data, by calculating the percentage of mussels in a size class that progressed to the next size class as the target weight was approached (Fig. 3.7). The graduation factor was only calculated for the transition from medium to large size classes and from large to commercial size classes, because it was not possible to accurately distinguish the progression of small mussels to the medium size class. Therefore it was assumed that proportion of individuals moving from one size class to the next was constant across all sizes. The model ran for 8 months with a calculation time step of half-a-day. This time step was chosen to facilitate coupling of the population dynamics model with future hydrodynamics and physiological models, where tidal cycles may have an important role in food renewal.

The size frequency distribution predicted by the model for Brito Cove was different from that observed in the study (χ^2=376.407, df=31, P<0.001), with 25% of the size classes across the study incorrectly estimated. This was largely a function of the model having problems estimating the proportion of small mussels in the populations (Fig 3.8A). The model also had problems in month 6, where it underestimated the proportion of large mussels and overestimated the proportion of harvestable in the population. Although the predictions in these size classes were accurate in the final month. Although the model produced a different size frequency from the observed at Porto Belo (χ^2=397.96, df=27, P<0.001), with 13% of the size class across the study incorrectly estimated this was not due to the small size class. Instead the proportion of medium and large mussels in the population were poorly predicted in months 3 and 6 (Fig 3.8B). Like Brito Cove the model for Porto Belo over-estimated the proportion of harvestable mussels in month 6 (Fig 3.8.B).

The model was most sensitive to rates of seed attachment, followed by the graduation factor, individual growth rates, and mortality rates (Table 3.3). Both the growth rate and graduation factor relate to the number of animals that move from one size class to the next. As a consequence, the proportion of harvestable individuals was relatively more sensitive to changes in parameters because the wet weight at age is highly variable particularly in individuals in the large size class. Conversely, the proportion of individuals in the smallest size-class was less affected by changes in the main parameters of the model, because the size at age of these individuals in less variable.

Fig. 3.7. Graduation factor for medium (A) and large size classes (B).

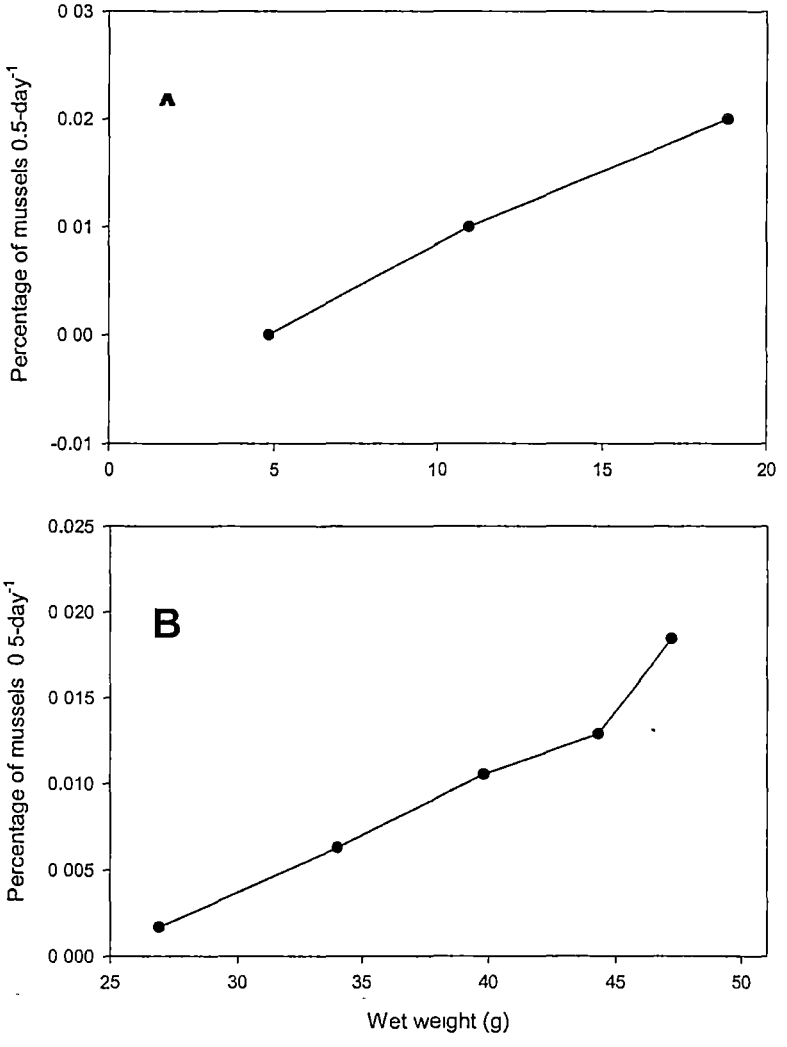

Fig. 3.8. Observed and predicted mussel size frequency distributions for Brito Cove (A) and Porto Belo (B).

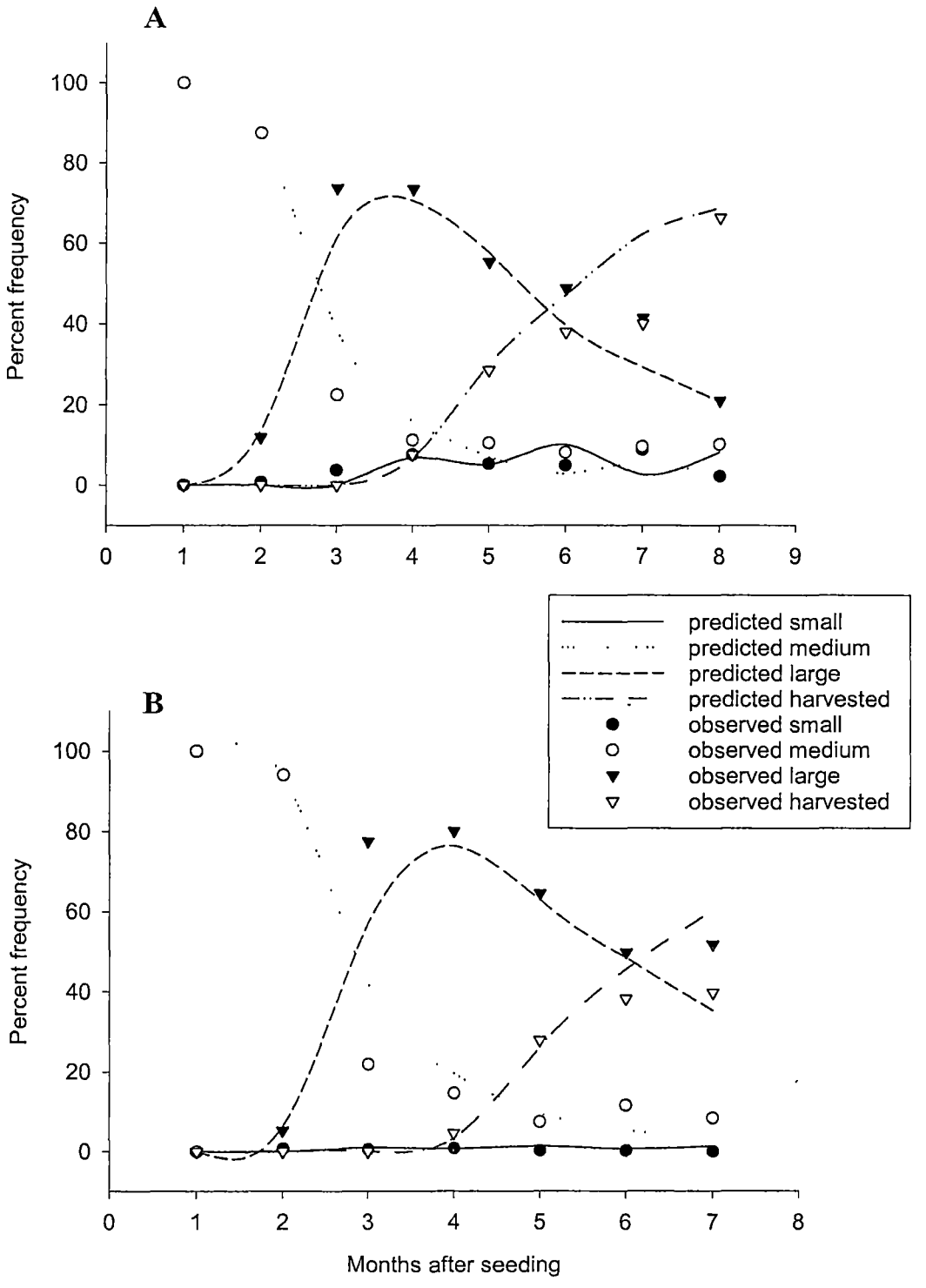

Table 3.3. Sensitivity analysis of the percentage of the population in each of the four shell length size classes to changes of ± 10% in the parameters of the population dynamics model.

	Sensitivity of model outputs at the end of the integration period			
Parameter	Percentage of small mussels	Percentage of medium mussels	Percentage of large mussels	Percentage of harvestable mussels
Graduation fraction Small	0.259	0.633	0.104	1.941
Graduation fraction Medium	0.000	0.201	0.342	3.249
Graduation fraction Large	0.000	0.142	0.062	1.557
Mortality	0.000	0.076	0.087	0.818
Seed attachment	1.121	1.686	1.326	3.849
Growth rate S	0.000	0.025	0.028	0.989
Growth rate M	0.000	0.000	0.081	1.733
Growth rate L	0.000	0.038	0.040	1.734

3.5. Discussion

Shell length growth rates of *P. perna* in Southern Brazil estimated in this study are the fastest reported for this species and are comparable to other fast-growing mussel species farmed in coastal upwelling areas (e.g. *Mytilus galloprovincialis* in Saldanha Bay, South Africa (Heasman *et al.*, 1998). The influence of temperature on mussel growth is well known (Bayne and Newell, 1983), but factors like seed origin, i.e. from spat collectors or rocky shores (Babarro *et al.*, 2000; Aquini and Ferreira, 2000), food availability (Bayne and Worrall, 1980), parasites, dissolved oxygen, and water current speed may also influence growth rates (Marques *et al.*, 1998). It is likely that growth rates are governed collectively by all these parameters and stocking density. *Perna perna* seed from collectors grow up to 46% faster than seed obtained from rocky shores (Aquini and Ferreira, 2000). In this study using seed from commercial collectors 81.1-84.7 % of mussels were > 55 mm after 3 months. In comparison, *P. perna* grown at the same temperatures as this study (19 -29 °C), but collected from the rocky shores (initial size 20 - 40 mm), take 6-8 months for 80% of the population to reach 50 mm (Marques *et al.*, 1998).

The decrease in growth rate with increase in length is well documented for various mussel species (Jørgensen, 1976). This is explained as a gradual decrease in feeding efficiency resulting from the increased energy requirements of a larger body (Hickman, 1979). The growth rates of *P. perna* in Santa Catarina were 25 to 400% faster than the same species in other locations (Table 3.4). Furthermore, in a comparison of

growth rates among cultured mussels (*M. edulis, P. viridis, M. galloprovincialis* and *P. perna*) growth rates ranged from 0.06 to 0.25 mm day^{-1} (Marques *et al.*, 1998). These rates are all, well below the rates of 0.34 and 0.38 mm day^{-1} reported here for Brito Cove and Porto Belo respectively.

Table 3.4. Monthly growth rate of *P. perna* available on the literature.

Country	Growth rate (mm $month^{-1}$)	Source
South Africa	2.4	van Erkon Schurink and Griffiths, 1993
South Africa	6.2	Berry, 1978
Angola	8.6	Mota and Machado, 1974
Venezuela	8.1	Carvajal, 1969
Brazil	10.0	this study

Our results demonstrate that mussels from the same rope grow at different rates, which may be a function of genetic differences among individuals (Hawkins and Bayne, 1991, 1992) and/or competition for food and space (Fréchette *et al.*, 1992). Although seed was collected from one site we cannot differentiate between these two processes. The variability in shell length will affect the evaluation of the economical feasibility of a mussel farm business plan, as growers should not expect to harvest 100% of the stock after a growing period. It will be necessary to reattach the slower growing animals (as much as 30% of the crop) for a second harvest a few months later, or sell these mussels for a lower price. It is not recommended that harvest is delayed to ensure that a greater proportion of mussels reach commercial size because of the loss of mussels that fall off culture ropes after 9 months (Marques *et al.*, 1998). Using anti-slough discs and plastic pegs has helped to reduce losses due to mussels falling off (Scarratt, 2000). If reattached

mussels can increase their growth rates in conditions of lower density and match the growth rate of the fastest growing individuals, a second harvest could occur in two or three months. However, it may take longer if natural variability in growth is driving the rate at which animals reach commercial size.

Under standard farming practices in the shallow waters of Santa Catarina, (2 m ropes, on long lines with an average of 80 ropes, and up to 40 long lines ha^{-1}), our results estimate productivity, defined as the potential rate of incorporation of biomass under ideal conditions, of 325 tones ha^{-1} $year^{-1}$ and a standing crop of 80 tones ha^{-1}. This is similar to the farming load currently used in Brito Cove (84.6 tones ha^{-1}). However, the sustainable carrying capacity of Brito Cove must be carefully evaluated as the extension of the growing period to allow animals to reach commercial shell length has been observed in the last few years (industry, personal communication). It is thought that this is a function of the intensification of the farming effort (industry, personal communication).

Variability in shell length frequency distribution as reported in this study is also important for studies of carrying capacity. Existing models assume that all mussels grow at the same pace. However, filtration rate is generally calculated using allometric equations based on shell length (Powell *et al.*, 1992), therefore the population filtration rate is often erroneously calculated. A more accurate model for predicting total population filtration rate will only be achieved if population size distribution is considered, rather than using the average filtration rate for all size classes. In a review of

previous studies relating shell length (mm) to filtration rate (l h^{-1}), Powell *et al.* (1992) proposed a general relationship to estimate filtration rates in unstudied species. If we apply this equation to a range of mussel shell lengths, we find that mussels of 3, 5, and 8 cm shell length filter 0.49, 1.04, and 2.14 l h^{-1} respectively. If we apply these filtration rates to a rope of 200 mussels m^{-1}, these values are increased to 97, 208 and 428 l h^{-1}. The error associated in assuming filtration rate of only one size class can be enormous if we consider a farming area like Brito Cove were we estimate the number of mussels to be 23.3 million.

There are many similarities between this work and another population dynamics model developed for oyster culture in Thau lagoon, France (Gangnery et al., 2001). These authors used the same methodology to estimate growth rate, using simultaneous introduction of homogeneous sets of individuals and measuring shell increase over time. They also relied on industry inquiries about seeding periods to set an appropriate input of new individuals in the system. Constant seeding of new mussels occurred all year, except during summer when it was zero. These authors also used weight classes, with the model simulating the variation in time of the abundances in each weight class. Similarly, the movement of individuals between weight classes was controlled by target weight for each class until they reach a minimum weight set for harvest.

Variability in growth and growth equation has over estimated growth of large individuals. A species that is growing so quickly may require more intense temporal sampling that would provide a better estimate of the transition rates between size classes.

More intense temporal sampling can also improve estimates of the graduation factor, a fundamental parameter of the model that acted together with growth rate to move mussels between size classes. It is possible that variation in growth rates within a lease will be problematic in estimating growth, suggesting the model may need to take into account the position in large leases. The development of a population dynamics model based solely on the coefficients from the Gompertz growth curve and its associated relative growth rate gave realistic size frequency distributions in some months for both Brito Cove and Porto Belo. The model will be improved if the relative growth rate employed here is replaced by a dynamic scope for growth model for individual mussels including features like energy intake, expenditure, and allocation into soft tissues, and organic shell. This approach was used in an oyster population dynamics model (Gnaiger et al., 2001), where growth rate was controlled by an allometric function of chlorophyll a and individual weight.

The model generated was sensitive to rates of seed attachment, mortality and growth. Therefore, we used location specific rates when generating predicted population size structures for Brito Cove and Porto Belo. Given the sensitivity of the model to these rates, we recommend that this model can be applied to other tropical locations provided that these population parameters are obtained. It appears that of these only seed attachment rates are temporally variable (Acuña, 1977; Berry, 1978) and it will be necessary to obtain this information over a longer time period. The rate of seed attachment is an important factor that appears to be unique for each location. The model was sensitive to rates of seed attachment and therefore it was important to assume an order of magnitude difference in this rate at Brito Cove and Porto Belo to generate

realistic population predictions. This study presents valuable information about *P. perna* population dynamics, both for aquaculture purposes as well as for further development of models for carrying capacity analysis in mussel farms. With this objective in mind, this model will be integrated with models of mussel energy physiology, primary production, and hydrodynamics to estimate sustainable stocking densities for mussel farming in Brazil.

Chapter 4

An ecophysiological model for the brown mussel *Perna perna* grown under suspended culture in Santa Catarina, Brazil.

4.1. Abstract

A dynamic simulation ecophysiological model of suspension-feeding, energy allocation, and growth is presented for *Perna perna* grown under suspended culture in Santa Catarina, Brazil. The model was divided in four sectors; seston, feeding, energy allocation, and growth. This facilitated descriptions and explanations of the functions controlling feeding and metabolic responses to changing food availability and seawater temperature. The seston sector included time-series of seston variables likely to influence food and energy acquisition in mussels. It also included relationships among these seston variables to estimate the energy content of phytoplankton and detritus, the main components of mussel diet. The feeding sector described mussel suspension-feeding behavior measured using natural seston. Rates of filtration, rejection, ingestion, and absorption were directly related to the quantity and quality of available seston. In the energy allocation sector absorbed matter was transformed to absorbed energy using estimates of energy content of food provided in the seston sector. After accounting for the maintenance requirements of the mussels (heat loss, excretion, and mucus production), surplus energy, or the scope for growth, was directed to the growth sector. The growth sector included byssus, organic shell, and soft tissue production based on energy partitioning estimated from monthly measurements of tissue (somatic and reproductive) and shell growth. The model successfully predicted mussel shell length and dry tissue weight during the study and provided estimates of the response to food acquisition, energy expenditure, and allocation to growth. This was the first attempt to model the ecophysiology of this fast growing tropical and sub-tropical mussel. Given the

results obtained in the growth predictions, we suggest that it can be used in furthering studies of carrying capacity analysis of shellfish culture in Brazil.

4.2. Introduction

As the mollusk aquaculture industry grows there is increasing demand for new farming leases, this combined with over-stocking of existing areas may depress of growth rates of bivalves (Grant *et al.*, 1993). The exploitable carrying capacity of shellfish farms is defined here as the stock size at which maximum yield of the marketable cohort is achieved (Smaal *et al.*, 1998). Many predictive models of carrying capacity have been developed both at ecosystem and local scales in the last twenty years. However, there is increasing consensus that modelling of ecophysiological processes is of primary importance in these predictive models (Smaal *et al.*, 1998). Some general relationships in the feeding physiology of suspension-feeding bivalves have been described (Hawkins *et al.*, 1998b). However, there are subtle yet significant interspecific differences in the response of feeding activity to changing quantity and quality of seston (Hawkins *et al.*, 2002). Similarly, important interspecific differences in bivalve physiology related to energy balance directly affect scope for growth (e.g. van Erkon Schurink & Griffiths, 1992).

Although the pathways by which bivalves consume food and produce biomass are complex and still the subject of debate in the literature, predicting bivalve growth through simulation modelling is becoming an increasingly important tool in the

management of cultured stock (Grant & Bacher, 1998). These models generally attempt to reproduce the physiological responses of bivalves to changing availability of food quantity and quality to predict the scope for growth. Scope for growth, in these models, is calculated as the net result of energy gain by feeding and energy loss by maintenance (respiration and excretion) and reproduction (Scholten & Smaal, 1998). Such models are valuable because they enable the integration of ecophysiological knowledge for a given species, the identification of knowledge gaps, and can be used as a management tool in eutrophication and carrying capacity studies (Scholten & Smaal, 1998).

Most mussel ecophysiological models have been developed for *Mytilus edulis*, a temperate species that experiences marked seasonal changes in food availability and temperature (e.g. Scholten & Smaal, 1999; Brylinski & Sephton, 1991; Van Haren & Kooijman, 1993; Campbell & Newell, 1998). As a result, *M. edulis* displays distinct seasonal variation in feeding, absorption, and use of available energy (Hawkins & Bayne, 1985), which is reflected in clear annual cycles of gametogenesis and spawning (Bayne, 1976). In contrast, closer to the equator there are less pronounced seasonal changes in food availability and temperature. Therefore different environmental forcing functions will have an effect on primary production at different latitudes (Taylor *et al.*, 1997). There is a need to specifically develop models that use environmental forcing functions appropriate for tropical environments. The physiological energetics of *Perna perna* (Linnaeus, 1758), in relation to body size, ration, and temperature are described for South African conditions (van Erkon Schurink & Griffiths, 1992). However, it is unclear if these can be applied in a general way to all tropical environments. In Brazil mussel

farming is an important socio-economic activity with production increasing from 150 to 12,000 tones in the last decade (Suplicy, 2001).

The aim of this study was to generate a model that simulated food uptake, energy balance and therefore predicted growth for this mussel species in tropical waters. This will then allow management of this industry based on the biological characteristics of the growing areas in tropical and sub-tropical environments. This was achieved by integrating the available knowledge about *P. perna* physiology to produce a responsive ecophysiological model for mussels kept under suspended culture conditions in a sub-tropical environment. A focus was given in the characterization of physiological outputs and feedbacks to the environment and its effect on mussel growth. STELLA® software (High Performance System, Hanover, USA) was used to model the interaction between the bivalve energy budget and the feeding environment.

Modelling bivalve ecophysiology using STELLA® software is increasing (e.g. Grant & Bacher, 1998; Pouvreau *et al.*, 2000; Hawkins *et al.*, 2002). This multi-level, hierarchical environment for constructing and interacting with models, facilitates modelling for both model producers and users, and provides a valuable learning environment. An initial conceptual diagram was developed based on the model developed for *Mytilus edulis* (Scholten & Small, 1998, 1999), and for *Chlamys farreri* (Hawkins *et al.*, 2002). This conceptual diagram was simplified and adapted given the available physiological information for *Perna perna* in a model with a time step of 0.5-

day. To facilitate analysis and explanation the model was divided into four sectors; seston, feeding, energy balance, and growth (Fig. 4.1).

Figure 4.1. The relationship between the four sectors in the ecophysiological model. Thick arrows represent material flow between sectors and thin arrows represent feedback between sectors. (1) absorbed matter (mg), (2) scope for growth (J), (3) reabsorption (J), (4)TPM and OCS, (5) absorbed matter, (6) water temperature and food energy, (7) water temperature, (8) dry body weight, (9) heat loss, excretion, and mucus production.

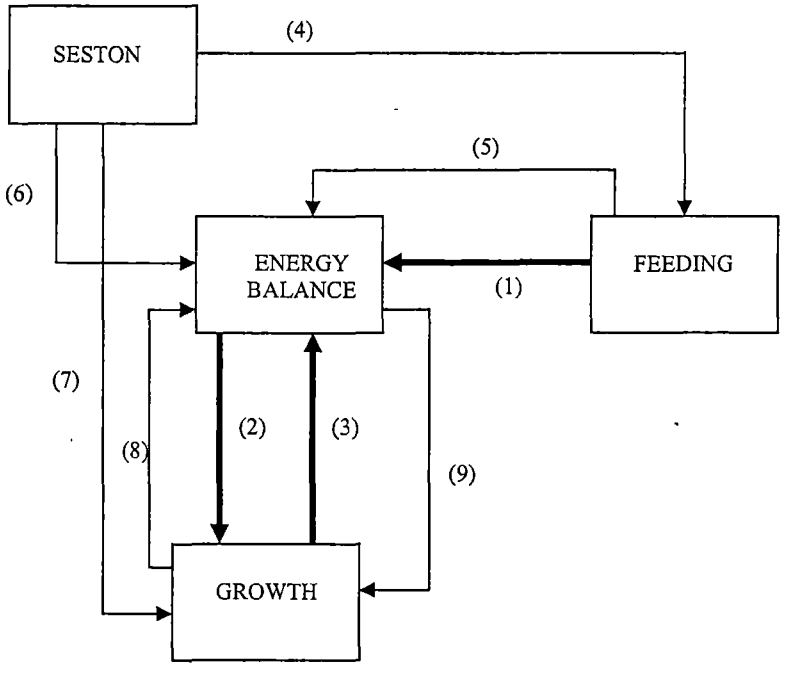

The feeding model was entirely reproduced from an earlier study (Chapter 1). All model sectors were intrinsically connected by feedback loops of parameters, model outputs, and forcing variables. As STELLA® is an iconographic modelling environment the functions and diagrams for each sector are provided. The relationships between

model parameters and state variables as well as associated statistical validation and explanations are described in the text.

4.3. Methods

4.3.1. Study site

Brito Cove, an intensive mussel *P. perna* farming area of Santa Catarina, Southern Brazil (27° 46' S, 48° 37' W), was selected for this study (Fig. 4.2). The cove has a total area of 3.7 km^2 and 43 farmers produced 1,370 tones of mussels in 16.2 ha of culture leases. The average and maximum depth were 1.5 and 3 meters respectively and mussels were grown on 1-m ropes suspended from long-lines. Mussel density in these farms was 300-500 mussels m^{-3} with a distance between long lines of 2-3 m. Strong south winds and tidal currents periodically resuspended the cove sediment (Suplicy, unpublished data) that produced considerable turbidity (6.72 ± 4.94 NTU, n = 60).

4.3.2. Data acquisition for the seston sector

Characteristics of the seston measured were total particulate matter (TPM, mgL^{-1}), particulate organic and inorganic matter (POM and PIM, mg L^{-1}), and chlorophyll a (CHL, μgL^{-1}). These parameters were measured weekly between November 2000 and May 2001 from 2 L seawater samples taken 0.5 m below the surface.

To determine TPM, PIM, and POM three 300-400 mL aliquots from each water sample were filtered onto pre-ashed and weighed Whatman GF/C filters (25 mm

diameter). Filters were rinsed with 15 mL distilled water to remove salts and dried at 60°C for 48 h before re-weighing allowing calculation of the total sample dry weight.

Figure 4.2. Sampling area in Brito Cove, Southeast Brazil.

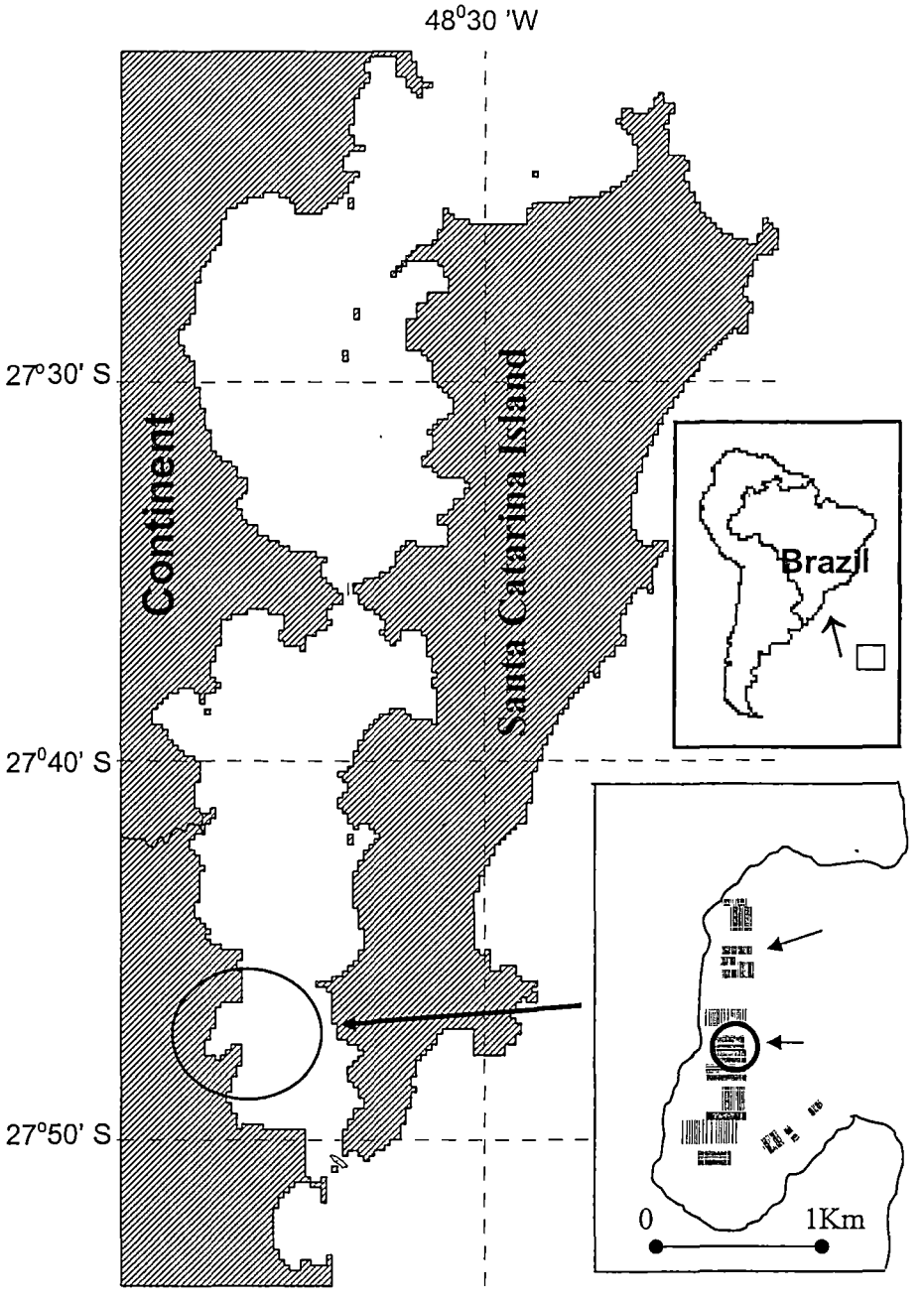

Each filter was ashed at 450°C for 4 h prior to final weighing, allowing calculation of both ash (inorganic) and ash-free (organic) mass. Chlorophyll-a was determined from 100 mL aliquots of the water sample, filtered in triplicate on 25 mm Whatman GF/C filters, fixed with potassium chlorite, and analyzed using a Turner Designs AU-10 fluorometer. Additionally, surface water temperature was monitored weekly where the mussel ropes were installed.

4.3.3. Modelling the seston sector

This included the time-series and calculations of the forcing functions of the model (Fig. 4.3, Table 4.1). Daily values of the measured seston variables were generated by applying an eight day moving average function to the weekly data. The organic content of seston (OCS) was calculated as POM/TPM.

Energy content of POM was partitioned into a phytoplankton and a detritus component (Grant & Bacher, 1998; Hawkins *et al.*, 2002). The phytoplankton carbon content was estimated by multiplying Chlorophyll by 50, based on values measured in nutrient-rich surface waters (Taylor *et al.*, 1997). This conversion factor is in accordance with C:Chl of 48 reported for estuarine areas in Southern Brazil (Proença *et al.*, 1994). Phytoplankton carbon was divided by 0.38 to estimate phytoplankton organic matter, based on an average conversion for natural algal blooms in near-shore waters (Platt & Irwin, 1973). The energy content of phytoplankton organic matter was assumed to be 23.5 J mg^{-1} (Slobodkin & Richman, 1961). As the energy content of detritus is highly

Table 4.1. Forcing variables, functions and parameters of the seston sector from the ecophysiological model for *Perna perna*.

Seston sector
Forcing variables
Chlorophyll a = (time-series) ($\mu g\ l^{-1}$)
POM = (time-series) ($mg\ l^{-1}$)
TPM = (time-series) ($mg\ l^{-1}$)
Water temperature = (time-series) (^{o}C)
Functions and parameters
POC = POM × POM: POC
POM: POC = 0.5
EPOM = ((0.62 + (0.086 × (POC ÷ (POM × 1000)) × 100)) × 4.187) ($J\ mg^{-1}$ POM)
Phytoplankton organic carbon = chlorophyll a × 50 ($\mu g\ l^{-1}$)
Phytoplankton organics = (phytoplankton organic carbon ÷ 0.38) ÷ 1000 ($mg\ l^{-1}$)
Phytoplankton energy = (phytoplankton organics × 23.5) ($J\ mg^{-1}$)
Detritus energy = ((POM × EPOM) - phytoplankton energy)) ÷ detritus organics ($J\ mg^{-1}$)
Detritus organics = POM - phytoplankton organics ($mg\ l^{-1}$)
Food energy = if (detritus energy > 0) then (detritus energy + phytoplankton energy) else (phytoplankton energy) ($J\ mg^{-1}$)
Organic content of seston = POM ÷ TPM (fraction)

Figure 4.3. The seston sector showing the calculation of forcing variables in the model based on TPM (mg l^{-1}), POM (mg l^{-1}), CHL (μg l^{-1}), POC (μg l^{-1}), and water temperature. Refer to Table 1 for equations. Measured forcing variables are marked with (~) inside the icon.

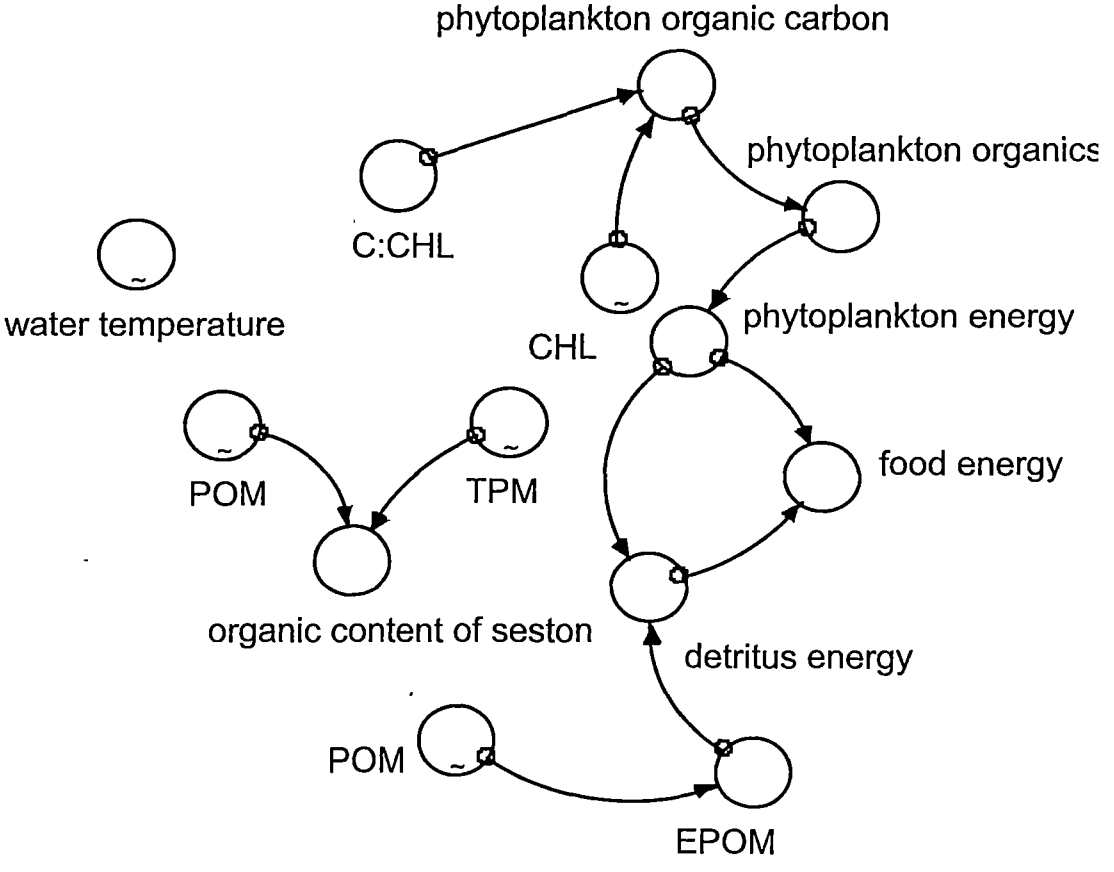

variable (Hawkins *et al.*, 2002), we used a standard factor (1 mg POM = 20.78 J) to calculate energy content of POM (EPOM, J mg POM^{-1}) (Crisp, 1971), and detritus energy was calculated as the difference between EPOM and phytoplankton energy

Detritus energy = [EPOM – (phytoplankton organics × 23.5)] (Equation 1)

Food energy (J mg^{-1}) was estimated by summing phytoplankton and detritus energy. To avoid negative values of detritus energy caused by high values of phytoplankton energy associated with algae blooms the following function was used:

Food energy = if (detritus energy > 0) then (detritus energy + phytoplankton energy) else (phytoplankton energy) (Equation 2)

Daily surface seawater temperature generated by applying an eight day moving average function to data collected weekly was also included in this sector.

4.3.4. Data acquisition for the feeding sector

All field experiments for characterization of suspension feeding behavior of *P. perna* exposed to natural variations of quantity and quality of seston are provided in Chapter 1.

4.3.5. Modelling the feeding sector

Although experiments of feeding behavior are not presented here, it was necessary to reproduce succinctly the model of the feeding physiology developed for *Perna perna* (Chapter 1), which described the feeding sector of this physiological model (Fig. 4.4., Table 4.2). This sector started with filtration (FR, mg h^{-1}) and rejection rates (RR, mg h^{-1}), which were dependent on seston quantity (TPM) and quality (OCS) according to Equations 3 and 4 (Chapter 1).

$$FR = 68.77 - (0.12 \times TPM) - (370.10 \times OCS) + (0.07 \times TPM^2) + (565.8 \times OCS^2)$$

(Equation 3)

$$RR = 52.43 - (0.97 \times TPM) - (362.47 \times OCS) + (0.02 \times TPM^2) + (589.79 \times OCS^2)$$

(Equation 4)

Ingestion rate (IR, mg 0.5-day^{-1}) was inserted in the model as FR – RR, and FR and RR values were multiplied by 12 hours to obtain 0.5-day rates.

Food entering the gut was divided into ingestion rates of organic and inorganic material. Net organic ingestion rate (NOIR, mg 0.5-day^{-1}) is dependent on TPM and total ingestion rate (IR) (Equation 5):

$$NOIR = 1.37 - (0.23 \times TPM) + (0.11 \times IR) + (0.01 \times TPM^2) + (0.004 \times IR^2)$$

($r^2_{adj} = 0.92$) (Equation 5)

Table 4.2. Forcing variables, functions and parameters of the feeding sector and sub-model from the ecophysiological model developed for *Perna perna*. Details of the sub-model Food in gut are provided in Chapter 1.

Feeding sector

Forcing functions

TPM = (time-series) (mg l^{-1}) {from the Seston sector}

Organic content of seston = POM ÷ TPM (fraction) {from the Seston sector}

Dry body weight = gonad dry weight + somatic dry weight (g) {from the Growth sector}

State variables and associated derivations

Initial filtered matter = 219.81 (mg)

Filtered matter (t) = filtered matter (t - dt) + (filtration - rejection - ingestion) × dt (mg)

Faeces (t) = faeces (t - dt) + (egestion) × dt (mg)

Filtration = (68.77 - 0.12 × TPM - 370.10 × organic content of seston + 0.07 × TPM^2 + 565.80 × organic content of $seston^2$) × 12 × ((dry body weight ÷ 1) $^{0.62}$) (mg 0.5-day^{-1})

Rejection = (52.43 + 0.97 × TPM - 362.47 × organic content of seston + 0.02 × TPM^2 + 589.79 × organic content of $seston^2$) × 12 × ((dry body weight ÷ 1) $^{0.62}$) (mg 0.5-day^{-1})

Ingestion = filtration - rejection (mg 0.5-day^{-1})

Egestion = egestion' (mg 0.5-day^{-1}) {roll-up from sub-model Food in gut}

Absorption = absorption' (mg 0.5-day^{-1}) {roll-up from sub-model Food in gut}

Initial faeces = 0 (mg)

Sub-model Food in gut

State variables and associated derivations

Initial food in gut = 36.46 (mg)

Food in gut (t) = food in gut (t - dt) + (organic matter in gut + inorganic matter in gut - absorption' - egestion') × dt (mg) {absorption' and egestion' are roll-downs from the main feeding model}

Organic matter in gut = organic (mg)

Inorganic matter in gut = inorganic (mg)

Organic (t) = organic (t - dt) + (net organic ingestion rate – organic matter in gut) × dt (mg)

Initial organic = 13.17 (mg)

Inorganic (t) = inorganic (t - dt) + (net inorganic ingestion rate - inorganic matter in gut) × dt (mg)

Initial inorganic = 23.29 (mg)

Ingested (t) = ingested (t - dt) + (ingestion' – net inorganic ingestion rate - net organic ingestion rate) × dt (mg) {ingestion' is a roll down from the main feeding model}

Initial ingested = 36.46 (mg)

Ingested matter = food in gut + organic + ingested + inorganic (mg)

Ingestion' = ingestion (mg 0.5-day^{-1}) {roll down from the main feeding model}

Absorbed matter (t) = absorbed matter (t - dt) + (absorption – energy absorption) × dt (mg)

Initial absorbed matter = 10 (mg)

Absorption = net organic absorption rate (mg 0.5-day^{-1})

Egestion = Inorganic matter in gut + (net organic ingestion rate - net organic absorption rate) (mg 0.5-day^{-1})

Net inorganic ingestion rate = ingested - net organic ingestion rate (mg 0.5-day^{-1})

Net organic ingestion rate = 1.37 - 0.23 × TPM + 0.11 × ingestion + 0.01 × TPM^2 + 0.004 × ingestion^2 (mg 0.5-day^{-1})

Net organic absorption rate = -2.62 + 0.012 × filtration + 15.73 × organic content of ingested + 0.0001 × filtration ^{2} - 9.22 × OCI^2 (mg 0.5-day^{-1})

Function and parameters

Inorganic matter = 0.22 + 0.81 × TPM (mg l^{-1})

Organic matter = TPM - inorganic matter (mg l^{-1})

Net organic selection efficiency = 0.30-0.21 × inorganic matter + 1.03 organic matter + 0.01 × inorganic matter ^{2} - 0.20 × organic matter^2 (fraction)

Organic content of ingested = 0.13 - 0.001 × TPM + 0.27 × net organic selection efficiency + 0.0002 × TPM^2 + 0.19 × net organic selection efficiency ^{2} (fraction)

Figure 4.4. The feeding sector showing the flow of food, faeces, and pseudofaeces, including state variables and parameters used to predict absorption of filtered matter in *Perna perna*. Refer to Table 4.2 for equations.

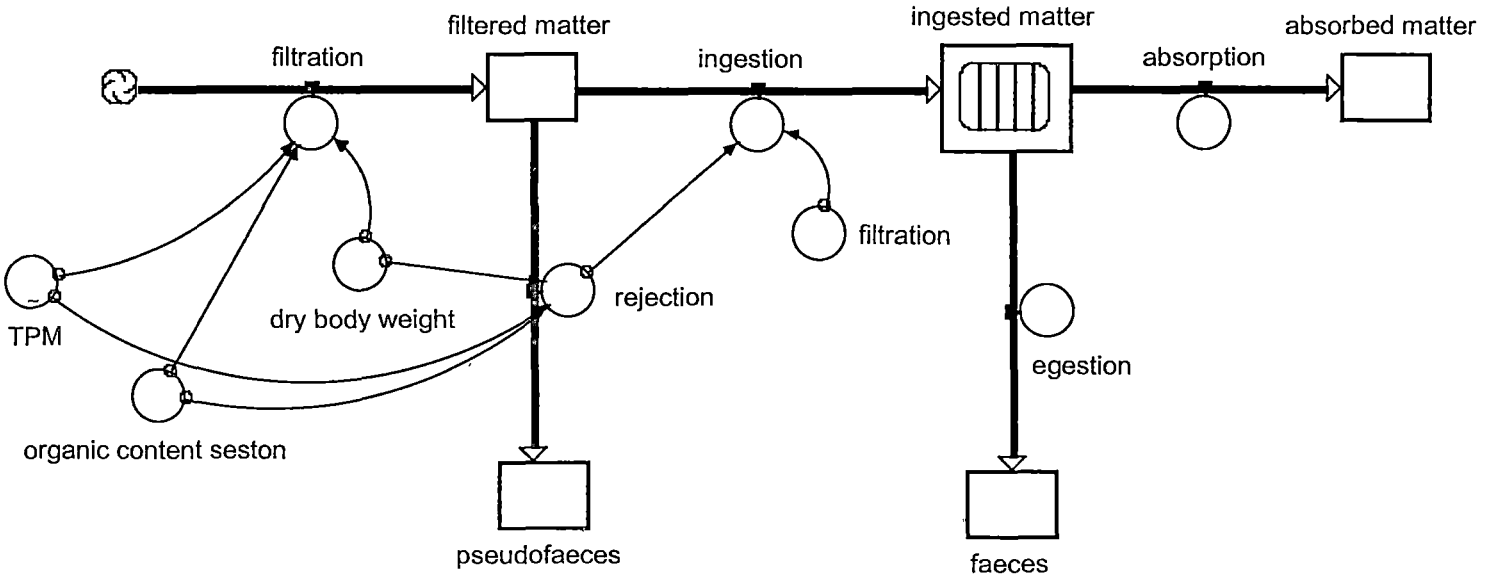

Inorganic ingestion rate was calculated as the difference between IR and NOIR. Net organic selection efficiency (NOSE, fraction) varied with organic and inorganic matter available in the seston in a relation described by a parabolic equation:

$$NOSE = 0.30 - (0.21 \times PIM) + (1.03 \times POM) + (0.01 \times PIM^2) - (0.20 \times POM^2)$$

$(r^2_{adj.} = 0.40)$ (Equation 6)

where POM and PIM are particulate organic and inorganic matter (mg L^{-1}) respectively.

Organic content of ingested matter (OCI, fraction) is dependent on NOSE and TPM as described in Equation 7:

$$OCI = 0.13 - (0.001 \times TPM) + (0.27 \times NOSE) + (0.0002 \times TPM^2) + (0.19 \times NOSE^2)$$

$(r^2_{adj.} = 0.75)$ (Equation 7)

The net organic absorption rate (NOAR, mg 0.5-day^{-1}) is dependent on OCI and filtration rate (FR) (Equation 8):

$$NOAR = -2.62 - (0.012 \times FR) + (15.73 \times OCI) + (0.0006 \times FR^2) - (9.22 \times OCI^2$$

$(r^2_{adj} = 0.90)$ (Equation 8)

The net absorption efficiency from ingested organics (NAEIO, fraction) was positively related to OCI as described in Equation 9:

$$NAEIO = 2.08 \times OCI / (1 + 0.22 \times OCI) \qquad (r^2_{adj} = 0.42) \qquad \text{(Equation 9)}$$

4.3.6. Modelling the energy balance sector

In the energy balance sector (Fig. 4.5, Table 4.3) absorbed energy was estimated by multiplying absorbed food by the energy content of food and by NAEIO. Energy content of food was the sum of phytoplankton and detritus energy content (Equation 3). Energy losses were partitioned into heat loss and excretion. Heat loss was calculated using values established for *Mytilus edulis* and other animals (Hawkins *et al.*, 1989) and previously used in the model proposed for *Clamys farreri* by Hawkins *et al.* (2002). The maintenance energy cost was 4.005 J h^{-1} g^{-1} dry soft tissue and active heat loss was linearly related to energy intake and associated with costs of feeding (Equation 10):

$$\text{Heat loss} = 4.005 + (0.23 \times \text{energy absorption}) \qquad \text{(Equation 10)}$$

Energy loss by excretion was estimated from the allometric relationship (Equation 11) describing ammonia-N excretion in *Perna perna*, (van Erkon Schurink & Griffiths 1992):

$$NH_4\,(\mu g) = 24.38 \times \text{dry weight}^{0.73} \qquad (r^2 = 0.97) \qquad \text{(Equation 11)}$$

Table 4.3. Forcing variables, functions and parameters of the energy balance sector from the ecophysiological model developed for *Perna perna*.

Energy balance sector

Forcing variables

Water temperature = (time-series) (°C) (from the Seston sector}

Food energy = if (detritus energy > 0) then (detritus energy + phyto energy) else (phyto energy) (J mg^{-1}) (from the Seston sector}

Rejection (mg 0.5-day^{-1}) {from the Feeding sector}

Dry body weight = gonad dry weight + somatic dry weight (g) {from the Growth sector}

State variables and associated derivations

Initial absorbed energy = 100 (J)

Absorbed energy (t) = absorbed energy (t - dt) + (energy absorption + reabsorption – heat losses – excretion rate – surplus - mucus production) × dt (J)

Energy absorption = absorbed matter × food energy = if (detritus energy > 0) then (detritus energy + phyto energy) else (phyto energy) (J 0.5-day^{-1})

Energy absorption rate = absorbed energy × (time) - absorbed energy × (time - dt) (J 0.5-day^{-1})

Heat losses = 0.23 × energy absorption + maintenance heat loss (J 0.5-day^{-1})

Excretion rate = (((24.38 × dry body weight $^{\text{excretion allometric b}}$) × 0.024) × 12) (J 0.5-day^{-}

$^{-1}$)

Mucus production = 0.1 × rejection (J 0.5-day^{-1})

Surplus = absorbed energy - (excretion rate + heat losses + mucus production) (J 0.5-day^{-1})

Energy for growth (t) = energy for growth (t - dt) + (surplus – soft tissues allocation – organic shell allocation – byssus production) × dt (J)

Initial energy for growth = 0 (J)

Energy surplus rate = energy for growth × (time) – energy for growth × (time - dt) (J 0.5-day^{-1})

Reabsorption = if ((excretion rate + heat losses) > absorbed energy) then ((excretion rate + heat losses + mucus production) - absorbed energy) else (0) (J 0.5-day^{-1}) {from the Growth sector}

Functions and parameters

Excretion allometric b = 0.73

Respiration allometric b = 0.72

Temperature effect on heat loss = exp (0.074 × water temperature) ÷ exp (0.074 × 23)

Maintenance heat loss = 4.005 × 12 × temperature effect on heat loss × (dry body weight ÷ 1) $^{\text{respiration allometric b}}$ (J 0.5-day^{-1})

Figure 4.5. The energy balance sector showing the flow of absorbed energy, energy expenditure by heat loss, excretion rate, and mucus production, including state variables and parameters used to predict energy surplus for growth in *Perna perna*. Refer to Table 4.3 for equations

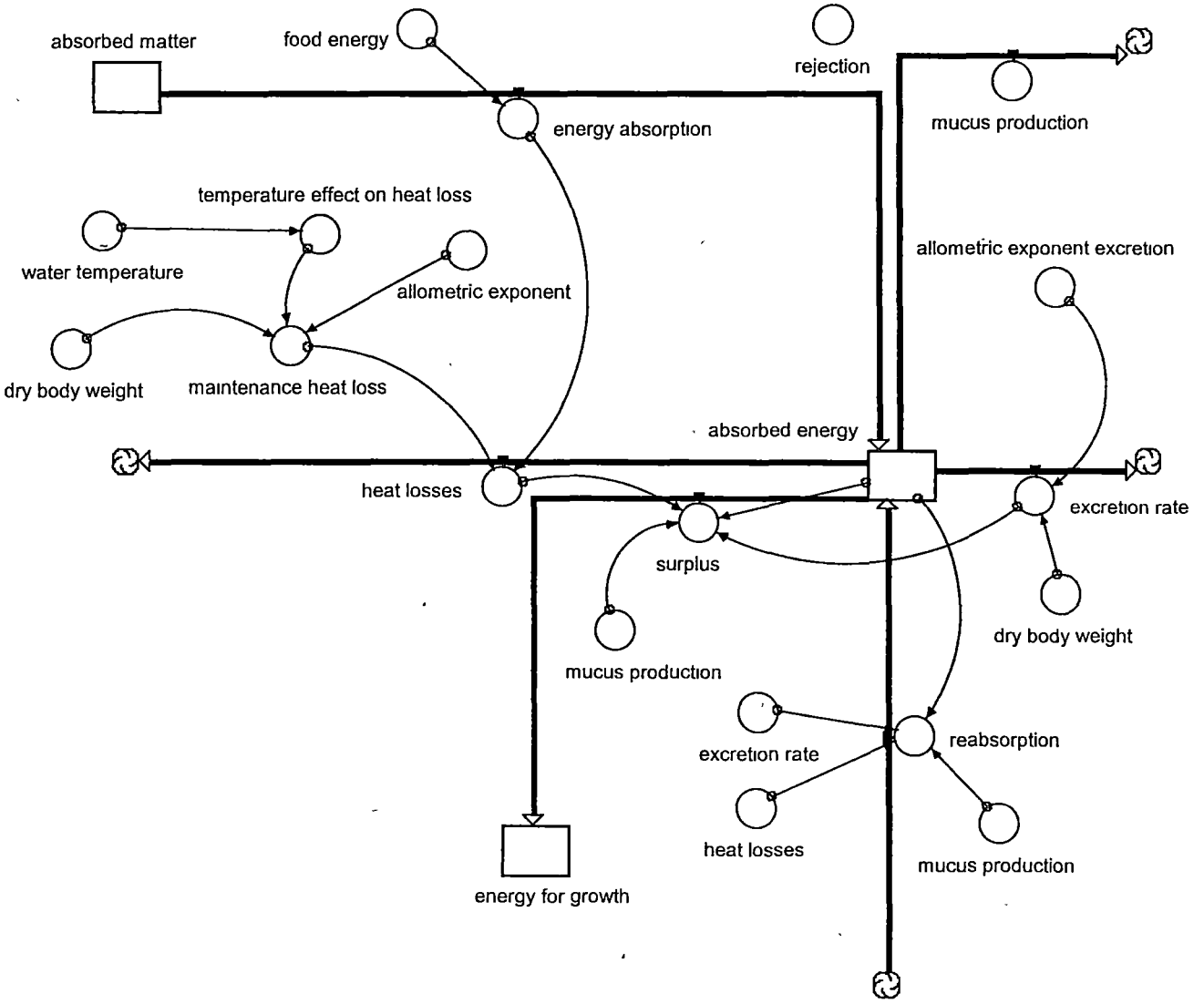

using the conversion 1 mg NH_4-N = 24.87 J (Elliot & Davison, 1975), to obtain Equation 12:

$$\text{Excretion rate (J 0.5-day}^{-1}) = (((24.38 \times \text{dry weight}^{0.73}) \times 0.024) \times 12) \quad \text{(Equation 12)}$$

A correction factor was calculated that described the effect of temperature on heat loss using a standard Q_{10} of 2.1 and water temperature of 23°C, (Equation 13), (Hawkins *et al.*, 2002):

$$\text{Temperature effect} = \exp(0.074 \times T) \div \exp(0.074 \times 23) \quad \text{(Equation 13)}$$

The amount of mucus production was directly related to rejection rate (Urrutia *et al.*, 2001). In the absence of information about energy loss due to mucus production in bivalves we assumed this loss to be proportional to pseudofaeces production and used 0.1 × rejection rate (J 0.5-day^{-1}) (Urrutia *et al.*, 2001). Surplus energy for growth was calculated as the difference between energy absorbed and energy used for maintenance metabolism (i.e. heat loss, excretion, and mucus production).

Mucus production, excretion, and heat loss equations were derived from other studies, (Urrutia et al., 2001; van Erkon Schurink & Griffiths 1992; Hawkins et al., 1989)

based on empiric measurements with *Perna perna* and other bivalves, and they were not verified in this study. This information was available in the separate papers listed above and it has never integrated with other components of bivalve physiology, like food uptake and assimilation, to produce an energy budget model applied to a time series of food quantity and quality. By applying physiological information available in the literature in a predictive integrated model it is now possible to predict the physiological responses of *Perna perna* to a range of environmental conditions.

4.3.7. Data acquisition for the growth sector

Mussel shell and soft tissue growth were measured monthly over 7 months using mussels grown using suspended culture methods. These measurements were obtained from mussel growth measurements in a population dynamics study where 24 1-m ropes were seeded with 200 mussels (3.5 - 4.5 cm shell length). Each month 12 mussels from the ropes were randomly sampled, externally cleaned, and shell length and whole live weight measured and shell and soft tissues separated. For six of these mussels the somatic and reproductive tissues were separated. Soft tissues and shell were dried for 48 hours at 60 °C and weighed to the nearest mg. Using the dry weight the condition index (CI) was calculated (Equation 14):

$$CI = (\text{dry soft tissue weight (g)} \times 1000) \div \text{internal shell cavity (g)} \quad \text{(Equation 14)}$$

where internal shell cavity is the difference between dry shell weight (g) and whole live weight (g) (Crosby & Gale, 1990).

4.3.8. Modelling the growth sector

In the growth sector (Fig. 4.6, Table 4.4) energy allocation for organic shell, soft tissues, and byssus was calculated from the increase in soft tissue dry weight and organic shell weight, multiplied by the calorific content of *Perna perna* tissues (Berry, 1978;

Table 4.5). Byssus production was estimated using Equation 15 (Berry, 1978), relating acid treated dry byssus weight to shell length in *P. perna* in the size range 2 – 11 cm:

Byssus weight (g) = $7.22 \times 10^{-4} \times$ shell length (cm) $^{3.06}$ ($n = 660$, $r^2 = 0.93$) (Equation 15)

Figure 4.6. Growth sector showing the flow of surplus energy to organic shell, byssus, soft tissues, somatic, and gonad tissues in *Perna perna*. Refer to Table 4.4 for equations.

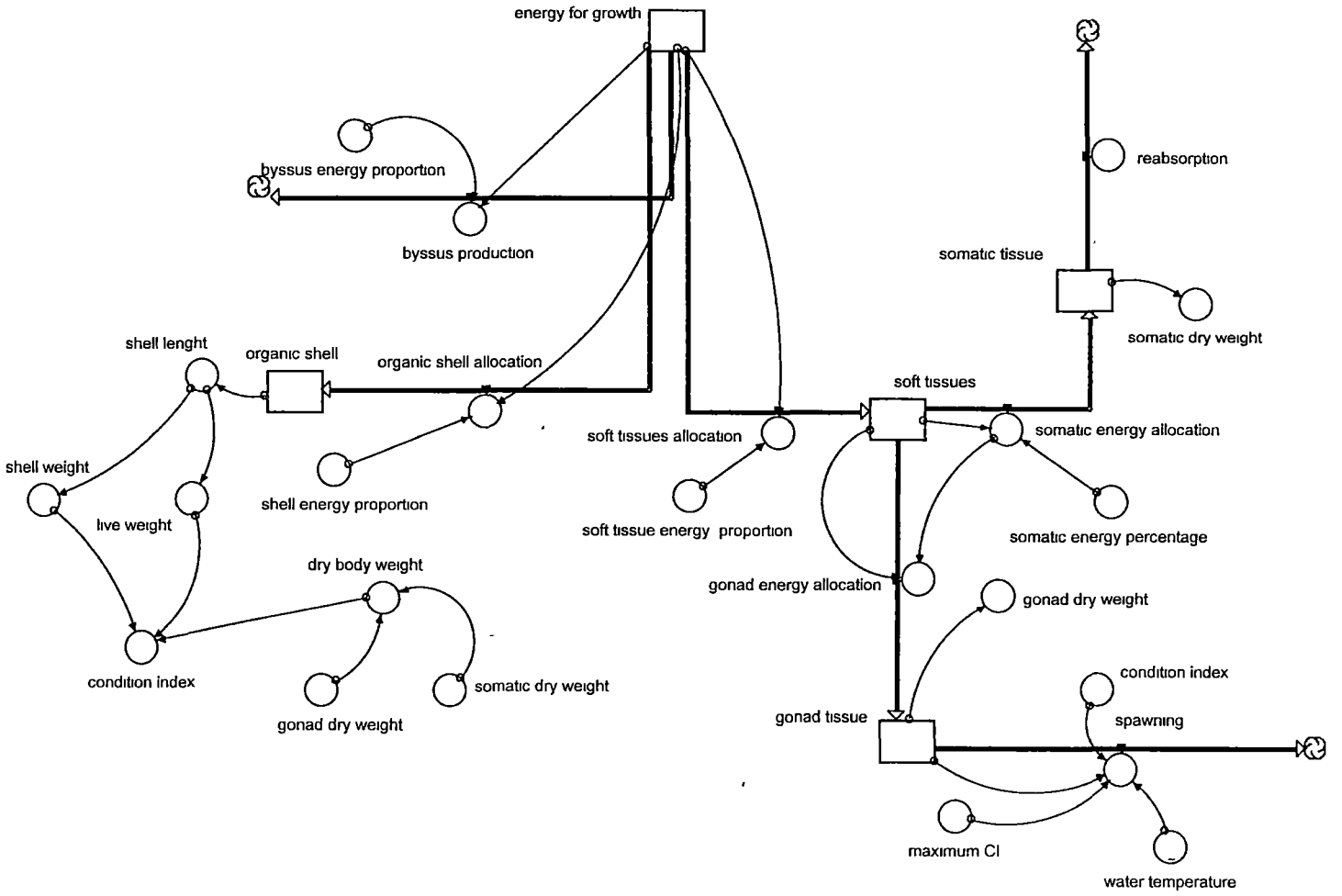

Table 4.4. Forcing variables, functions, parameters and outputs of the growth sector from the ecophysiological model developed for *Perna perna*.

Growth sector

Forcing functions

Water temperature = (time-series) (°C) (from the Seston sector}

State variables and associated derivations

Initial organic shell = 4643 (J)

Organic shell (t) = organic shell (t - dt) + (organic shell allocation) × dt (J)

Organic shell allocation = energy for growth ×shell energy percentage allocation (J 0.5-day^{-1})

Initial soft tissues = 21415 (J)

Soft tissues (t) = soft tissues (t - dt) + (soft tissues allocation – somatic energy allocation – gonad energy allocation) × dt (J)

Soft tissues allocation = energy for growth × soft tissue percentage energy allocation (J 0.5-day^{-1})

Gonad tissue (t) = Gonad tissue (t - dt) + (gonad energy allocation - spawning) × dt

Initial somatic tissue = 15961 (J)

Somatic tissue (t) = somatic tissue (t - dt) + (somatic energy allocation - reabsorption) × dt

Somatic energy allocation = soft tissues × somatic energy percentage (J 0.5-day^{-1})

Initial gonad tissue = 5454 (J)

Spawning = if (condition index > = maximum condition index) and (water

temperature > 22) then (gonad tissue × 0.9) else (0) (J 0.5-day^{-1})

Gonad energy allocation = soft tissues - somatic energy allocation (J 0.5-day^{-1})

Byssus production = energy for growth × byssus percentage energy allocation (J 0.5-day^{-1})

Functions and parameters

Byssus percentage energy allocation = 0.02 (fraction)

Shell percentage energy allocation = 0.27 (fraction)

Soft tissues percentage energy allocation = 0.7 (fraction)

Somatic percentage energy allocation = 0.8 (fraction)

Condition index = (1000 × dry body weight) ÷ (live weight - shell weight)

Maximum CI = 120

Model outputs

Shell length = 8.41+ 2.28 × log N (organic shell ÷ 18997) (cm)

Shell weight = exp (0.34 × shell length) (g)

Live weight = exp (0.44 × shell length) (g)

Gonad dry weight = gonad tissue energy ÷ 21774 (g)

Somatic dry weight = somatic tissue ÷ 17336 (g)

Dry body weight = gonad dry weight + somatic dry weight (g)

Somatic and gonadal tissue energy allocation was estimated from the relationship between the energy content of the respective tissues and the total energy of total soft tissue.

4.3.9. Reabsorption

Reabsorption is the mobilization of metabolic reserves when insufficient absorbed energy is available for heat loss, excretion, and mucus production (Bayne & Newel, 1983; Scholten & Smaal, 1999). A function was inserted into the model that controlled reabsorption of somatic tissue in conditions of low energy intake (Equation 16).

Reabsorption (J 0.5-day^{-1}) = if ((excretion rate + heat losses) > absorbed energy) then ((excretion rate + heat losses)-absorbed energy) else (0) (Equation 16)

4.3.10. Condition index and spawning

In our model a simple function involving maximum condition index and water temperature was used to trigger a spawning event (Scholten & Smaal, 1999). In this function at the maximum condition index (120) and at water temperature > 22 °C (Velez

& Epifanio, 1981) spawning resulted in loss of gonad tissue, otherwise no loss occurred (Equation 17)

Spawning (J 0.5-day^{-1}) = if (condition index > = maximum CI) and (water temperature > 22) then (gonad tissue) else (0) (Equation 17)

4.3.11. Effect of mussel size

The model included feedback-reinforcing loops between mussel dry body weight and functions in the feeding and energy balance sectors. In the feeding sector, filtration and rejection rates were corrected to mussel size by standardizing these rates for an equivalent mussel of 1 g dry soft tissue weight using the formula $Y_s = (W_s/W_p)^b \times Y_p$, where Y_s is the standardized parameter, W_s is the standard weight (1 g), W_p is the weight of dry soft tissue predicted by the model, Y_p is the uncorrected parameter, and b is the allometric exponent. An exponent of 0.62 was used for filtration and rejection rates (Hawkins *et al.*, 2001). Another feedback loop between growth and energy balance sectors was used to account for the positive relationships between soft tissue dry weight and each of heat loss and excretion rates, using the allometric equations presented in section 2.4.

4.3.12. Sensitivity analysis

To determine the sensitivity of the model to changes in the forcing variables and main parameters we ran the model three times. Each time the forcing variables or main parameters values were changed by ± 10% from the parameter values generated by the model. The average percentage change in the model outputs i.e. shell length, live weight, dry soft tissue weight, somatic and gonad weight produced from these changes were used as a measure the sensitivity of the model.

4.4. Results

4.4.1. The seston sector

Phytoplankton blooms between days 120 – 150 and 180 – 200 were responsible for the variability in the time-series of TPM, POM and POC (Fig. 4.7). Water temperature ranged from 17 °C at the beginning of winter (day 190) to 29 °C in the middle of summer (day 50) (Fig. 4.7). Estimated energy content of food (J mg^{-1}) varied between 2 - 82 J mg^{-1}, while phytoplankton energy content was in the range 1.2 - 25 J mg^{-1}.

4.4.2. The feeding sector

Rates of filtration, rejection, ingestion, and absorption all varied positively with TPM (Fig. 4.8A and 4.8B). Ingestion and absorption rates were not strongly affected by variation in TPM because of the food selection efficiency of mussels (Chapter 1). Filtration rates ranged between 47 - 936 mg 0.5-day^{-1}, and rejection rates between 0 - 748 mg 0.5-day^{-1}, representing up to 75% of filtered matter. Ingestion rate ranged between 7 - 188 mg 0.5-day^{-1} and absorption rate ranged between 0.5 - 101 mg 0.5-day^{-1} with the model predicting values between 3 - 40 mg 0.5-day^{-1} for most of the observed periods. Organic content of ingested matter (OCI) varied negatively with organic content of seston (OCS) (Fig. 4.8C).

Fig. 4.7. Seston variables CHL (μg l^{-1}), TPM (mg l^{-1}), POM (mg l^{-1}), and water temperature (°C) in Brito Cove and the moving average used to obtain daily values that were used as forcing variables in the ecophysiological model. Arrows indicate times of algae blooms.

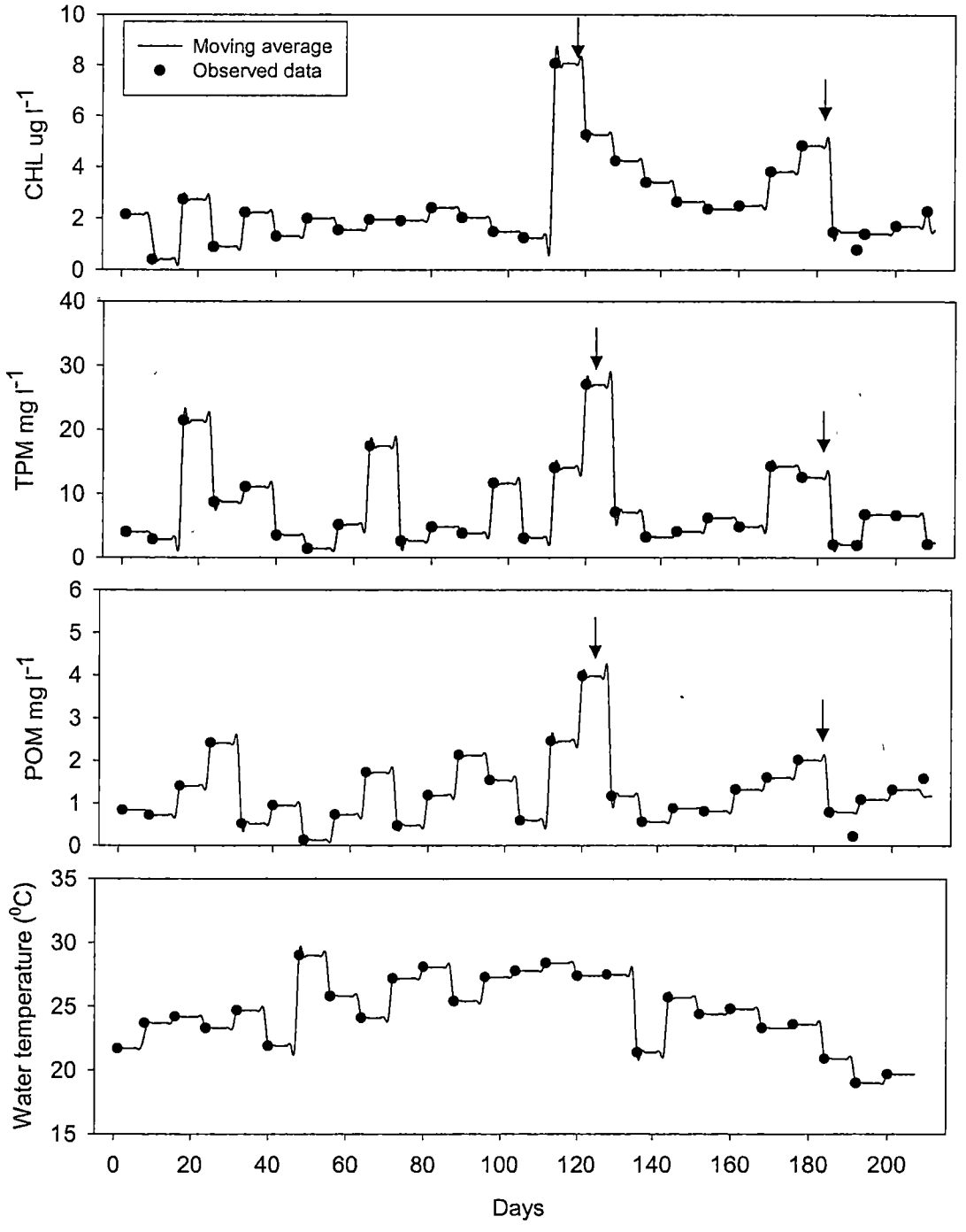

Fig. 4.8. Model predictions for the feeding sector. (A) filtration rate (FR, mg 0.5-day^{-1}), rejection rate (RR, mg 0.5-day^{-1}), and total particulate matter (TPM, mg l^{-1}); (B) ingestion rate (IR, mg 0.5-day^{-1}), absorption rate (AR, mg 0.5-day^{-1}) and TPM; and (C) organic content of seston (OCS, fraction), and organic content of ingested matter (OCI, fraction).

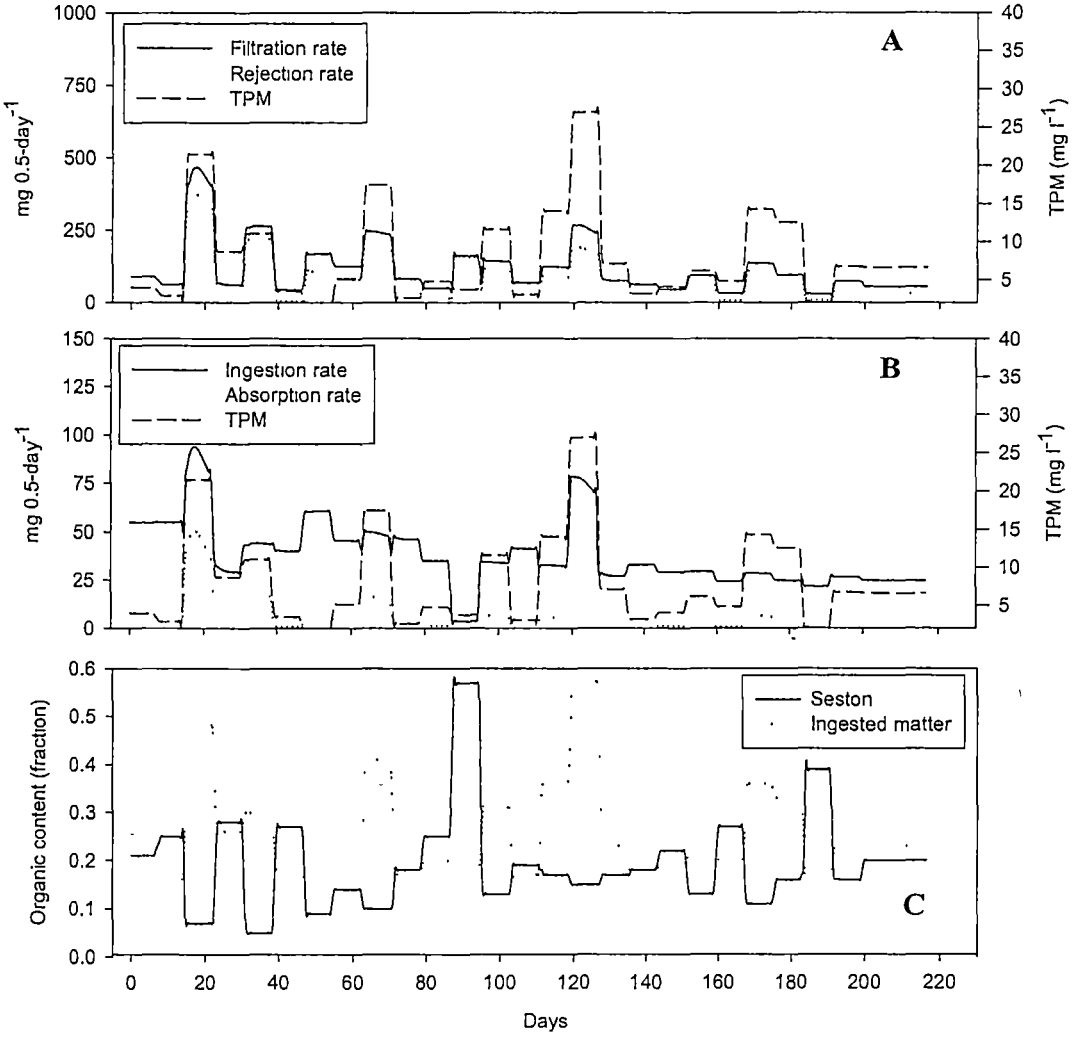

4.4.3. The energy balance sector

Predicted energy absorption (3.5 - 2004 J 0.5-day^{-1}) followed the oscillation in food energy (Fig. 4.9A). Heat losses and excretion rates ranged from 0-100 and from 6-17 J 0.5-day^{-1} respectively (Fig. 4.9B and 4.9C). The amount of energy lost due to mucus production was intermediate between energy loss associated with heat loss and excretion rates, with a maximum of 75 J 0.5-day^{-1} (Fig 4.9D). Maximum surplus energy for growth was 1608 J 0.5-day^{-1}. Reabsorption rates of 0 - 25 J 0.5-day^{-1} occurred a number of time during the study when filtration rates and food energy were smallest (Fig. 4.9E). The model predicted maximum values of energy absorption and energy surplus for growth during the largest algae bloom recorded during the study, with secondary peaks associated with high levels of detritus energy (Fig. 4.9A and 4.9E).

4.4.4. The growth sector

Energy increases in shell, byssus, and soft tissues were estimated at c. 0.27, 0.02, and 0.70 % of energy allocated for growth respectively, derived from linear equations (Fig. 4.10A). The relationship between soft tissue energy content and somatic and gonadal tissues energy content was c. 0.8 and 0.2 % of energy allocated for soft tissue growth respectively (Fig. 4.10B).

Fig. 4.9. Model predictions for the energy balance sector. (A) energy absorption (J 0.5-day^{-1}), (B) heat loss (J 0.5-day^{-1}), (C) excretion rate (J 0.5-day^{-1}), (D) mucus production (J 0.5-day^{-1}), and (E) energy surplus for growth and energy reabsorption from somatic tissue (J 0.5-day^{-1}).

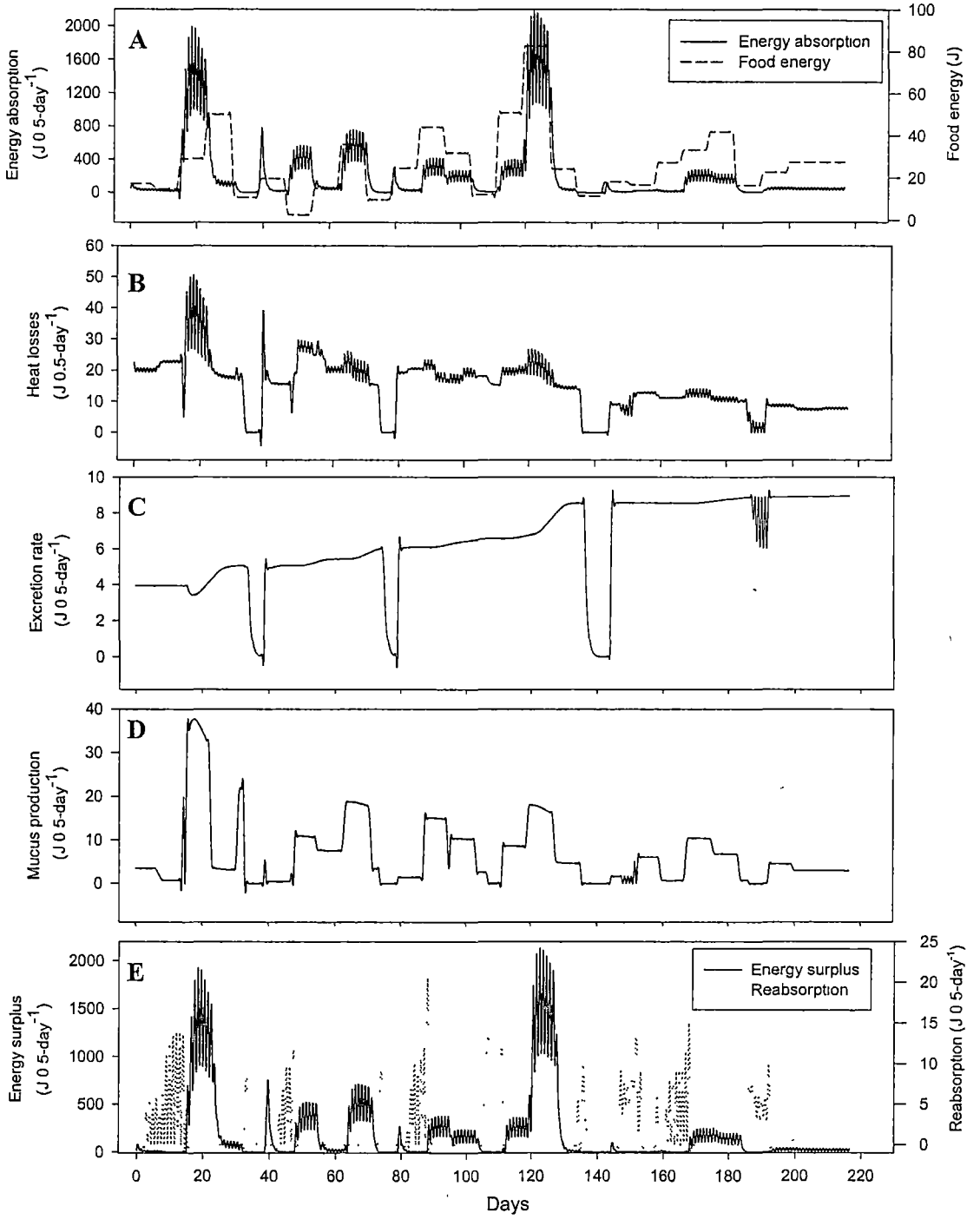

Fig. 4.10. Energy surplus for growth partitioned into (A) total dry soft tissue, organic shell, and byssus and (B) allocation of energy for somatic and gonad tissues from the energy allocated to total soft tissues Data measured from mussels 5-10 cm shell length.

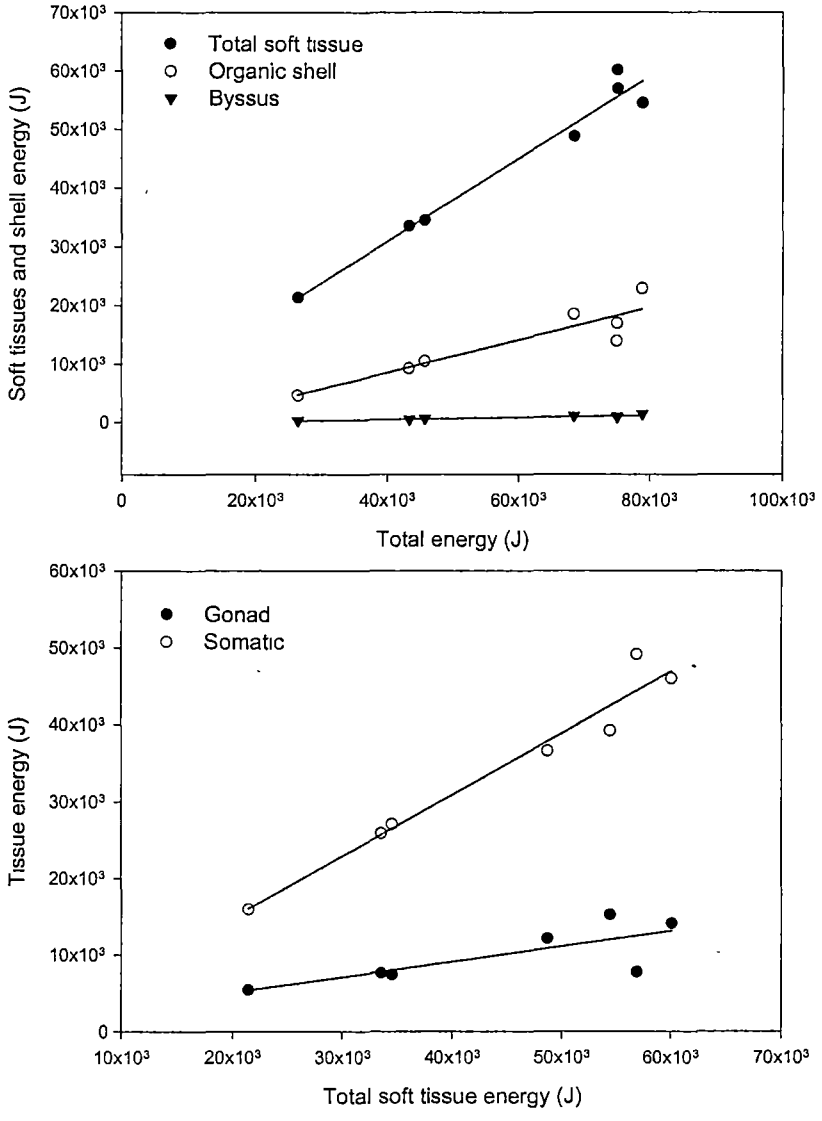

Predicted values of shell length, live weight, and shell weight were obtained from organic shell weight (Fig. 4.11A) and shell length (Fig. 4.11B and 4.11C), based on shell measurements in Brito Cove to obtain the equations on Table 4.6. The weight of organic shell, byssus, somatic, and gonad tissues were calculated by dividing the energy allocated to these state variables by their energy content (Table 4.5). Total dry body weight was calculated by summing somatic and gonad weight, and predicted condition index was calculated using Equation 1. The model was able to predict values of somatic dry weight, total dry weigh, live weight, and shell length that were comparable to the values obtained in the study (Fig. 4.12). However the model failed to produce gonad weights that matched the real data (Fig. 4.12).

4.4.5. Sensitivity analysis

The model was sensitive to changes in the both forcing functions and parameters (Table 4.7). TPM was the forcing function that appeared to be the most sensitive, causing 3-26% changes in the model outputs. POM and chlorophyll a were the second most important inputs of the model, leading to changes of 0 - 11% and 0 - 4% respectively in the model outputs.

The parameters the model was most sensitive to was the percentage energy allocated to shell and soft tissue, particularly in predictions of gonad tissue dry weight

Table 4.5. Calorific content of *Perna perna* somatic tissue, gonad tissue and organic shell. Reproduced from Table 6 in Berry (1978).

	Mean energy content (J g^{-1})	Range (J g^{-1})	Coefficient of variation (%)
Flesh	20277	17336 - 23205	9.57
Gametes	21774	20116 - 23675	8.80
Organic shell	18997	18997 - 19762	3.51
Byssus	19679	19217 - 20286	2.79

Table 4.6. *Perna perna*. Equations from the relationships plotted on Fig. 4.12A and 4.12B, used to calculate shell length (cm), live weight (g), and shell weight (g) from organic shell weight (mg).

Equation	Statistics
Shell length = 8.41+2.28 × log N (organic shell weight)	r^2= 0.89, df 1,81, F = 714.90, P<0.001
Live weight = exp (0.44 × shell length)	r^2= 0.90, df 1,46, F = 465.49, P<0.001
Shell weight = exp (0.33 × shell length)	r^2= 0.89, df1, 46, F = 399.67, P<0.001

Table 4.7. Model sensitivity analyses, calculated as the average percentage change in the model outputs resulting from adjustments of ± 10% in the forcing functions and main parameters (refer to Methods).

Model forcing functions	Original value	Average percentage change in model output to ±10 % adjustments				
		Shell length	Whole live weight	Soft body dry weight	Somatic tissue dry weight	Gonad tissue dry weight
Total Particulate Matter (TPM)	3.7 mg L^{-1}	10	11	3	10	26
Chlorophyll a	7.8 μg L^{-1}	1	2	0	2	4
Particulate Organic Matter (POM)	1.3 mg L^{-1}	2	2	0	2	11
Water temperature	24.5 °C	0	1	0	1	2

Model parameters	Parameter value	Shell length	Whole live weight	Soft body dry weight	Somatic tissue dry weight	Gonad tissue dry weight
Ratio of chlorophyll to carbon	50	1	2	0	2	4
Phytoplankton organic energy content	23.5 J mg^{-1}	1	1	0	1	4
Feeding allometric exponent	0.62	4	4	1	4	11
Heat loss allometric exponent	0.72	0	0	0	0	2
Shell % energy allocation	0.27	2	1	2	7	46
Soft tissues % energy allocated	0.70	3	1	2	9	54

Fig. 4.11. Relationships between (A) organic shell weight (g) and shell length (cm), (B) shell length and shell weight (g), and (C) shell length and live weight (g).

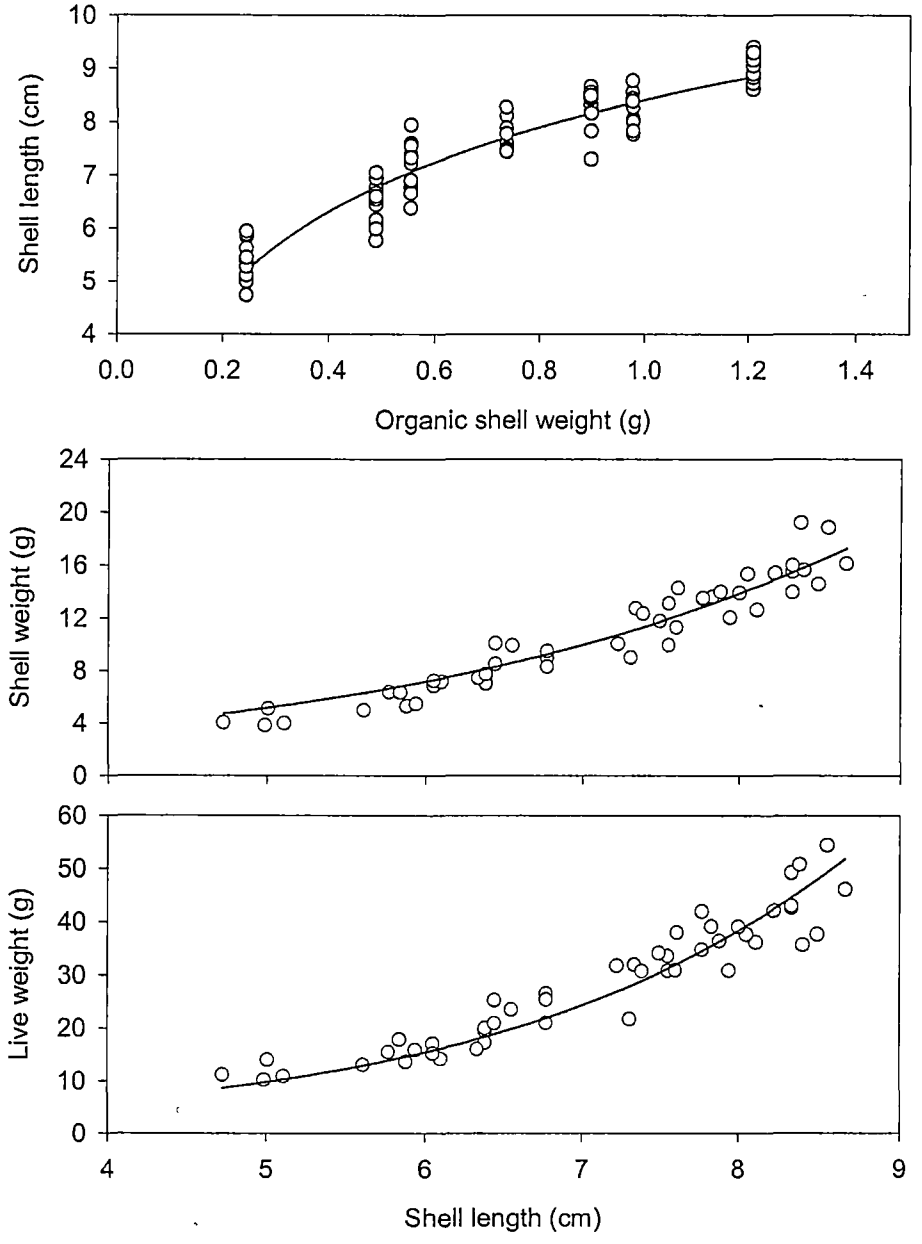

Fig. 4.12. Model predictions of gonad tissue weight, somatic tissue weight, total dry tissue weight, shell length and live weight (—), together with observed data of mussel growth in Brito Cove (•). Graphs on the right are scatterplots of observed against predicted values, with 95% confidence limits on the slope of the plot. If the confidence limits encompass one, then this was evidence that the model provided a close fit of the observed values

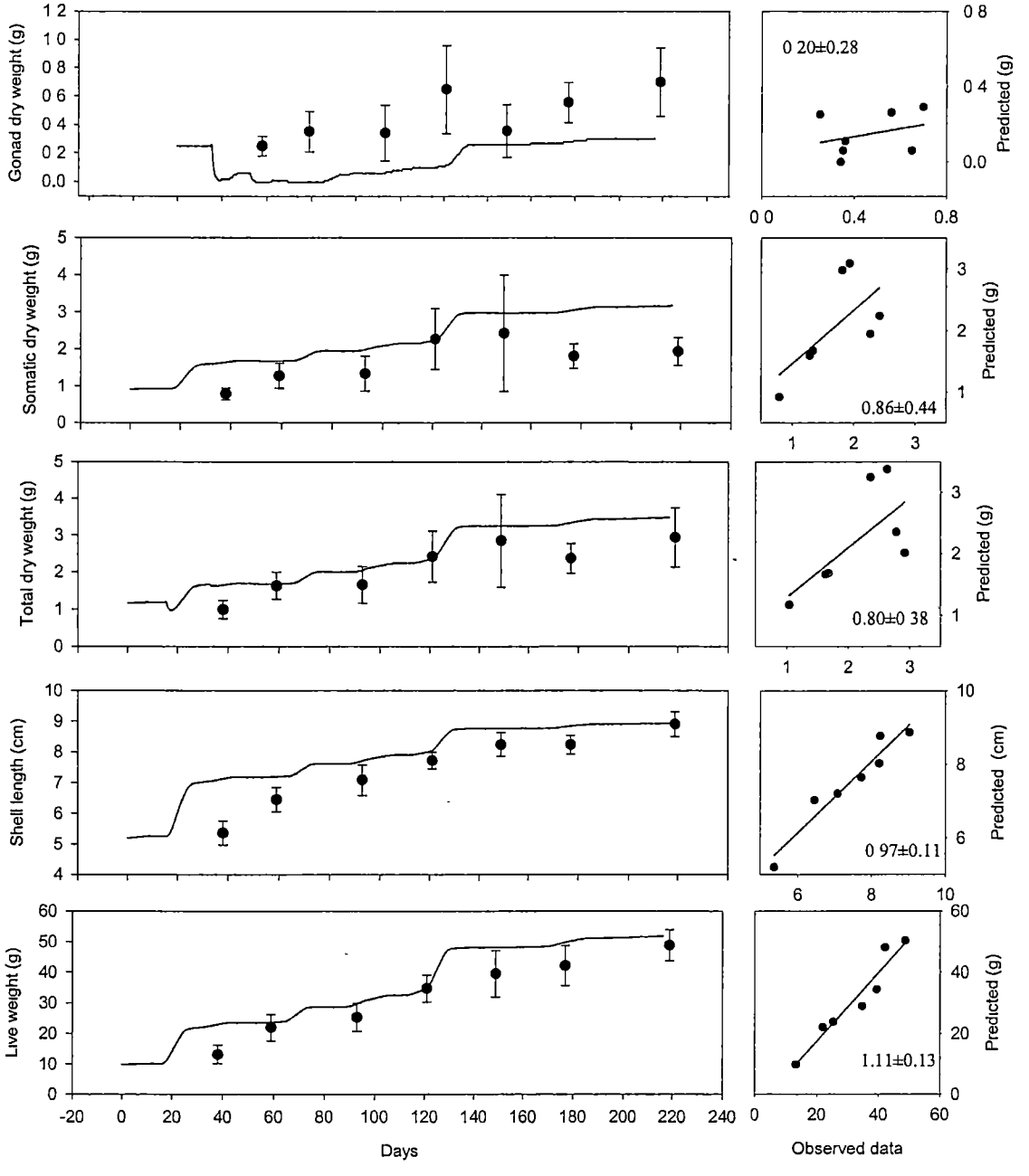

(46% and 54% respectively). The feeding allometric exponent also provided changes in the range of 1 - 11 % (Table 4.7). Variations in the ratio of chlorophyll to carbon, and in the energy content of phytoplankton organic matter caused a maximum change of 4% in the outputs, observed in predictions of gonad dry weight. The model was not sensitive to variations in the heat loss allometric coefficient at a level of 10% change.

4.5. Discussion

The model produced was successfully able to predict the average size shell and body tissues of cultured mussels in Brito Cove through time. We wanted to maintain a low level of complexity in the model structure, but include the full range of physiological compensations available to bivalve mollusks to optimize energy acquisition in spite of fluctuations in seston quantity and quality. The use of food and the incorporation of energy into bivalve tissue involved several steps all of which were simplified. As a result our model did not include detailed aspects of mussel physiology, like absorption efficiency as a function of gut residence time, protein recycling, and protein turnover rates. Although these simplifications may violate some biological features it was necessary to assist in the building and application of the model (Pouvreau *et al.*, 2000). Furthermore, gaps in our knowledge about mussel ecophysiology hindered building a model with all the physiological steps between food acquisition and growth. In particular, little is known about the allocation of energy to different body compartments and mucus production, and the physiological controls of gametogenesis and spawning (Scholten & Smaal, 1998). Nevertheless, keeping the model simple is important if the

final purpose is to apply physiological and growth rate predictions to environmental studies of carrying capacity, where the number of variables and complexity will be significantly increased. Furthermore, as the model becomes over-parameterized it becomes harder to perform calibrations, sensitivity analysis, and detect important forcing variables and feedback loops in the model structure (Scholten & Smaal, 1998, 1999).

The development of this model made use of the STELLA® software concept of mass/energy conservation, instead of using only parameters and mathematical formulas. An exception was the seston sector had no flows or state variables and as a result all calculations were based on parameters. Estimating food energy content based on POM data was problematic because of the complexity of organic suspended particles in the water (Grant & Bacher, 1998). However the close agreement between predicted and observed shell length suggested that our estimate of food energy content based on POM was probably a realistic estimate of energy content of seston. Detritus energy comprised 20-90% of the total energy content of seston in the *Clamys farreri* model of Hawkins *et al.* (2002), a value similar to our model predictions (14–95%). Given that detritus comprises up to 94% of the diet of mussels (Berry & Schleyer, 1983) it is likely that *Perna perna* is predominantly a detritivore. Therefore, characterizing suspended food, particularly the detrital portion, is important. A disadvantage of calculating organic content of seston (OCS) by assuming an inverse relationship with TPM was that when TPM was high, due to algae blooms, unrealistically low values of OCS were obtained. Despite this, the organic content of ingested matter increased with increasing chlorophyll because of the positive effect of the blooms on POM. The high organic content of

ingested matter when the organic content of seston was low suggests that sorting between organic poor and rich particles was occurring under these conditions.

In the feeding sector, basic relationships reported as being general patterns in the feeding behavior of bivalves were included (Hawkins *et al.*, 1998b). The application of the feeding model enabled further validation of the set of equations describing the feeding physiology of *Perna perna* using a time series of forcing variables. This allowed a description of the responses in the feeding sector through time, rather than static values reported in Chapter 2. As the feeding model was developed on values of *P. perna* feeding on natural seston, the feeding rates reported should be realistic and accurately describe the response of mussels to varying food quantity and quality. The filtration and rejection rates covaried in such a way as to maintain ingestion rates relatively constant and independent of fluctuations in food availability. Filtration rates above the point that production of pseudofaeces occurred did not limited ingestion rate to a maximum as previously reported (Griffiths & Griffiths, 1987; Widdows *et al.*, 1979), but it further increased substantially during the algae bloom. The series of equations describing and quantifying suspension-feeding behavior in *P. perna* successfully reproduced the enrichment of ingested food in relation to the organic content of seston and filtered matter, following a common pattern in bivalve feeding (Bayne, 1998). Sector outputs of pseudofaeces and faeces are important when integrating the ecophysiological model with a population dynamics model (Chapter 3), because it allows the production of biodeposits released during a growing season to be estimated. The importance of sedimentation and

remineralization of biodeposits as a bivalve feedback to the surrounding environment will depend on the residence time of water in them (Doering *et al.*, 1986).

Energy absorption rate predicted by this model is similar to values reported for *Mytilus californianus* (Bayne & Newell, 1983). Suggesting that estimating absorbed energy by multiplying absorbed matter by the estimated energy content of phytoplankton and detritus was successful. However, one of the most difficult issues to deal with when modelling energy gains is the relationship between temporal variation in food supply, ingestion rates, and ultimately growth rates (Grant, 1996). The prediction of energy acquisition, expenditure, and resultant scope for growth did predict the amount of surplus energy with reasonable precision based on the agreement between predicted and observed growth of shell and dry body weight. Indeed, the scope for growth predicted by the model is similar to previous calculations for *Perna perna* (252–1224 J 0.5-day^{-1}) (van Erkon Schurink & Griffiths, 1992). Ammonia excretion contributed c. 5-10% of energy losses as previously reported for *Mytilus edulis* (Bayne & Newell, 1983), and respiration rate was positively associated with temperature and feeding activity as reported in many studies of bivalve physiology (Bayne & Newell, 1983).

Reabsorption of nutrient reserves from tissues to accommodate periods of low energy does occur in a number of bivalves (Hawkins *et al.*, 1985; Bayne & Newell, 1983) and is included in mussel physiological models (Scholten & Small, 1998; 1999). This physiological response is used in conditions of food limitation. Periods of high temperatures associated with low TPM, as observed in this study, represent a severe

physiological stress in mussels (Gabbott & Bayne, 1973), and will force them to use energy reserves. Our model predicted a linear rate of net energy deposition in tissues in relation to the rate of energy acquisition and resultant scope for growth as seen for *Mytilus edulis* by Hawkins & Bayne (1991).

Parameter values produced by this model are only suitable for the site from which the data were collected. Applying this model to other sites will require estimates of seston energy content and energy partitioning among tissues, shell, and byssus. When this model was applied to another site in Brazil, with lower TPM and POM values, the model failed to reproduce the observed growth of mussels. Suggesting that it is necessary to accurately characterize available seston energy and mussel energy acquisition and balance under conditions of lower food availability. This model was the first to model the physiology of *Perna perna* under conditions of varying food and temperature and refinement will occur as the physiology of this species is elucidated, particularly processes controlling gametogenesis and spawning.

Chapter 5

Modelling ecophysiological feedbacks between mussel *Perna perna* populations and the ecosystem: a preliminary investigation of carrying capacity for bivalve aquaculture in Santa Catarina, Brazil.

5.1. Abstract

In this chapter, information previously provided about mussel population dynamics and ecophysiology were integrated in a population level ecophysiological model. This enabled the quantification of important relationships between mussel population and the environment such as rates of filtration, excretion, and biodeposition. Measurements of bay area and volume, associated with oceanographic measurements, enabled the calculation of water residence time inside the bay and the time required by the mussel population to filter a volume of water relative to the volume of the bay. In periods without seed attachment, the average population clearance rate was much lower than estimates derived by summing the different clearance rates observed in each size class. Collection of long time-series of selected seston parameters did not revealed strong seasonal patterns in primary production and particulate matter in the water column. Instead, particulate matter in this shallow system appears to be mainly influenced by resuspension caused by wind and current action. An attempt to apply the model in a carrying capacity analysis was partially hampered by the lack of information about other steps in the nitrogen cycle. Important aspects to be investigated in Brito Cove are rates of sediment remineralization, other natural and anthropogenic fluxes of nitrogen, and zooplankton grazing on phytoplankton.

5.2. Introduction

Mussel farming in Southern Brazil is a fast growing industry with production increasing by more than 6000% in the last ten years. As sessile organisms, mussels are dependent on the availability of food brought by wind or current, which is generated by local primary production or by resuspension of detritus and benthic algae from the bottom (Sobral & Widdows, 2000). Filter feeders play a major role in estuarine and coastal ecosystems because they remove large quantities of suspended material from the water column, excrete abundant amounts of reactive nutrients, and enhance the vertical particle flux as they reject non-ingested material as phytodetritus (Dame, 1993; Proença & Schettini, 1998). High density mussel farming and poor food replenishment can reduce growth rates of mussels and increase the time taken to reach marketable size. Sites under these extreme conditions are said to have reached their exploitation carrying capacity (Smaal *et al.*, 1998).

Local authorities and aquaculture decision makers need to the right tools to evaluate the exploitation carrying capacity of bivalve shellfish farms to avoid economic and, in more extreme cases, environmental losses (Dankers, 1993). At a local scale carrying capacity depends on physical constrains such as substrate, shelter, and food supply by tidal currents. Therefore, predictive models of carrying capacity are characterized by details of hydro and geodynamic processes coupled with sub-models of organism and population levels processes (Smaal *et al.*, 1988). To avoid growing

bivalves at densities that result in food depletion models of local environmental patterns involved in organic seston production and transport need to include both tidal and seasonal variation (Fréchette *et al.*, 1991). Data at both these temporal scales can be used to generate a model that predicts food availability under different mussel stocking rates through out the growing period.

Most of the available information about seston dynamics is for temperate mussel farms, consequently, most bivalve carrying capacity studies have been developed for temperate latitudes (e.g. Incze *et al.*, 1981; Carver & Mallet, 1990; Brylisnky & Sephton, 1991; Raillard & Ménesguen, 1994; Dowd, 1997), with few examples in tropical latitudes (e.g. Pouvreau *et al.*, 2000). Temperate waters are characterized by spring and summer phytoplankton blooms followed by low food availability in autumn and winter (Smaal & Haas, 1997; Widdows *et al*, 1979). In the semi-tropical waters of Southern Brazil, this pattern is not so obvious and food is available throughout the year (unpublished data). Therefore, carrying capacity models applied to bivalve aquaculture in these environments needs to use patterns of food availability described for semi-tropical environments.

The total biomass supported by a given ecosystem is a function of the water residence time, primary production time, and bivalve clearance time (Dame & Prins 1998). From an economic perspective the exploitation carrying capacity must consider the stock size at which a maximum yield of the marketable cohort is achieved (Smaal *et al.* 1998). It is possible that at high stocking rates maximal yield may occur, but due to low individual growth rates the stock is largely made up of undersized individuals. Sub-models of water

transport, population dynamics, and bivalve physiology are necessary for development of exploitation carrying capacity models (Smaal *et al.*, 1998). Any model or conceptualization of the role of bivalve filtration in coastal waters should account for system water mass residence time, phytoplankton primary production or replacement time, and clearance time by the majority of filtering organisms (Bacher *et al.*, 1998). This chapter aims to integrate models of population dynamic and mussel physiology previously developed for *Perna perna* (Linnaeus, 1758) with preliminary measurements of primary production and water renewal in Brito Cove, a mussel farming area in Southern Brazil. In this chapter, information previously provided about mussel population dynamics and ecophysiology was integrated in a population level ecophysiological model. This will deliver valuable information about seston dynamics on different time scales, primary production, and major feedbacks between the bivalve population and the environment. In this way rates of clearance, biodeposition, and excretion by the culture population can be incorporated in a detailed environmental model of seston dynamic for this location. Additionally, this study provides important site-specific information relating to carrying capacity analysis such as bay clearance, water residence, and phytoplankton turnover time (Dame & Prins, 1998).

5.3. Methods

5.3.1. Site characterization

Brito Cove, (48° 34' W, 27° 46' S) is a small embayment (3.7 km^2) in Southern Brazil where mussels have been intensively cultivated for the last 10 years. It was specifically

selected for this study because local growers are reporting that an increase in stocking density is already reducing mussel growth rates (industry, personal communication). The cove is at the south part of Florianópolis Bay, which is characterized by two interconnected basins separated by a narrow passage, with each basin having its own opening to the ocean (Fig. 5.1). The southern part of the bay has an average depth of 3.5 m and a non-uniform bathymetry with a number of channels and shoals and is linked to the ocean through a very narrow entrance. Inside Brito Cove there are four farm leases shared by 44 mussel growers.

The mussel standing stock inside Brito Cove was estimated from the dimensions of the four leases and the number of long lines in each lease. The length of mussel culture ropes, the distances between the mussel culture ropes, and the distances between long lines were also measured. The coordinates of the shoreline, vortices of the mussel farm leases, and position of oceanographic instruments were determined using GPS with 20 m precision. Additionally, a bathymetric profile of the whole cove, to calculate its volume and surface area, was obtained using an echosounder.

5.3.2. Seston characterization

Water samples (2 L) were taken next to the long-lines inside lease B (Fig. 5.2) from near surface and bottom waters, stored on ice, and taken to the laboratory within 2 hours of collection. Seston parameters measured included turbidity (TURB, NTU), total

particulate matter (TPM, mg L^{-1}), particulate organic and inorganic matter (POM and PIM respectively, mg L^{-1}), organic content of seston calculated as OCS (POM/TPM,

Figure 5.1. Location and bathymetry of Florianópolis Bay, Brazil. Brito Cove is the area indicated by the black circle.

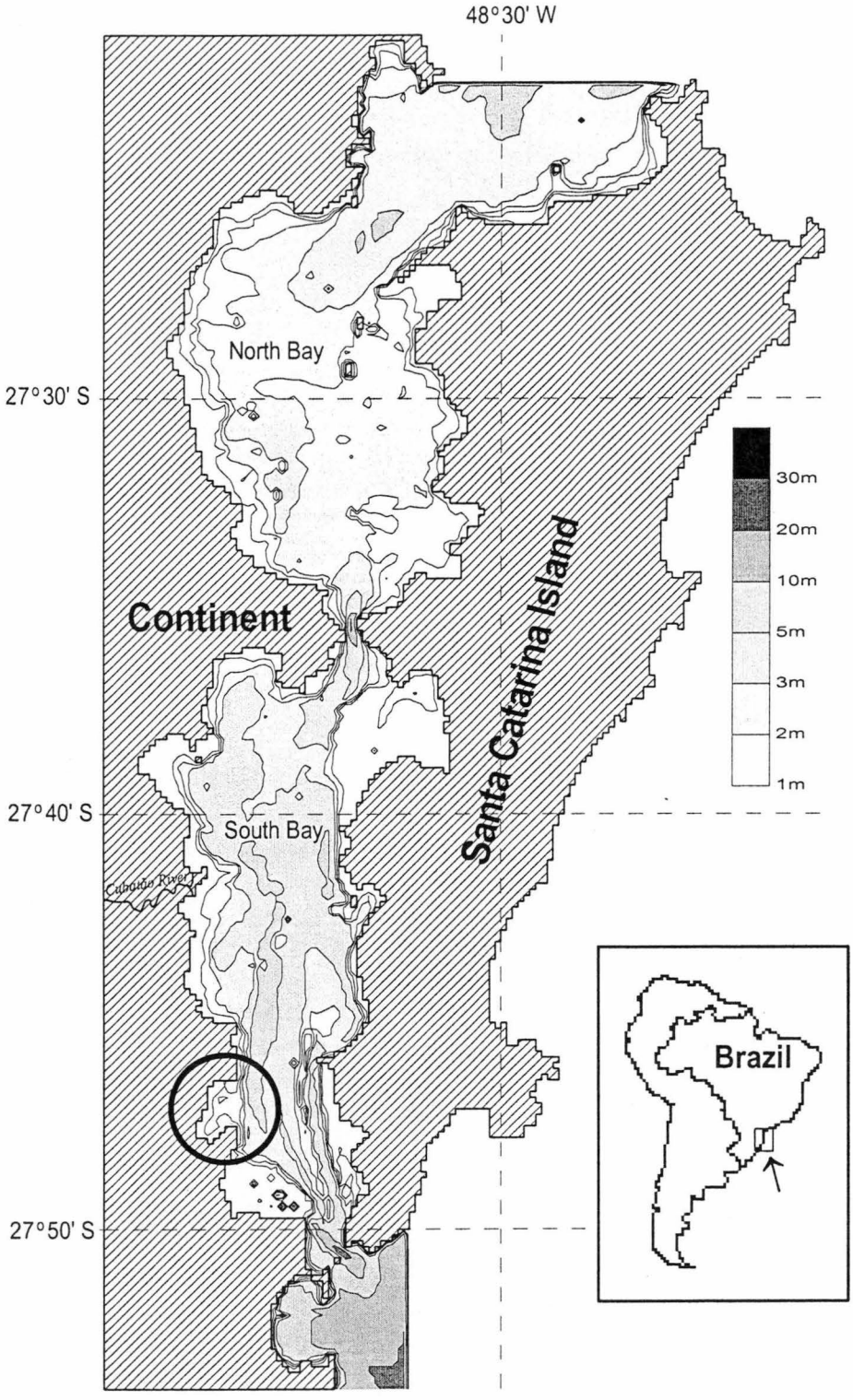

fraction), and chlorophyll-a (CHL, μg L^{-1}). Triplicate aliquots of water samples (50 and 200 ml) were filtered through pre-ashed and weighed Whatman GF/C filters (25 mm). These were rinsed with 15 mL distilled water to remove salts and dried at 60°C before re-weighing and calculation of the total sample dry weight per sample. Each sample was ashed at 450°C for 4 h prior to final weighing, allowing calculation of both ash (inorganic) and ash-free (organic) mass of each filtered sample. Chlorophyll-a was determined from triplicate 100 mL aliquot water samples filtered through Whatman GF/C filters (25 mm), then fixed with potassium chlorite and analyzed using a Turner Designs AU-10 fluorometer.

Seston sampling was carried out at three temporal scales; two hourly, weekly, and fortnightly, allowing the identification of seasonal and tidal influences on seston variables important for bivalve physiology and growth. Fortnightly measurements of both surface and near bottom waters inside lease B (Fig. 5.2) were taken from September 1998 to August 2002. Weekly measurements were taken from September 2000 until August 2002, on the first long-line (outside) furthest from shore and on the last long-line closest to the shore (inside), both inside lease B (Fig 5.2). The distance between the two stations was ca. 200 m and depth was 2 and 1.2 m respectively. Additionally, water temperature and salinity were measured at each sampling station. Incident solar radiation data was obtained from the local meteorological station.

To evaluate tidal influence on seston, TPM, POM, and CHL were measured at lease B every 2 hours for 24 hours on two occasions, during a spring (June 6, 2001) and a

Fig. 5.2. (A) Position of the four mussel farm leases inside Brito Cove. The white triangle indicates the position of the water level recorder, current meter, and outside sampling station. The black triangle indicates the inside sampling station. (B) Three dimensional plot of Brito Cove used to calculate the volume of the cove. Axes are coordinates in UTM.

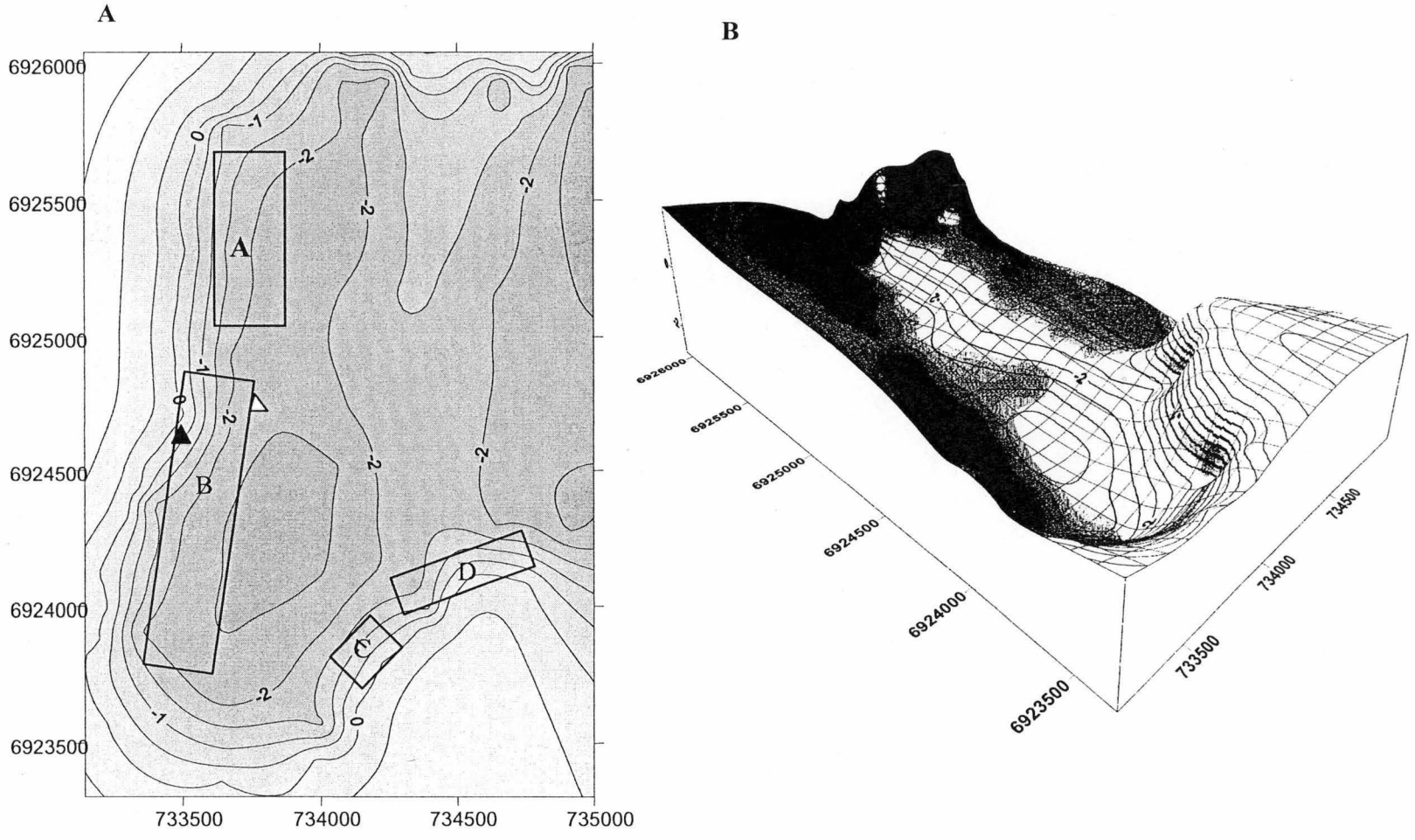

neap tide (July 12, 2001). Every 30 minutes over each 24 h period wind velocity was recorded with a portable anemometer (Simerl Instruments), water current velocity and direction recorded using a mini current meter (Sensordata SD-6000), and tidal height was recorded using a water level recorder (Aanderaa Instruments WLR-7). Additional oceanographic data in the same site was also collected over longer periods in 2001, from June 5 to July 13 (tide level), and from October 8 to October 23 (tide level and current speed).

5.3.3. Primary production measurements

Primary production was estimated using the incubation method using a high dilution technique adapted from Gallegos & Vant (1996). High dilution was necessary to exclude zooplankton grazing during the incubation period and was achieved by diluting 2.4 L of seawater (screened through 230 μm) in 40 L of filtered (1 μm) seawater. Two liter aliquots of the diluted sample were incubated for 24 hours in six bottles; three submerged close to the surface and three close to the bottom at 1.8 m. A rack with the incubation bottles was attached to a long line in a lease in the bay. At T_0 200 mL samples from the bottles were collected to quantify CHL, ammonium, nitrate, and phosphate. After 24 hours a further 200 mL were collected for analysis of the same variables. Surface and bottom primary production were averaged to give a value representative of the water column. Incubation experiments were conduced once a month between November 2002 and December 2002. Phytoplankton growth rate was calculated (Equation 1):

$$G = (1/\Delta t) \times \ln ((C_0 + \Delta C)/C_0) \qquad \text{(Eq. 1)}$$

where Δt = 1 d, C_0 = initial phytoplankton biomass (µg chlorophyll a L^{-1}), ΔC = daily increase of phytoplankton biomass due to production. This equation is derived from the exponential growth equation and is commonly used to calculate growth rates from biomass or cell count data (Brush *et al.*, 2002).

5.3.4. Model structure

To estimate clearance time (time needed by the mussels to filter all the cove volume), water residence time, and phytoplankton turnover rate, the model included population dynamics, mussel physiology, and general hydrodynamics of Brito Cove. The model reproduced the mussel population ecophysiology during a growing season when the mussels reached commercial size within 7-8 months. The population dynamics model for *P. perna*, standardized to one meter of culture rope, included in this carrying capacity analysis was developed using data acquired in Brito Cove (Chapter 3). The physiological model for *P. perna*, including response to variation in seston quantity and quality as presented in Chapter 4. Detailed characterization and modelling of feeding behavior of this species is presented in Chapter 2. In the model of *P. perna* population dynamics in suspended culture, the transition of mussel between size classes (see Chapter 3) was determined by growth rates measured in the field and used average lifetime values. In this model the predicted growth rates of individuals in each of the three size classes was

dependent upon the environmental conditions experienced, i.e. the quantity and quality of food and water temperature.

Mussel standing stock inside the cove was calculated by integrating the number and wet weight of individuals in each size class (small, medium, large, and harvestable), multiplied by the quantity of culture rope (in meters) inside each lease. The size of the population could increase through natural attachment of new seed and farm seeding. Farm seeding was estimated to be directly related to harvest rates, on the assumption that available space inside the lease would be restocked with new mussel culture ropes. Model predictions included feedbacks between the bivalve population and the ecosystem i.e. clearance time, excretion, and biodeposition rates. Individual mussel clearance rates were calculated by dividing predicted filtration rates ($L.0.5\text{-}day^{-1}$) by total particulate matter (TPM mg L^{-1}). These individual clearance rates were integrated over the size classes and multiplied by the mussel standing stock to obtain total clearance rate (m^3 $0.5\text{-}day^{-1}$). Clearance time (days) by the cultured mussel population was defined as the time taken for the total mussel biomass within an ecosystem to filter particles from a volume of water equivalent to the total system volume (Dame & Prins, 1998). This was estimated by dividing the volume of water in the cove by the bivalve clearance rate.

Excretion rates of the total cultured mussel population (g NH_4 day^{-1}) was based on an allometric equation proposed for individual *P. perna* (van Erkon Schurink & Griffiths, 1992). Excretion rates for a mussel culture rope was calculated by applying this equation to the soft tissue dry weight predicted for individuals in each size class,

multiplied by the number of mussels in each of the three size classes (μg NH_4 m of rope^{-1} day^{-1}). This value was then multiplied by the length of mussel culture rope in the cove (sum of rope meters in the four leases) to obtain the cultured mussel population excretion rate. Similarly, biodeposition rates for the same population were calculated by integrating the quantity of faeces and pseudofaeces produced by each individual mussels, multiplied by the number of individuals in each size class (mg of biodeposits m of rope^{-1} day^{-1}), and multiplied by total length of culture rope to give the population biodeposition rate (tones day^{-1}). Biodeposition rates on the sediment beneath the mussel leases (g m $^{-2}$ day^{-1}) were calculated by dividing the population biodeposition rate by the total lease surface area.

The rate of water renewal in the cove (m^3 day^{-1}) was calculated by multiplying the cove surface area (m^2 x10^6) by tidal height (m). Tidal height, measured as the water level recorded both on spring and neap tide, estimated variability in water renewal, and a time series of tidal heights in Brito Cove was used as a forcing function in the model. Two small creeks enter the bay, however freshwater input was assumed to have had a minimal contribution to water renewal, which was considered to be predominately controlled by tidal exchange. Water mass residence time (days) for the cove was calculated by dividing cove volume (m^3 *10^6) by the rate of daily water renewal.

The primary production model was driven by phytoplankton growth rates measured between November and April 2002. Phytoplankton growth rates acted as a

forcing function in a Lotka-Volterra predator-prey equation, describing the relationship between phytoplankton biomass and the filter-feeding population (Equation 2):

$$P/\Delta t = P\,(k_p - m_p) - P \times F \times B - P/RT + P_e/RT \qquad \text{(Eq. 2)}$$

where P = phytoplankton biomass (μg chlorophyll a L^{-1}); Δt = 1 d, B = filter feeding population (g fresh weight m^{-3}), k_p = phytoplankton growth rate (d^{-1}), m_p = mortality rate of phytoplankton resulting from causes other than grazing by mussels (day^{-1}), F = biomass-specific clearance rate of mussels (m^3 g fresh weight of $animal^{-1}$ day^{-1}), RT = water mass residence time (days), and P_e = phytoplankton concentration in advected water (here assumed to be 5 μg l^{-1}) (Herman, 1993; Dame & Prins, 1998). Grazing by mussels is directly proportional to algal concentration and suspension feeder biomass, but local depletion and larger spatial gradients are not taken into account (Herman, 1993). Primary production time describes the time taken for primary production within the system to replace the standing crop biomass of phytoplankton within the system (Dame & Prins, 1998). Primary production time was defined as the ratio of phytoplankton biomass (P) to phytoplankton primary production ($P \times k_p$) within the system.

5.4. Results

5.4.1. Area and volume of Brito Cove

A 3-dimensional plot of coordinates (UTM) and depth calculated the volume (6.3 $m^3 \times 10^6$) and surface area (2.7 $m^2 \times 10^6$) for Brito Cove (Fig 5.2). The area used for mussel farming was 162.2 m^2 x 10^3, which was equivalent to 6% of the total cove area. Assuming 200 mussels of 45 g per meter of culture rope the estimated harvestable standing stock inside the cove was 1367.8 tones, which corresponded to 27.3 x 10^3 individual mussels.

5.4.2. Seston dynamics at different time scales

CHL, measured in the fortnightly seston samples taken between 1998 and 2002, varied from <1 to 8 $\mu g\ L^{-1}$, and there was a weak seasonal pattern with peaks in late summer and spring (Fig. 5.3A). TPM ranged between 2-35 $mg\ L^{-1}$ and POM was <1-6 $mg\ L^{-1}$. Seasonal patterns in TPM and POM from the fortnightly measurements were not evident (Fig. 5.3B and 5.3C). Both water temperature and solar radiation followed a seasonal pattern and ranged between 16-30°C and 180-400 Cal respectively (Fig. 5.3.D and 5.3F). Water salinity ranged from 28 to 33 ‰ and there was no evidence of major seasonal patterns (Fig. 5.3E).

In the weekly series of data there were no differences between the two positions in the lease for CHL (t=0.72, df 61, P=0.47), TPM (t=1.78, df 54, P=0.08), POM (t=0.83,

df 54, P=0.40), and OCS (t=0.94, df 54, P=0.34) concentrations (Fig. 5.3). During the year highest CHL concentrations were observed in March, confirming the late summer bloom observed in the longer time-series. The two CHL peaks observed in March and April contributed to the increase in POM and TPM during these months (Fig. 5.4.A, 5.4.B and 5.4.C). In spite of this, OCS did not increase substantially during the algae bloom (Fig. 5.4.D). This was due to probably a positive correlation between PIM and wind speed (Pearson correlation = 0.64, n = 33, $P<0.001$) causing a dilution effect as sediments are resuspended by wind driven water movement (Fig. 5.5.B). CHL was inversely related to the availability of total dissolved nitrogen (Fig. 5.5.A) in a common pattern where nitrogen is either associated with phytoplankton organic matter or available as dissolved nutrient. Ammonium was the major form of nitrogen in water inside the mussel lease, representing 72% of total dissolved nitrogen.

Fig. 5.3. Results of the long time-series (1998-2002) of seston parameters (A) CHL, (B) TPM, (C) POM, and other environmental parameters (D) water temperature, (E) water salinity and (F) solar radiation likely to influence algae production recorded fortnightly measurements. Solar radiation was plotted using monthly average values from daily measurements.

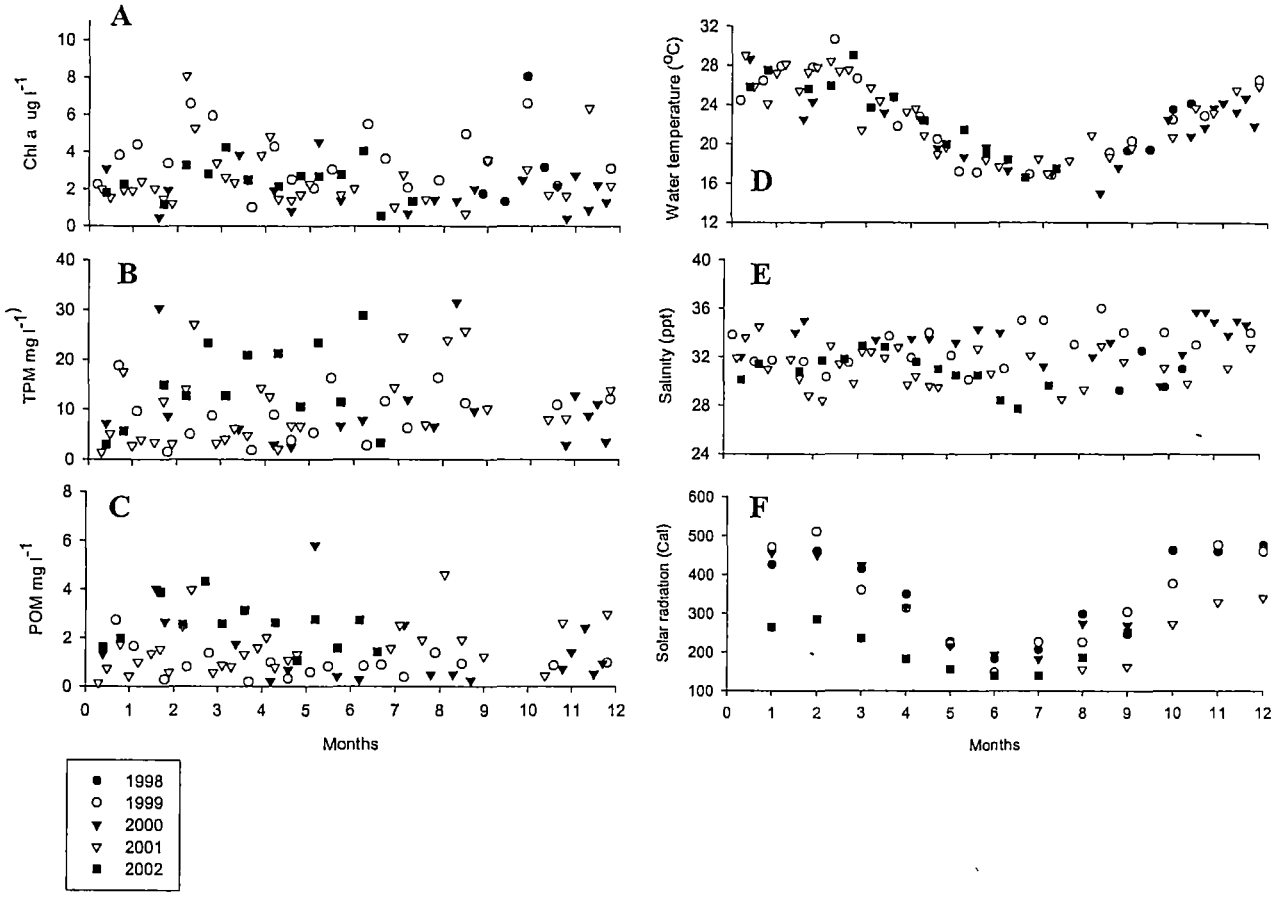

Fig. 5.4. Results of the short time-series (2000-2001) of weekly measurements of seston parameters (A) CHL, (B) TPM, (C) POM, and (D) OCS for the two sampling stations indicated in Fig. 5.2. TPM, POM and OCS samples between months June and July were lost.

P

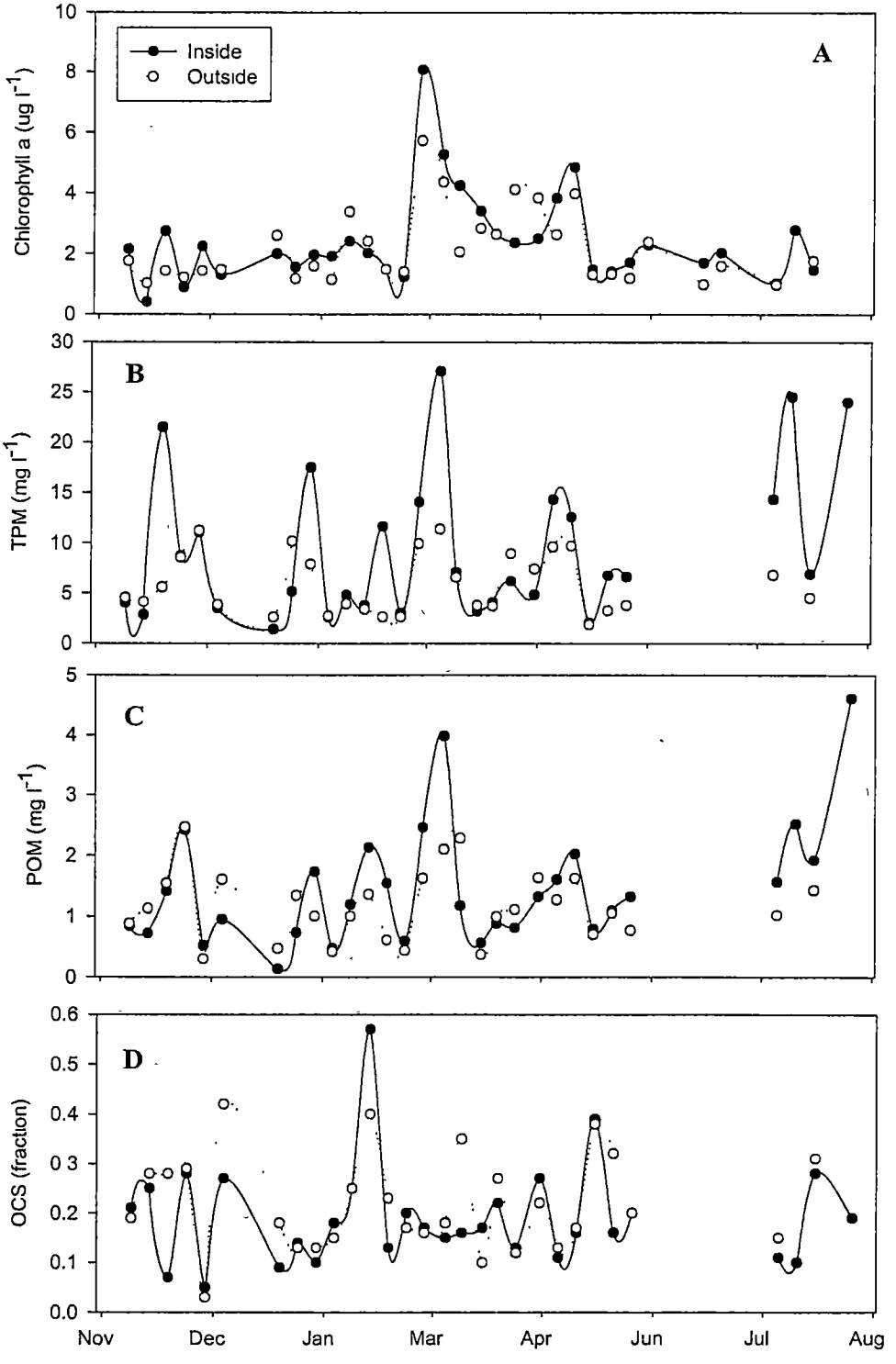

Pearson's correlation analysis on both the weekly and fortnightly series of seston measurements revealed a positive correlation between TPM at near surface and bottom samples (Table 5.2). There was also a strong correlation between TPM and PIM (Table 5.2), suggesting that most of the total particulate matter suspended in the water column was inorganic matter (PIM), which corresponded to an average of 79.4% (± SD 11.4, n=30) of TPM in the short weekly series. CHL at surface and bottom waters were correlated in both series of measurement and in surface waters only, while CHL was weakly correlated with POM (Table 5.2).

Over a 24 h period there were no significant correlations between wind, current speed, and tide level and TPM, possibly because of the limited number of observations (N=13). However, Fig. 5.6 and 5.7 suggested evidence of a non-linear association between these variables and the availability of TPM. Evidence of resuspension was indicated by a positive correlation between bottom turbidity and wind speed during the spring tide ($r = 0.80$, $n=13$ $P = 0.001$).

Fig. 5.5. Selected seston parameters from the short time-series of weekly measurements. (A) Surface CHL, NO_3, and NH_4, and (B) PIM and wind speed. Samples of PIM between months June and July were lost.

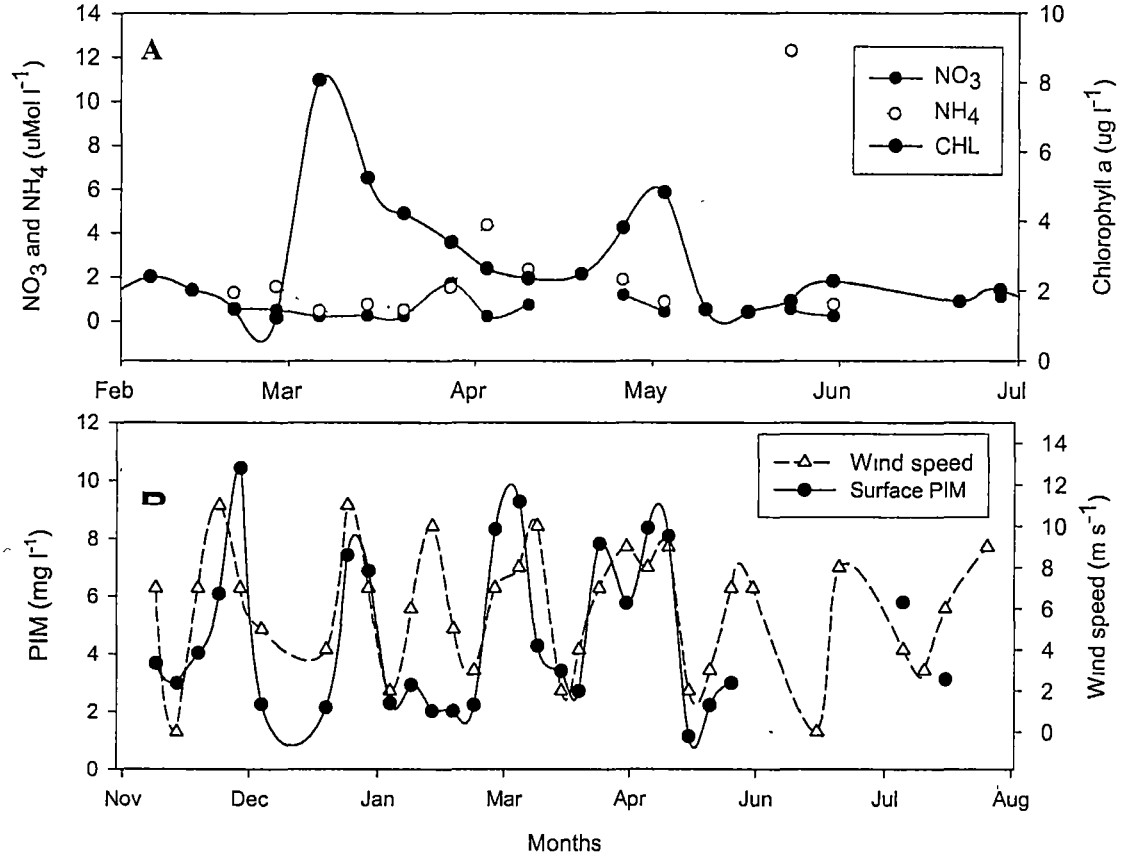

Table 5.1. Area, standing stock, and mussel population (assuming 200 mussels per m of rope) in the four commercial mussel leases inside Brito Cove.

Lease	Area ($m^2 \times 10^3$)	Standing stock (Tones)	Number of mussels ($\times 10^6$)
A	31.1	288.8	5.7
B	101	818.7	16.4
C	10.5	91.1	1.8
D	19.5	169.2	3.4
Total	162.2	1367.8	27.3

Table 5.2. Pearson correlation coefficients calculated for CHL, TPM, PIM, and POM measured at near surface and bottom waters. Series refer to long biweekly (1998-2002) and short weekly (2000-2001) series. All correlations are significant at $P<0.001$. The number of samples is provided next to each correlation factor.

	Series	R (n)
CHL (surface) vs CHL (bottom)	(1998-2002)	0.712 (90)
	(2000-2001)	0.544 (32)
CHL (surface) vs TPM (surface)	(1998-2002)	0.295 (80)
CHL (surface) vs POM (surface)	(1998-2002)	0.314 (78)
	(2000-2001)	0.474 (29)
TPM bottom vs surface	(1998-2002)	0.510 (79)
	(2000-2001)	0.550 (30)
TPM (bottom) vs PIM (bottom)	(1998-2002)	0.997 (78)
	(2000-2001)	0.996 (31)
TPM (bottom) vs POM (bottom)	(1998-2002)	0.870 (78)
	(2000-2001)	0.778 (31)
PIM (surface) vs TPM (surface)	(1998-2002)	0.998 (79)
	(2000-2001)	0.976 (30)
PIM (surface) vs PIM (bottom)	(1998-2002)	0.508 (79)
PIM (surface) vs POM (bottom)	(1998-2002)	0.369 (78)
	(2000-2001)	0.508 (30)
PIM (bottom) vs POM (surface)	(1998-2002)	0.830 (78)
	(2000-2001)	0.727 (31)
TPM (surface) vs POM (surface)	(1998-2002)	0.314 (78)
	(2000-2001)	0.474 (29)
POM (surface) vs POM (bottom)	(1998-2002)	0.510 (78)
	(2000-2001)	0.718 (30)

Fig. 5.6. TPM measurements presented with wind and current speed, and tide height during a spring tide cycle.

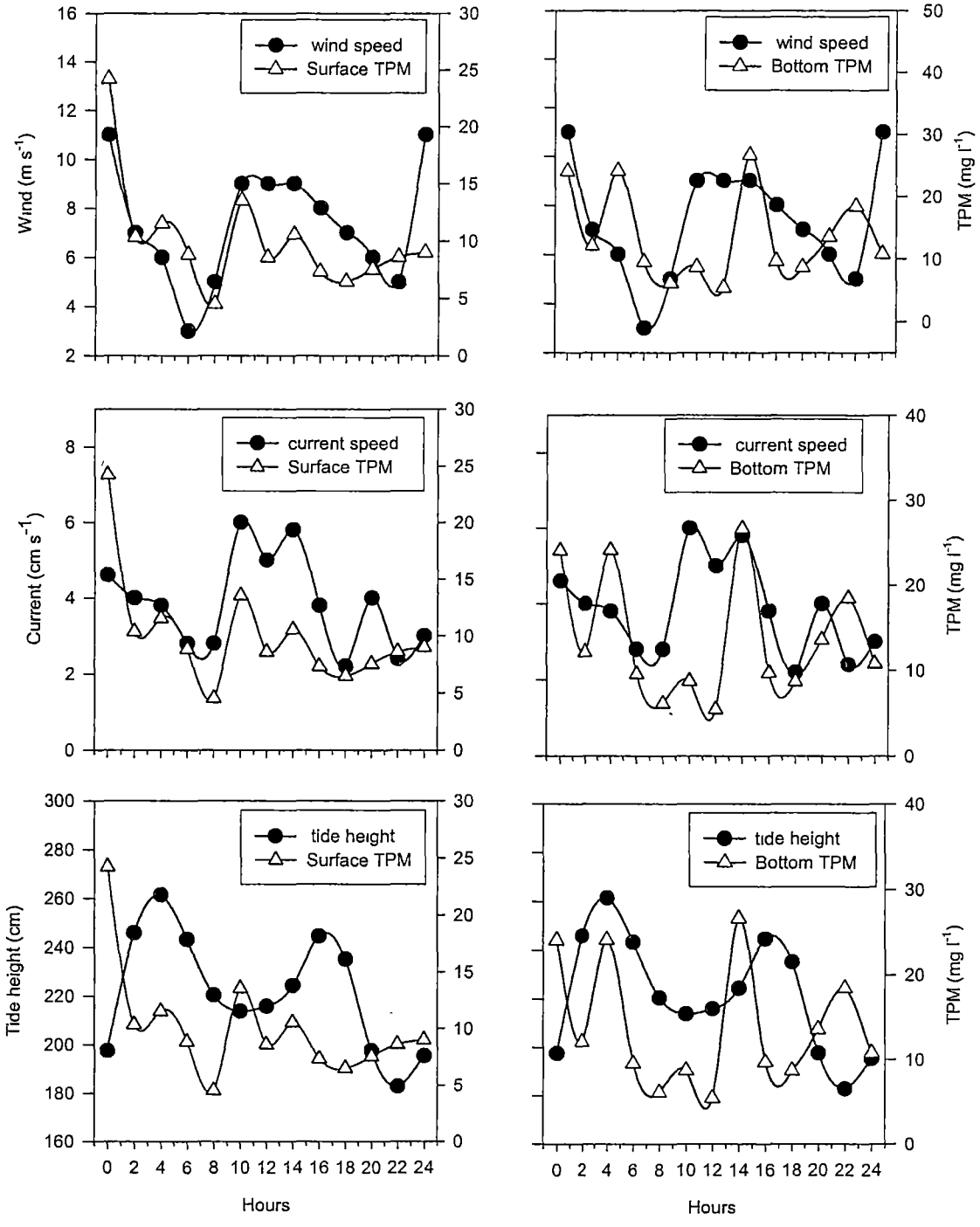

Fig. 5.7. TPM measurements presented with wind and current speed, and tide height during a neap tide cycle.

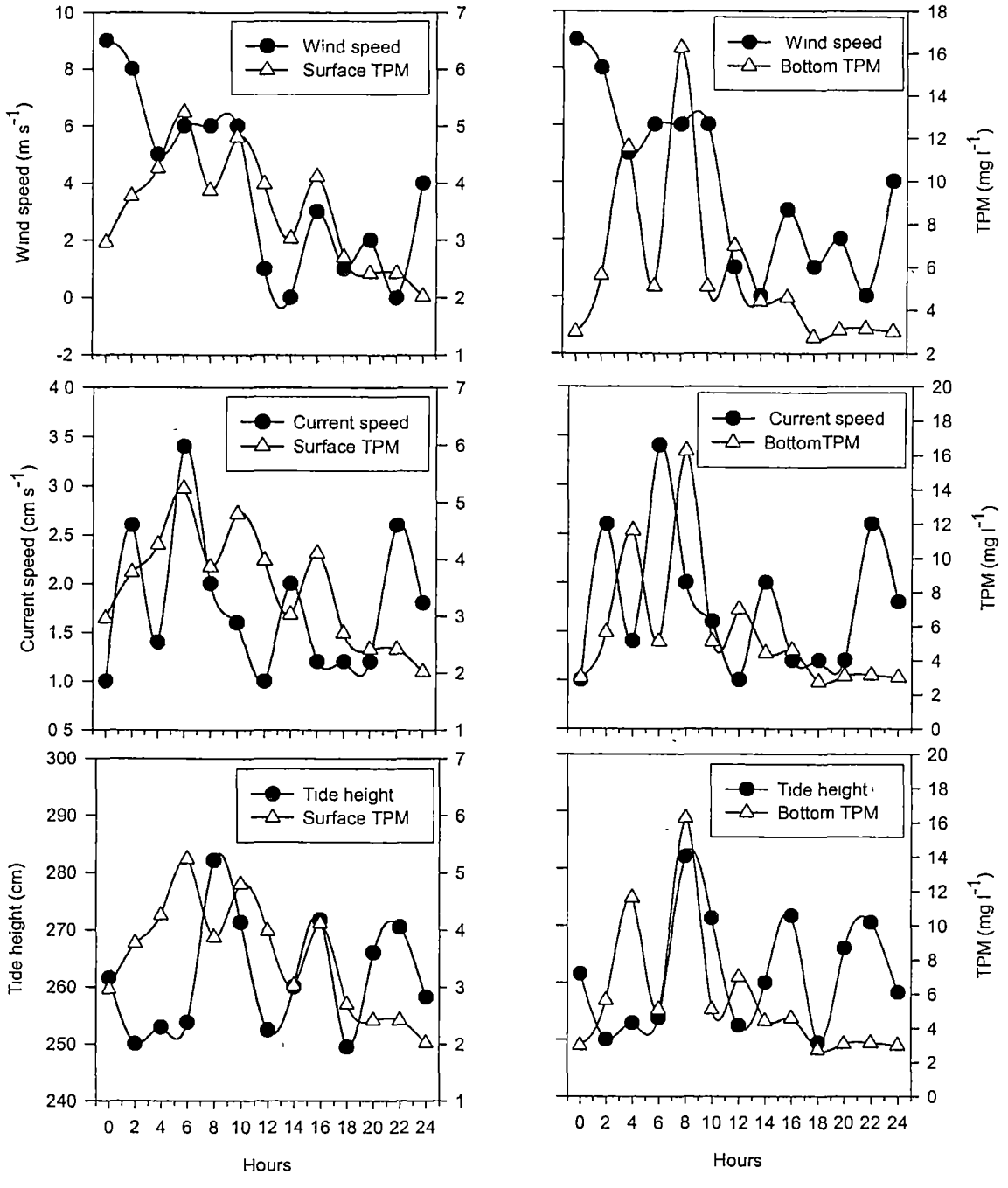

Fig. 5.8. Tide height and current and wind speed in Brito Cove in (A and B) June – July, 2001 and (C) tide height and current speed in October, 2001.

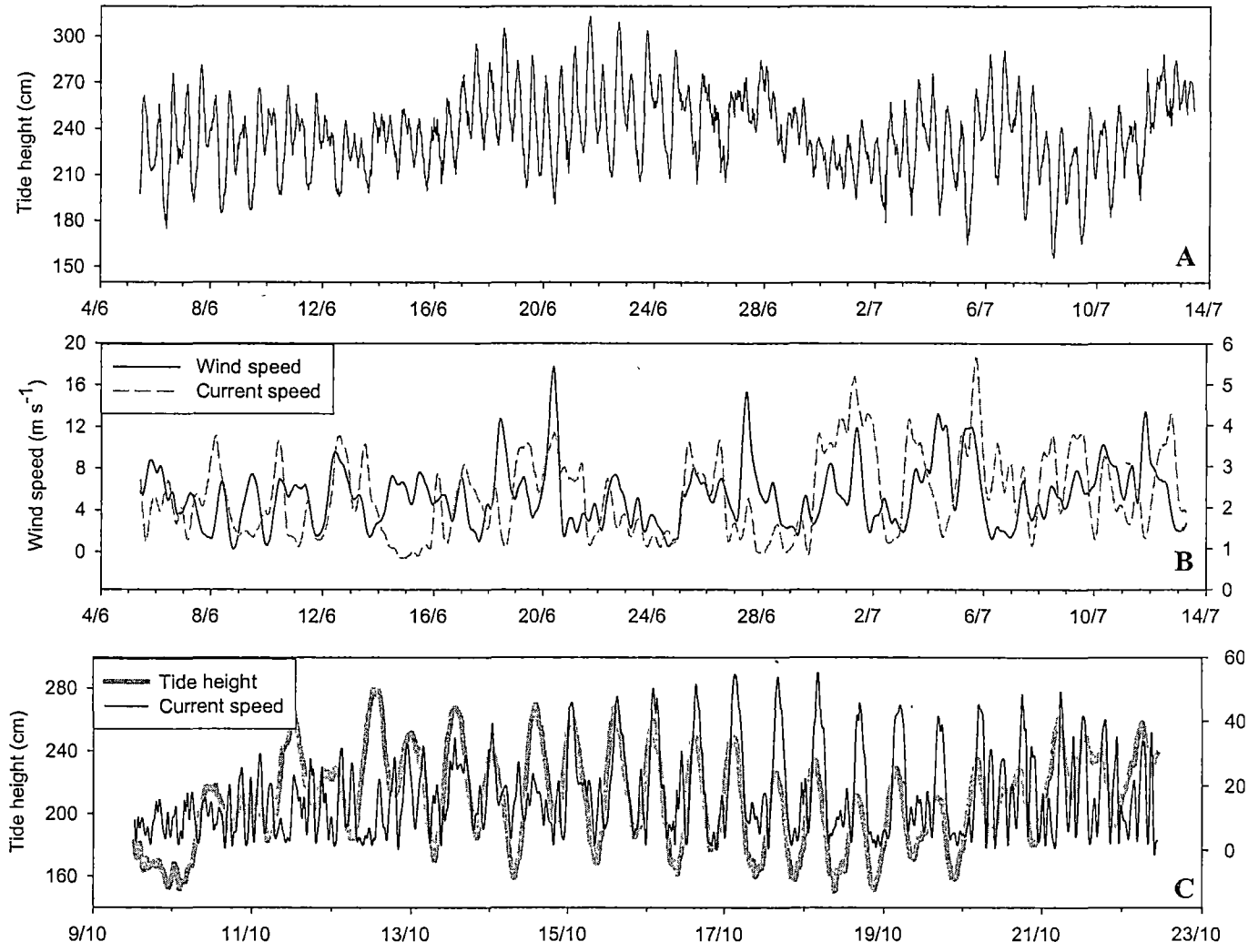

Tidal height measured over three spring and neap tides cycles in June–July ranged from 180 to 310 cm (Fig. 5.8A). When multiplied by cove surface area this corresponded to a water mass renewal ranging between ca. 5.5 – 10.5 $m^3 \times 10^6$ day^{-1}. Wind and current speed data recorded every half an hour were transformed applying a moving average with a period of 13 h to give average values over half a day. Maximum wind speed recorded over June-July was 16 m s^{-1}, and the significant, but weak, correlation between wind and current ($r = 0.20$, $n = 1818$, $P<0.001$) was due to the large number of records (Fig 5.8B). A weak correlation was also detected between tide and current speed over neap and spring tides in October ($r = 0.41$, $n = 620$, $P<0.001$), particularly during spring tides (Fig. 5.8C).

The variation of biweekly and weekly data of seston concentration was 100% and 50% greater than the variation in tidal measurements in surface waters (Table 5.3). The coefficients of variation for bottom samples were similar for all temporal scales and this was interpreted as a result of common forcing variables acting in the dynamics of these seston concentrations, more specifically the action of wind and currents re-suspending the sediment in this shallow bay. The coefficients of variation for seston concentration measured at three temporal scales (tidally, weekly, and fortnightly) for different periods (24 h, eight months, and four years) are presented in Table 5.3.

Phytoplankton growth rate varied between 0.63–1.03 and 0.42–1.04 μg CHL l^{-1} day^{-1}, in surface and bottom samples respectively. Greater primary production was observed in December, February, and March with values declining towards April (Fig

5.9A). Water temperature peaked at 29°C in March, total dissolved inorganic nitrogen (DIN) peaked in April (6.13 μM l^{-1}), and ammonium peaked in December (1.96 μM l^{-1}) (Fig 5.9B).

Table 5.3. Coefficient of variation of seston concentrations (CV, %), measured in different temporal scales at near surface and near bottom waters: Weekly (2000-2001), biweekly (1998-2002) and spring and neap tides (24 h).

	Spring tide			Neap tide			Weekly			Biweekly		
	S	B	n	S	B	n	S	B	n	S	B	n
TPM	48	53	13	28	69	13	78	68	30	104	69	80
PIM	49	54	13	28	88	13	82	71	30	107	70	80
POM	43	48	13	50	80	13	68	57	30	93	71	80
OCS	23	20	13	50	110	13	53	40	30	61	42	80
CHL	37	29	13	38	30	13	62	58	32	59	64	90

5.4.3. Model predictions

Bivalve population size predicted by the population dynamics model (Chapter 2) varied between 6.2 and 7.5 million mussels inside the cove (Fig. 5.10A). The decrease in population was due to natural mortality of 0.006 individuals.day^{-1} (Chapter 3) and an increase in population size occurred when the model predicted natural settlement of spat. Total biomass increased from < 200 t to ca. 1000 t during the growing season (Fig. 5.10B). Predicted CHL concentrations were greater than observed values during 83% of the growing period (Fig 5.10C). Chlorophyll a concentrations ranged between 0.4-8.07 $\mu g\ l^{-1}$in the observed values and between 0.84-6.86 $\mu g\ l^{-1}$ in the predicted values. Although observed and predicted CHL series were different ($F = 5.76$, $df = 2, 210$, $P<0.001$), model predictions reproduced the main patterns of phytoplankton dynamics in this system, with highest concentrations occurring in March (approximately day 120) (Fig. 5.10C).

The model of the culture rope population dynamics predicted that the total mussel population size decreased from 200 to 110 mussels m^{-1}, then stabilized after six months (Fig. 5.11A). An assumption in the model was that all growers would seed their lease until fully stock at time 0, which does not reflect the real lease management practiced in Brito Cove. Therefore, the number of mussels on the ropes is realistic and reflects a situation where leases are not always at maximum stocking density and seeding and harvesting are carried out a number of times throughout the year. The model also showed that initially small mussels in the population were responsible for most of the water clearance. Large mussels were dominant in the

population close to harvesting time and clearance rates were a function of their abundance. The contribution of small mussels to the total population clearance rate was limited to short periods just after the spawning season (Fig. 5.11B). The model, using average clearance rates, predicted elevated clearance activity by the mussel population during the seed attachment season. In periods without seed attachment, the average population clearance rate was much lower than estimates derived by summing the different clearance rates observed in each size class (Fig. 5.11C).

Bivalve feedbacks to the system predicted by the model included population clearance rate (5 – 35 $m^3 \times 10^6$ day^{-1}) (Fig. 5.12A), biodeposition rate (0.5 – 9 tones day^{-1}) (Fig. 5.12B), and excretion rate (1.8 – 2.2 g NH_4 day^{-1}) (Fig. 5.12C). The clearance and biodeposition rates of the mussel population tracked changes in the quantity and quality of seston. However, population excretion rates were predominantly influenced by predictions of total bivalve biomass as the model did not considered excretion rate to be controlled by any variable other than mussel dry body weight and the number of individuals (Fig. 5.10A). Excretion rates inside mussel leases ranged between 0.38 – 0.5 μmol NH_4 m^3 day^{-1}. Cultured mussel population biodeposition rates divided by total lease surface area ranged between 3 – 5 g biodeposits m^{-2} day^{-1}.

Fig. 5.9. Surface and bottom phytoplankton growth rate (μg CHL l^{-1} day^{-1}) measured through 24 hours incubation between November and April in Brito Cove (A). Water temperature, dissolved inorganic nitrogen (DIN) and ammonium measured during the incubation experiments (B).

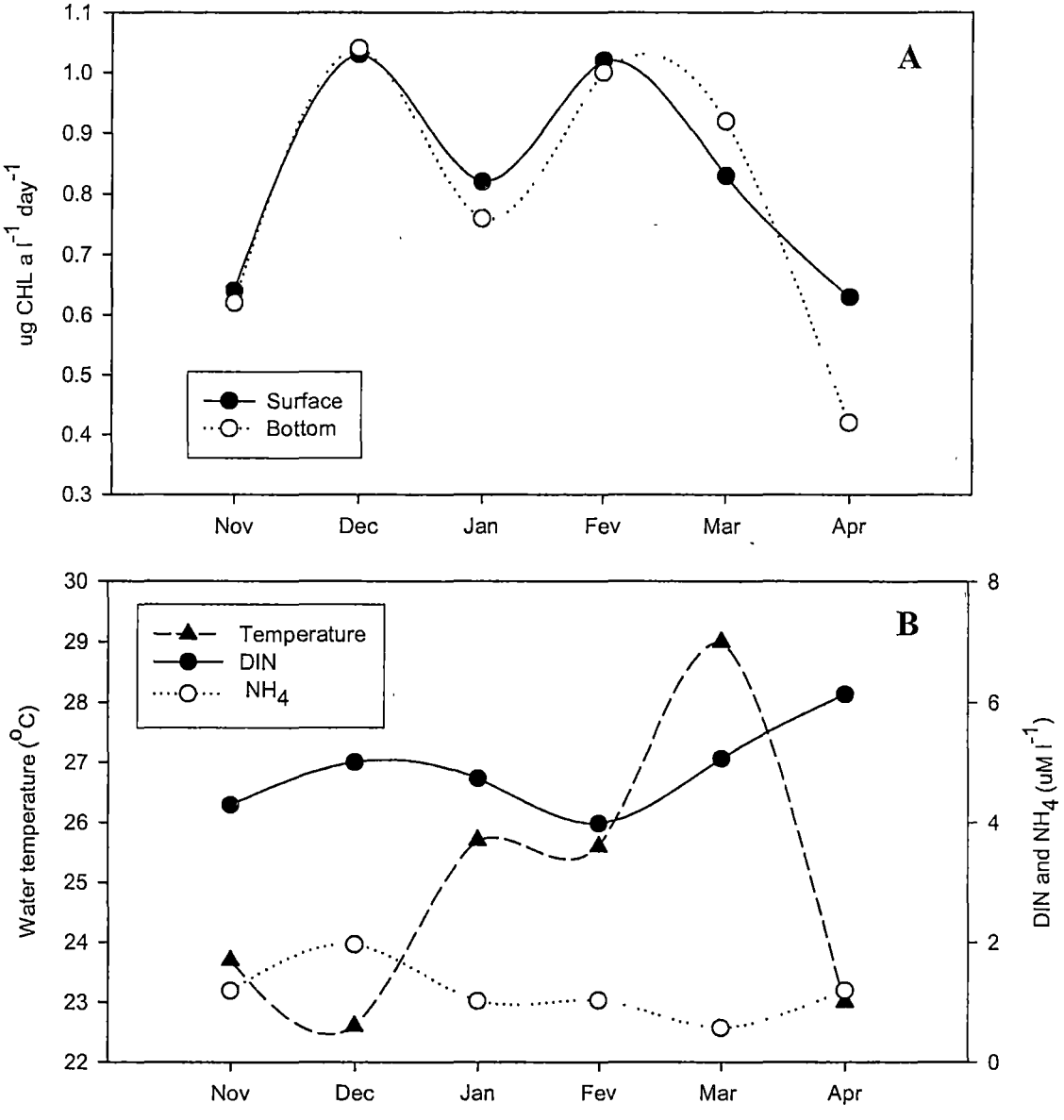

Fig. 5.10. Model predictions of total bivalve population (A), total bivalve biomass (B), and chlorophyll a (C).

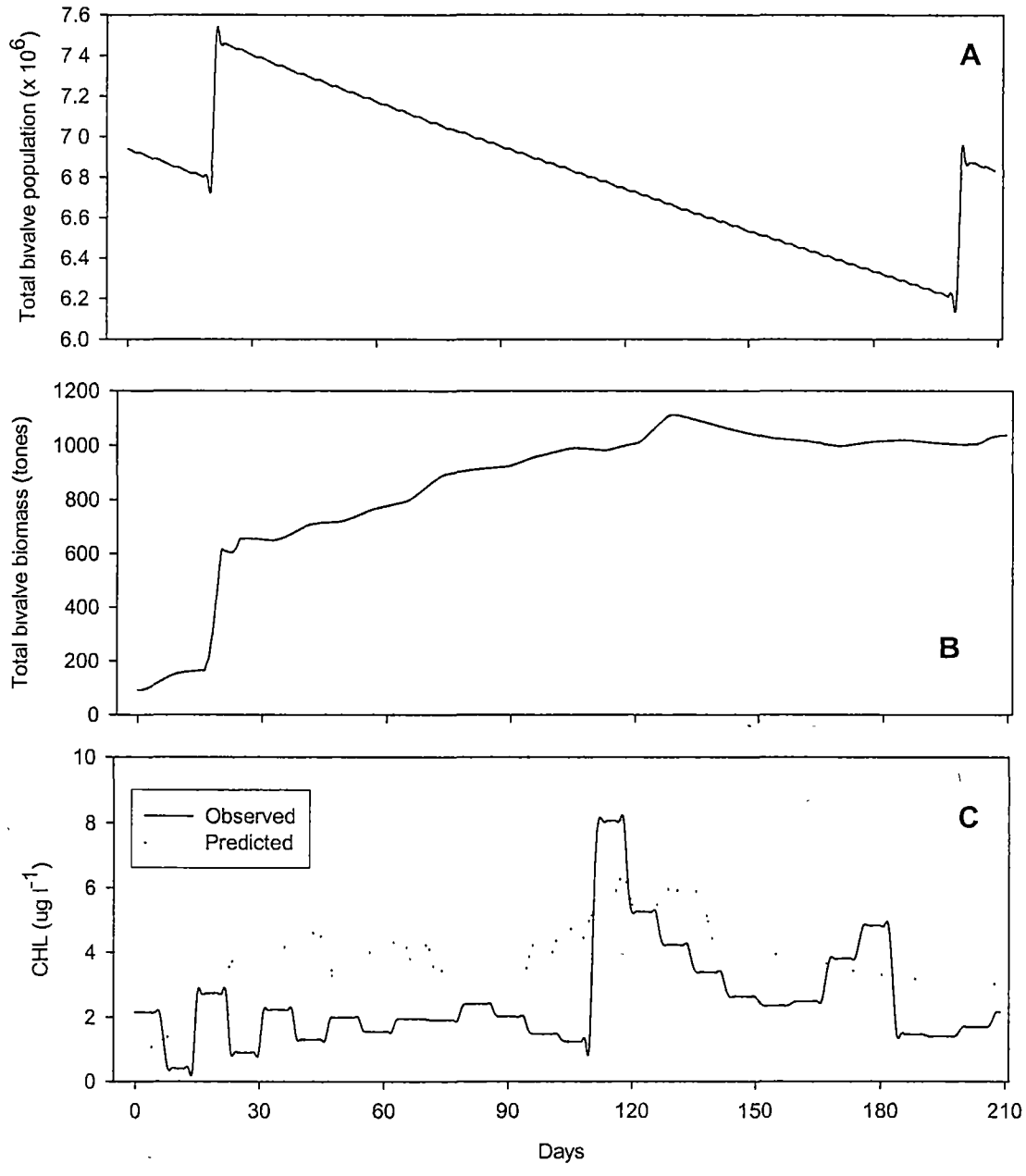

Fig. 5.11. Mussel size class density distribution in one meter of rope (A), clearance rate separated by size class (B), and mussel rope clearance rate calculated averaging clearance rate across size classes (average clearance) and calculated considering mussel size class distribution (predicted clearance) (C).

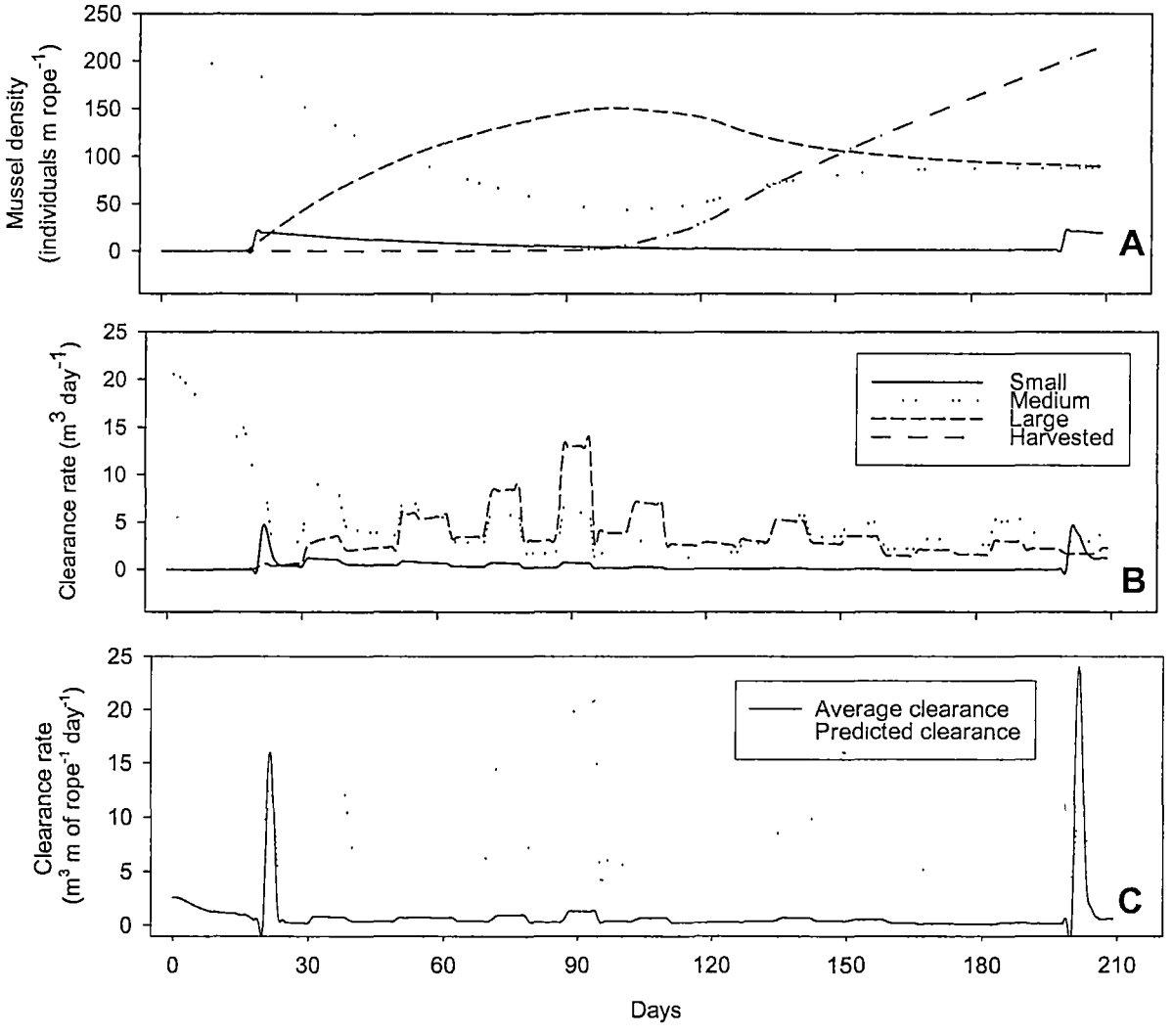

Fig. 5.12. Model predictions of population clearance rate (A), biodeposition rate (B), and excretion rate (C).

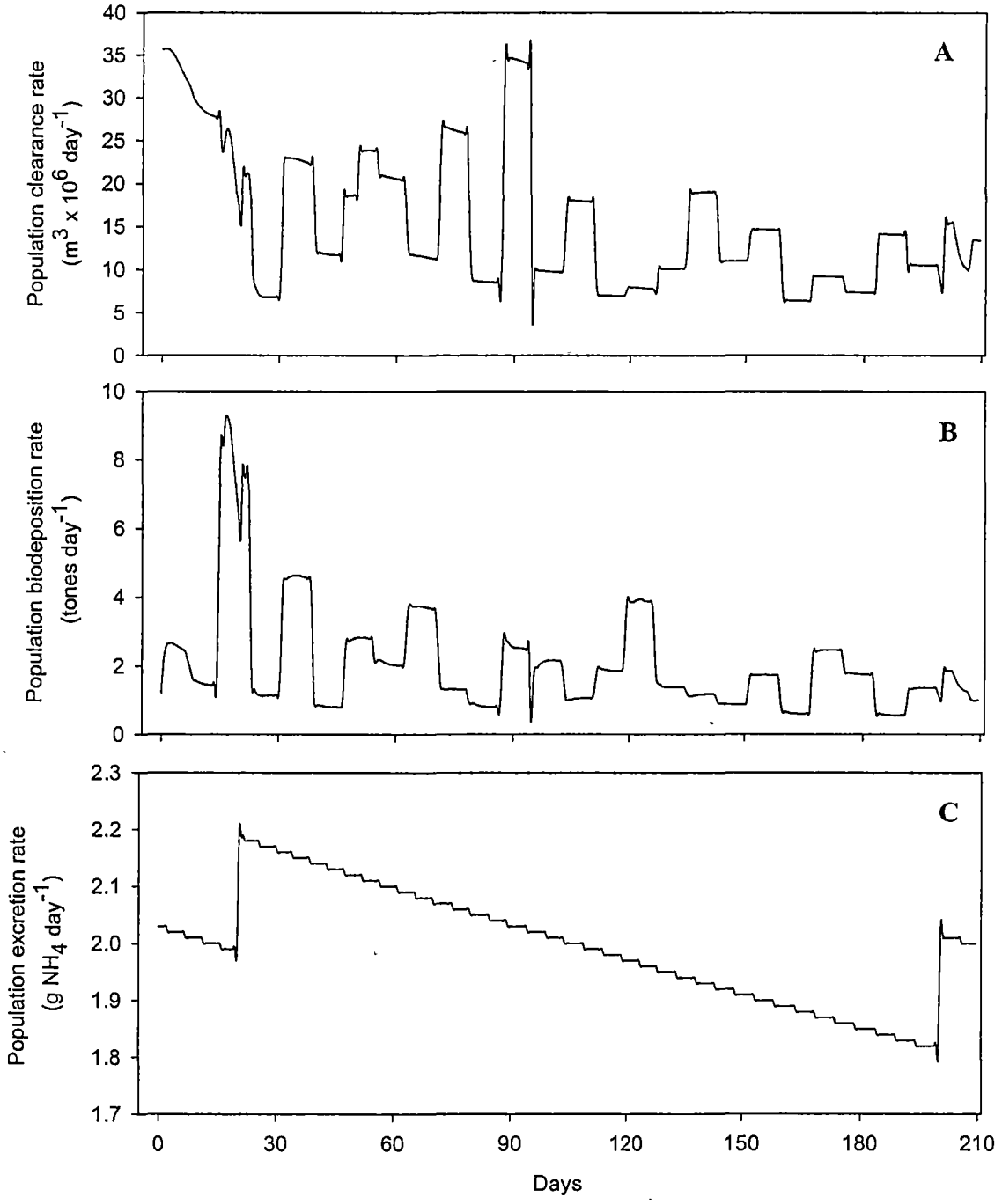

Fig. 5.13. Model predictions of water residence time (A), primary production time (B), and bay clearance time (C).

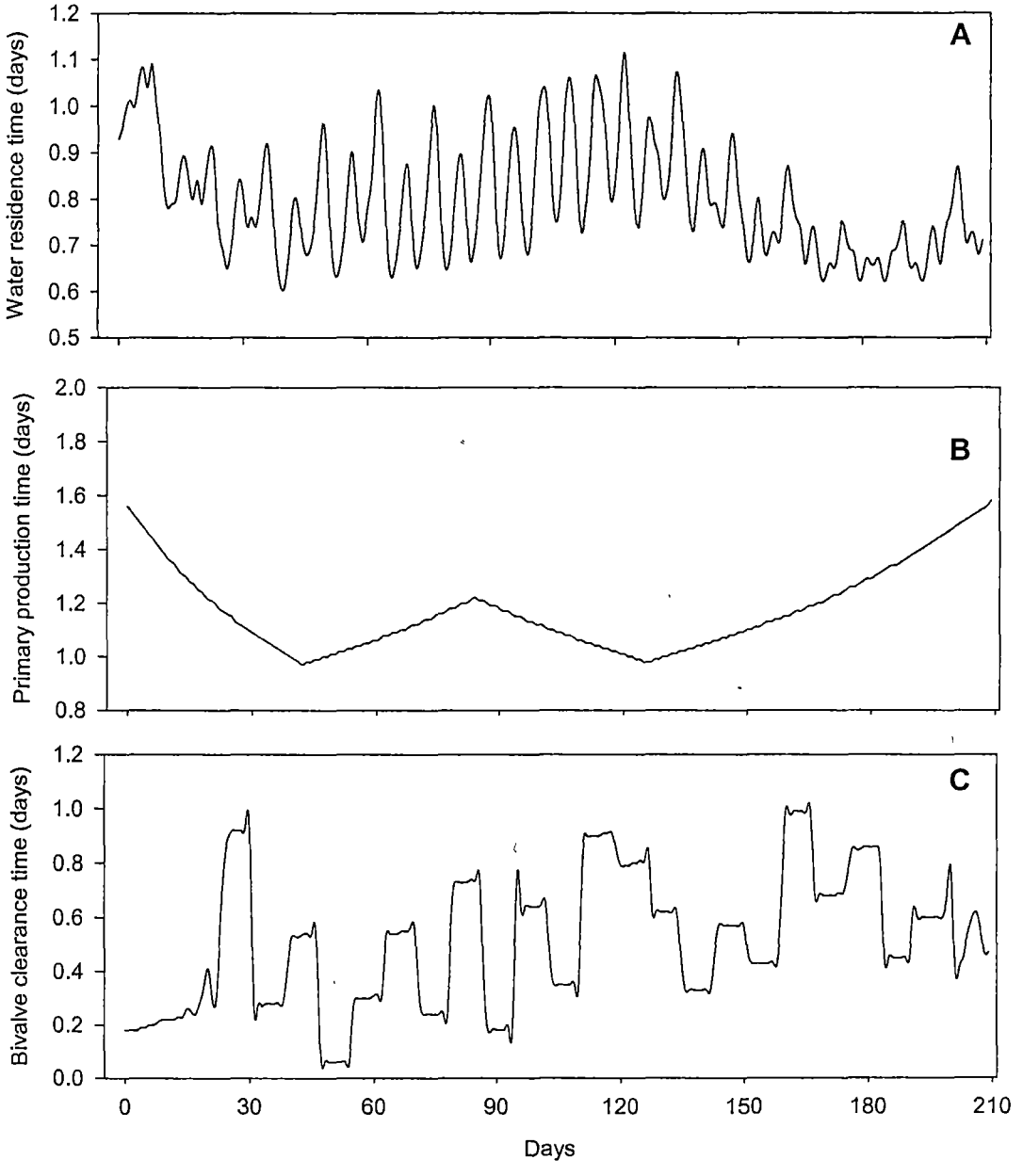

Relevant factors for analysis of carrying capacity predicted by the model were water mass residence time (0.6 – 1.1 day) (Fig. 5.13A), primary production time (1.0 - 1.6 days) (Fig. 5.13B), and bay clearance time (0.1 – 1 day) (Fig. 5.13C). Water residence time was influenced by water renewal both in spring and neap tides (see methods), however the frequency of tide amplitude was set to vary more smoothly than the real semidiurnal cycle that would be harder to visualize in the graph. Primary production time was mainly controlled by the growth rate measured by the primary production incubation experiments. Bay clearance time was a function of bivalve population and standing stock subject to the control mechanisms observed in the filter-feeding behavior of mussels to optimize the organic content of ingested food in seston with varying quantity and quality conditions.

Sensitivity analysis of the model was provided separately for *P. perna* feeding behavior (Chapter 2), population dynamics (Chapter 3), and ecophysiology (Chapter 4), and it will not be provided here as the main model outputs: 1) bivalve population feedback to the system and 2) water residence, primary production, and clearance times, are obviously controlled by the coupling of population dynamics, feeding and ecophysiology models, and by tidal height and measured primary production respectively.

5.5. Discussion

In general the smaller the basin the shorter the water mass residence time (Bacher *et al.*, 1998). This is true for Brito Cove where the whole water mass is renewed up to twice daily and is less than the primary production time. This normally implies that the ecosystem is overwhelmingly dominated by tidal forces (Dame & Prins, 1998). Mussel clearance times were less than water residence and primary production times. This suggests that phytoplankton must be advected into the cove for the cultured mussel population in this system to be sustained. This is characteristic of ecosystems where phytoplankton abundance is controlled by bivalves (Dame & Prins, 1998). In coastal ecosystems with dense bivalve populations, these organisms represent a major functional component that consumes large amount of phytoplankton and couples benthic and water column processes (Dame, 1996).

The population biodeposition rates predicted by the model means that two tones of biodeposits were released per day inside the four mussel leases in Brito Cove. Although current and wind may spread this material, most of it settles beneath the mussel farms. This affects benthic fauna, which becomes dominated by polychaete worms and scavenging gastropods (Stenton-Dozey *et al.*, 1999; Kaspar *et al.*, 1985), and phytoplankton detritus in form of phaeophytin. Biomass in the sediment can be increased by a factor of three compared to a reference site as a result of biodeposition associated with bivalve aquaculture (Kaspar *et al.*, 1985). This material, together with microphytobenthic biomass, will be resuspended by strong tidal currents and winds, making it available to suspension-feeders (Héral, 1985). By grazing particulate organic nitrogen present in phytoplankton and excreting ammonium, the form of

nitrogen preferentially taken up by phytoplankton, bivalves can short-circuit pelagic nutrient processing and rapidly recycle nitrogen in a process which benefits both phytoplankton and bivalves (Dame, 1996).

The strong feedback between shellfish culture and the plankton ecosystem, through phytoplankton consumption and nutrient regeneration, implies that estimates of carrying capacity need to applying tools that quantify these feedbacks (Ross *et al.*, 1999). Much of the effort in developing carrying capacity models is taken up in determining the rates at which concentrations of food change throughout the marine system (James & Ross, 1996). However, the processing of nitrogen is a complex sequence of biological processes. Nitrogen undergoes numerous transformations in addition to state changes as it cycles through the environment, making measurements difficult and most of the time incomplete (Dame, 1996).

This model tried to couple primary production with nitrogen recycled by mussels. Unfortunately predictions were poor due to lack of information about many other physical and biological components involved in modelling nitrogen budgets applied to phytoplankton growth. Particularly information about sediment remineralization rates, other natural and anthropogenic fluxes of nitrogen, and zooplankton grazing on phytoplankton in Brito Cove. The successful modelling of this feedback loop between the role of bivalves in the nutrient cycle and primary production is vital to developing exploitation carrying capacity models. As these processes act together under the influence of bivalve standing stock and local hydrodynamics to allow predictions of stocking density at which production of marketable mussels is maximized. Although the relationship between stocking

density and growth reduction is a desirable in developing carrying capacity models, this is a surprisingly rare output in most studies (Grant, 1999), probably related to the difficulty in closing this feedback loop.

This study provided a first attempt to elucidate the main interactions between bivalve filter feeders populations and the environment in an aquaculture system in Southern Brazil. The predictions of biodeposition and excretion rates presented here for *P. perna* are important information that can be readily incorporated in more complex model of nitrogen budget applied to carrying capacity analysis. The coupling of *P. perna* feeding and energetic physiology with population dynamics enabled estimations of physiological feedbacks of mussel populations to the system. Oceanographic measurements associated with a detailed characterization of the cove enabled an understanding of how fast water is exchanged in this ecosystem. Finally, the integration of all these information indicated that the reduction in growth rate observed in the recent years, are likely to be associated with the increased culture density and the depletion of food before it can be replaced by primary production or advection from boundary areas.

Chapter 6

Thesis Conclusion

The investigation of phytoplankton dynamics as a mussel food source is complex and depends on various biological, physical, and chemical processes which operate over a large range of spatial and temporal scales. The sustainable production of mussels in suspended culture depends on the understanding of how these processes and their multiple feedbacks act together as a function of farm density. Models that reproduce these interactions can be used to evaluate the effect of farm densities on mussel growth and sediment dynamics. The present study described and modelled some aspects of *Perna perna* feeding behavior and physiology, in an attempt to understand the main mechanisms controlling growth of this species in the semi-tropical waters of South Brazil. Important feedbacks between mussel populations and the environment resultant from grazing and metabolism were presented like filtration, biodeposition and excretion rates.

Short and long time-series of chlorophyll-a presented here demonstrated that seasonal patterns in primary production are much weaker in semi-tropical than in temperate environments. Indeed, instead of strong seasonal patterns, phytoplankton is relatively abundant throughout the year. Food abundance associated with reduced temperature amplitude throughout the year directly reflects in higher growth rates as reported here. As food abundance and bivalve growth rate are crucial components in modelling carrying capacity, the findings reported here are significant as they provide ground knowledge to further studies of carrying capacity in Southern Brazil.

Mussels accelerate nutrient cycling by removing phytoplankton from the column and encapsulating it as biodeposits that sink rapidly. Filtration at large seston concentrations leads to the production of large amount of biodeposits (Chapter 2). This intense sedimentation of organic matter can transform sediments from a net sink of dissolved nitrogen in a source with increased ammonium release (Hatcher *et al.*, 1994). Ammonium is also the main excretory product of mussels as it is the nitrogen compound preferentially utilized by phytoplankton to promote growth. Ammonium plays an important role in the nitrogen cycle in mussel farms and any model of exploitable carrying capacity in these systems depends of the successful modelling of this benthic-pelagic coupling.

The increase of ammonium concentration inside mussel farms as a result of excretion and biodeposition rates has been documented by Kaspar *et al.*, (1985). They report that although nitrate and nitrite pools were similar in sediments from a mussel farm and a reference site, the ammonium pool was twice as high in farm sediment. Measurements of nitrogen availability in the water column reports ammonium concentrations in the column up to 73 % higher than in a reference site (Souchu *et al.*, 2001). Nitrogen fluxes at the water-sediment interface under bivalve farms in a shallow lagoon in France, were 1-5 times higher for ammonium in the farm area compared to a reference site (Mazouni *et al.*, 1996). Herman & Scholten, (1990) also report that in Marennes–Oléron (France), a doubling of nutrient loadings is balanced by no more than a 2.5% increase in suspension-feeders biomass, which further confirms the important role of bivalves in the nitrogen cycle of coastal areas.

When calculating the carrying capacity on the basis of annual average budgets, a large number of assumptions have to be made. Given the time scale and the steady state assumption, it was not possible to include feedback mechanisms between mussel populations and the environment (Smaal, 1991). Furthermore, models with a one year time scale are not suitable to predict growth of *Perna perna*, a mussel that attains commercial size within months in the semi-tropical waters of Brazil. Models with shorter time scales reproducing dynamic interactions between bivalves, water column, and sediment are crucial in studies in these fast growing conditions.

The models of scope for growth and population dynamics presented here can be used as a tool for studies in similar sites. Although there was good agreement of the model prediction with the observed mussel growth data, the model needs to be tested with an independent set of data before it is can be used as a management tool. The model structure can be used, with minor modifications in the coefficients and parameters, to describe the scope for growth and population dynamics of other bivalve species. The physical aspects involved in carrying capacity analysis, like import and export of phytoplankton by tidal action, demand more detailed models of hydrodynamics and resuspension by wind, which are site specific and depend of intense measurements in every new site investigated. This makes the applicability of a general carrying capacity model questionable.

Mechanisms such as sediment resuspension and nitrogen cycling involve complex models because there are often orders of magnitude differences in the standing stocks of organic matter in sediments. There is a model that simulates changes in standing stocks and flows of organic matter resulting from sediment

resuspension in shallow coastal environments (Wainright & Hopkinson 1997). However, the integration of this model with the mussel ecophysiology and population dynamics presented in this study would generate an excessively complex model. Although the model becomes a more realistic reproduction of natural interactions, there is in an increasing loss of accuracy as new variables are added. As a result, more complex model becomes less precise in their estimates of maximum densities in exploitable mussel culture. The model produced in this thesis lacks details of how mussels control the nitrogen cycle both within the water column and sediment. Given the importance of nitrogen, future work needs to quantify the relationships between nitrogen release by mussel population and the sediment, primary production, and food availability (Fig. 6.1). The prediction of sustainable mussel biomass must account for the direct and indirect effects of mussel physiological activities on remineralization and local primary production.

Despite the number of studies about carrying capacity modelling, there is no general model that can be readily employed at different sites without extensive studies of local hydrodynamics, nutrient cycling and primary production. In spite of this, there is a demand for model that can be used to plan the development of mussel industry and minimize the deleterious effects of high densities in bivalve farming. This demand is particularly high in many developing countries where marine aquaculture is becoming an increasingly important alternative of income. As the development of the bivalve aquaculture is inevitable and currently underway bivalve farmers should observe guidelines of minimum distances between culture ropes, long lines and leases to avoid local food depletion and accumulation of biodeposits beneath culture sites. A precautionary approach associated with continuous monitoring of

food abundance and fluxes of standing stocks between water column and sediment should guide decisions of further increase or reduction in standing stocks, while a predictive model of carrying capacity with broad application is not available.

Figure 6.1. Main components involved in modelling the feedback between bivalve population ecophysiology and food renewal. The black arrow represents the feedback of nitrogen generated by mussel excretion and sediment release to primary production and food availability.

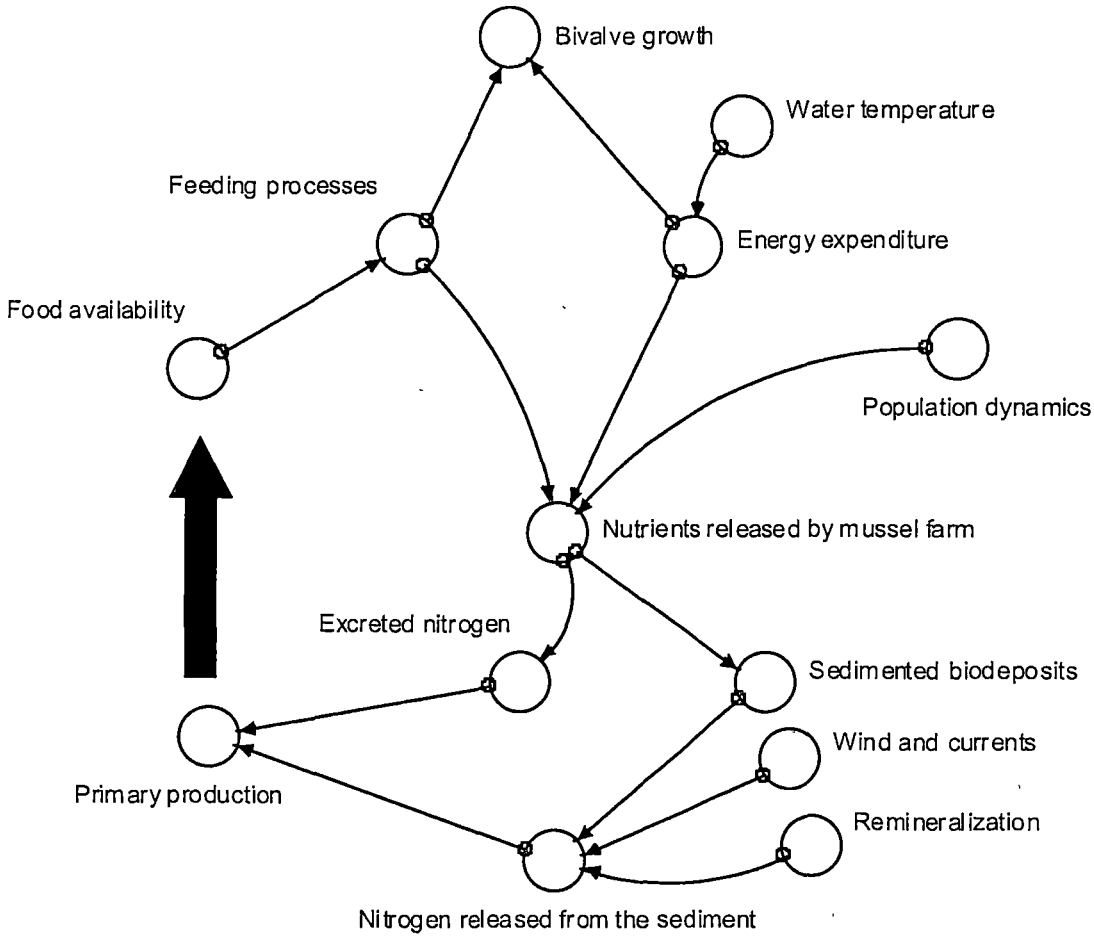

7. References Cited

Acuña, A. C., 1997. Variación estacional de la fijación larval Del mejillon *Perna perna* em los bancos naturales de la costa norte Del estado Sucre, Venezuela. Bol. Inst. Oceanogr. Univ. Oriente, 16: 79-82.

Aquini, E. N., Ferreira, J. F., 2000. Influence of seed origin on growth of the Brown mussel *Perna perna* (L.) in a culture system. In: Proceedings of the XI Brazilian Aquaculture Symposium, Florianopolis, Santa Catarina, Brazil. CD-rom.

Babarro, J. M. F., Fernández-Reiriz, M. J., Labarta, U., 2000. Growth of seed mussel (*Mytilus galloprovincialis* Lmk): effects of environmental parameters and seed origin. J. Shellfish Res., 19: 187-193.

Bacher, C., Duarte, P., Ferreira, J. G., Héral, M., Raillard, O., 1998. Assessment and comparison of the Marennes-Oléron Bay (France) and Carlingford Lough (Ireland) carrying capacity with ecosystem models. Aquatic Ecology, 31: 379-394.

Bayne, B. L., 1998. The physiology of suspension feeding by bivalve mollusks: an introduction to the Plymouth "TROPHEE" workshop. J. Exp. Mar. Biol. Ecol., 219: 1-19.

Bayne, B. L., Newell, R. C., 1983. Physiological energetics of marine mollusks. In: Wilbur, K. M., Saleuddin, A. S. (Eds.), The Mollusca, vol. 4. Academic Press, New York, p. 407-515.

Bayne, B. L., Hawkins, A. J. S., 1990. Filter–feeding in bivalve mollusks: control of energy balance. In: Mellinger, J. (Ed.), Animal nutrition and transport processes. 1. Nutrition in wild and domestic animals. Karger, Basel, p. 70-83.

Bayne, B. L., 1976. Aspects of reproduction in bivalve mollusks. In: Wiley, M. (Ed.), Estuarine Processes, Vol. 1, Uses, stresses and adaptations to the estuary. Academic Press, New York, p. 432-448.

Bayne, B. L., 1993. Feeding physiology of the bivalves: time-dependence and compensation for changes in food availability. In: Dame, R. (Ed.), Bivalve filter feeders in estuarine and coastal ecosystems processes. NATO ASI Series, G 33 Springer-Verlag, Berlin, p. 1-24.

Bayne, B. L., 1998. The physiology of suspension feeding by bivalve mollusks: an introduction to the Plymouth "TROPHEE" workshop. J. Exp. Mar. Biol. Ecol., 219: 1-19.

Bayne, B. L., Hawkins, A. J. S., Navarro, E., 1987. Feeding and digestion by the mussel *Mytilus edulis* L. (Bivalvia: Mollusca) in mixtures of silt and algal cells at low concentrations. J. Exp. Mar. Biol. Ecol., 111: 1-22.

Bayne, B. L., Hawkins, A. J. S., Navarro, E., 1988. Feeding and digestion in suspension-feeding bivalve mollusks: the relevance of physiological compensations. Am. Zool., 28: 147-159.

Bayne, B. L., Iglesias, J. I. P., Hawkins, A. J. S., Navarro, E., Héral, M., Deslous-Paoli, J. M., 1993. Feeding behavior of the mussel, *Mytilus edulis*: responses to variations in quantity and organic content of the seston. J. Mar. Biol. Ass. U.K., 73: 813-829.

Bayne, B. L., Klumpp, D. W., Clarke, K. R., 1984. Aspects of feeding, including estimates of gut residence time, in three mytilid species (Bivalvia, Mollusca) at two contrasting sites in the Cape Peninsula, South Africa. Oecologia, 64: 26-33.

Bayne, B. L., Worral, C. M., 1980. Growth and production of mussels *Mytilus edulis* from two populations. Mar. Ecol. Prog. Ser., 3: 317-328.

Berry, P. F., 1978. Reproduction, growth and production in the mussel *Perna perna* (Linnaeus), on the east coast of South Africa. Invest. Rep. Oceanogr. Res. Inst., 48: 1-28.

Berry, P. F., Schleyer, M. H., 1983. The brown mussel *Perna perna* on the Natal coast, South Africa: utilization of available food and energy budget. Mar. Ecol. Prog. Ser., 13: 201-210.

Brush, M. J., Brawley, J. W., Nixon, S. W. and Kremer, J. N., 2002. Modeling phytoplankton production: problems with the Eppley curve and an empirical alternative. Mar. Ecol. Prog. Ser., 238: 31-45.

Brylisnki, M., Sephton, T. W., 1991. Development of a computer simulation model of a culture blue mussel (*Mytilus edulis*) population. Can. Tech. Rep. Fish. Aquat. Sci., 1805 (viii + 81pp.).

Campbell, C. J., Newell, C. R., 1998. MUSMOD, a production model for bottom culture of the blue mussel *Mytilus edulis* L. J. Exp. Mar. Biol. Ecol., 219: 171-203.

Carvajal, J. R., 1969. Fluctuación mensual de las larvas y crescimento del mejillón *Perna perna* (L.) y las condiciones ambientales de la ensenada de Guatanapare e do Sucre, Venezuela. Bol. Inst. Oceanogr. Univ. Oriente, 8: 13-20.

Carver, C. E. A., Mallet, A. L., 1990. Estimating the carrying capacity of a coastal inlet for mussel culture. Aquaculture, 88: 39-53.

Chevarria, G. G., 1999. Caracterização biogeoquímica de uma área de cultivo de moluscos – Enseada de Armação do Itapocoroy – Penha/SC. Oceanography Degree Monograph. Universidade do Vale do Itajaí. Brazil.

Costanza, R., Duplisea, D., Kautsky, U., 1998. Ecological modelling and economic systems with STELLA. Ecol. Model., 110: 1-4.

Cranford, P. J., 2001. Evaluating the 'reliability' of filtration rate measurements in bivalves. Mar. Ecol. Prog. Ser., 215: 303-305.

Crisp, D. J., 1971. Energy flow measurements. In: Holme NA, McIntyre AD (Eds.), Methods for the study of marine benthos. IBP handbook no.16. Blackwell Scientific Publications, Oxford, p. 197-279.

Crosby, M. P., Gale, L. D., 1990. A review and evaluation of bivalve condition index methodologies with a suggested standard method. J. Shellfish Res., 9: 233-237.

Dame, R. F., 1993. Bivalve filter feeders and estuarine and coastal ecosystems processes: conclusions. In: Bivalve Filter Feeders in Estuarine and Coastal Ecosystems Processes. Dame, R. (Ed.). NATO ASI Series, vol. G 33. 579 pp.

Dame, R. F., Prins, T. C., 1998. Bivalve carrying capacity in coastal ecosystems. Aquatic Ecology, 31: 409-421.

Dame, R. F., 1996. Ecology of Marine Bivalves: An Ecosystem Approach. Marine Science Series, CRC Press, Boca Raton, Florida. 254 p.

Dankers, N., 1993. The role of scientists in the management of coastal ecosystems. In: Bivalve Filter Feeders in Estuarine and Coastal Ecosystems Processes. Dame, R. (Ed.). NATO ASI Series, vol. G 33. 579 pp.

Doering, P. H, Oviatt, C. A., Kelly, J. R., 1986. The effects of the filter-feeding clam *Mercenaria mercenaria* on carbon cycling in experimental marine mesocosms. J. Mar. Res., 44: 839-861.

Dowd, M. 1997. On predicting the growth of cultured bivalves. Ecological Modelling, 104: 113-131.

Elliot, J. M., Davison, W., 1975. Energy equivalents of oxygen consumption in animal energetics. Oecologia 19: 195-201.

Fréchette, M., Grant, J., 1991. An in situ estimation of the effect of the wind-driven resuspension on the growth of the mussel *Mytilus edulis* L. J. Exp. Mar. Biol. Ecol. 148: 201-213.

Fréchette, M., 1991. Carrying capacity and density dependence (Workshop Report). ICES Mar. Sci. Symp., 192: 78.

Fréchette, M., 1993. Physical factors: working group report. In: Dame, R. (Ed.). Bivalve Filter Feeders in Estuarine and Coastal Ecosystems Processes. NATO ASI Series, vol. G 33. 579 pp.

Fréchette, M., Aitken, A. E., Pagé, L., 1992. Interdependence of food and space limitation of a benthic suspension feeder: consequences for self-thinning relationships. Mar. Ecol. Prog. Ser., 83: 55-62.

Fréchette, M.; Booth, A. D.; Myrand, B., Bérard, H., 1991. Variability and transport of organic seston near a mussel aquaculture site. ICES Mar. Sci. Symp., 192: 24-32.

Gabbott, P. A., Bayne, B. L., 1973. Biochemical effects of temperature and nutritive stress on *Mytilus edulis*. J. Mar. Biol. Ass. U. K., 53: 269-286.

Gallegos, C. L., Vant, W. N., 1996. An incubation procedure for the estimating carbon-to-chlorophyll ratios and growth-irradiance relationships of estuarine phytoplankton. Mar. Ecol. Prog. Ser., 138: 275-291.

Gangnery, A., Bacher, C., Buestel, D. 2001. Assessing the production and the impact of cultivated oysters in the Thau laggon (Mediterranee, France) with a population dynamics model. Can. J. Fish. Aquat. Sci., 58: 1012-1020.

Gardner, J. P. A., Thompson, R. J., 2001. Naturally low seston concentration and the energy balance of the Greenshell mussel (*Perna canaliculus*) at Island Bay, Cook Strait, New Zealand. NZ J. Mar. Freshw. Res. 35: 457-468.

Gardner, J. P. A., 2002. Effects of seston variability on the clearance rate and absorption efficiency of the mussel *Aulacomya maoriana*, *Mytilus galloprovincialis* and *Perna canaliculus* from New Zealand. J. Exp. Mar. Biol. Ecol., 268: 83-101.

GESAMP (IMO/FAO/UNESCO-IOC/WMO/WHO/IAEA/UN/UNEP Joint Group of Experts on the Scientific Aspects of Marine Protection), 2001. Planning and management for sustainable aquaculture development. Rep. Stud. GESAMP, (68): 90 pp.

Grant, J., 1996 The relationship of bioenergetics and the environment to the field growth of cultured bivalves. J. Exp. Mar. Biol. Ecol., 200: 239-256.

Grant, J., Bacher, C., 1998. Comparative models of mussel bioenergetics and their validation at field culture sites. J. Exp. Mar. Biol. Ecol., 219: 21-44.

Grant, J., Dowd, M., Thompson, K., 1993. Perspectives on field studies and related biological models of bivalve growth and carrying capacity. In: Dame, R. F. (Ed.), Bivalve Filter Feeders in Estuarine and Coastal Ecosystem Processes. Coastal Carolina University. Nato Asi series, Serie G. Ecological Sciences. 33: 371-420.

Grant, J., 1993. Working group report: modelling. In: Dame, R. (Ed.), Bivalve filter feeders in estuarine and coastal ecosystems processes. NATO ASI Series, G 33 Springer-Verlag, Berlin, p. 549-555.

Grant, J., 1999. Preliminary models of seston depletion and growth variation in cultured mussels. Proceedings of the Workshop on Mussel Production Capacity (part 1), held at Aquaculture Canada'98. Bull. Aquacult. Assoc. Can., 2: 5-8.

Griffiths, C. L., Griffiths, R. J., 1987. Bivalvia. In: Pandian, T. J., Vernberg, F. J., (Eds.), Animal energetics. Vol. 2: Bivalvia through Reptilia. Academic Press, New York, p. 1-88.

Hatcher, A., Grant, J., Schofield, B., 1994. Effects of suspended mussel culture (*Mytilus* spp.) on sedimentation, benthic respiration and sediment nutrient dynamics in a coastal bay. Mar. Ecol. Prog. Ser., 115: 219-235.

Hawkins, A. J. S., Bayne, B. L., 1985. Seasonal variation in the relative utilization of carbon and nitrogen by the mussel *Mytilus edulis*: budgets, conversion efficiencies and maintenance requirements. Mar. Ecol. Prog. Ser., 25: 181-188.

Hawkins, A. J. S., Bayne, B. L., 1991. Nutrition of marine mussels: factors influencing the relative utilizations of protein and energy. Aquaculture, 94: 177-196.

Hawkins, A. J. S., Bayne, B. L., Bougrier, S., Héral, M., Iglesias, J. I. P., Navarro, E., Smith, R. F..M., Urrutia, M. B., 1998. Some general relationships in comparing the feeding physiology of suspension-feeding bivalve mollusc. J. Exp. Mar. Biol. Ecol., 216: 87-103.

Hawkins, A. J. S., Duarte, P., Fang, J. G., Pascoe, P. L., Zhang, J. H., Zhang, X. L., Zhu, M. Y., 2002. A functional model of responsive suspension-feeding and growth in bivalve shellfish, configured and validated for the scallop *Chlamys farreri* during culture in China. J. Exp. Mar. Biol. Ecol., 281: 13-40.

Hawkins, A. J. S., Fang, J. G., Pascoe, P. L., Zhang, J. H., Zhang, X. L., Zhu, M. Y., 2001. Modelling short-term responsive adjustments in particle clearance rate among bivalve suspension-feeders: separate unimodal effects of seston volume and composition in the scallop *Chlamys farreri* during culture in China. J. Exp. Mar. Biol. Ecol., 262: 61-73.

Hawkins, A. J. S., Salkeld, P. N., Bayne, B. L., Gnaiger, E., Lowe, D. M., 1985. Feeding and resource allocation in the mussel *Mytilus edulis*: evidence for time-averaged optimisation. Mar. Ecol. Prog. Ser., 20: 273-287.

Hawkins, A. J. S., Widdows, J., Bayne, B. L., 1989. The relevance of whole-body protein metabolism to measured costs of maintenance and growth in *Mytilus edulis*. Physiol. Zool., 62: 745-763.

Hawkins, A. J. S., Bayne, B. L., 1992. Physiological interrelations and the regulation of production. In: Gosling, E. (Ed.), The Mussel *Mytilus*: Ecology, physiology, genetics and culture. Elsevier, Amsterdam, p. 171-222.

Hawkins, A. J. S., Bayne, B. L., Bougrier, S., Héral, M., Iglesias, J. I. P., Navarro, E., Smith, R. F. M., Urrutia, M. B., 1998b. Some general relationships in comparing the feeding physiology of suspension-feeding bivalve mollusks. J. Exp. Mar. Biol. Ecol., 219: 87-103.

Hawkins, A. J. S., Fang, J. G., Pascoe, P. L., Zhang, J. H., Zhang, X. L., Zhu, M. Y., 2001. Modelling short-term responsive adjustments in particle clearance rate among bivalve suspension-feeders: separate unimodal effects of seston volume and composition in the scallop *Chlamys farreri*. J. Exp. Mar. Biol. Ecol., 262: 61-73.

Hawkins, A. J. S., James, M. R., Hickman, R. W., Hatton, S., Weatherhead, M., 1999. Modelling of suspension-feeding and growth in the green-lipped mussel *Perna*

canaliculus exposed to natural and experimental variations of seston availability in the Marlborough Sounds, New Zealand. Mar. Ecol. Prog. Ser., 191: 217-232.

Hawkins, A. J. S., Salkeld, P. N., Bayne, B. L., Gnaigerl, E., 1996. Novel observations underlying the fast growth of suspension-feeding shellfish in the turbid environments: *Mytilus edulis*. Mar. Ecol. Prog. Ser., 131: 179-190.

Hawkins, A. J. S., Smith, R. F. M., Bougrier S., Bayne, B. L., Héral, M., 1997. Manipulation of dietary conditions for maximal growth in mussels, *Mytilus edulis* L., from the Marennes-Oléron Bay, France. Aquat. Living Resour., 10: 13-22.

Hawkins, A. J. S., Smith, R. F. M., Tan, S. H., Yasin, Z. B., 1998a. Suspension-feeding behavior in tropical bivalve mollusks: *Perna viridis*, *Crassostrea belcheri*, *Crassostrea iradelei*, *Saccostrea cucculata* and *Pinctada margarifera*. Mar. Ecol. Prog. Ser., 166: 173-185.

Heasman, K. G., Pitcher, G. C., McQuaid, C. D., Hecht, T., 1998b. Shellfish mariculture in the Benguela System: raft culture of *Mytilus galloprovincialis* and the effect of rope spacing on food extraction, growth rate, production, and condition of mussels. J. Shellfish Res., 17: 33-39.

Héral, M., 1993. Why carrying capacity models are useful tools for management of bivalve mollusks culture. In: Bivalve filter Feeders in Estuarine and Coastal Ecosystems Processes. Dame, R. (Ed.). NATO ASI Series, vol. G 33. 579 pp.

Héral, M., 1985. Evaluation of the carrying capacity of mollusk shellfish ecosystems. Proceedings of Shellfish Culture Development and Management, La Rochele, France, March, 1985. p. 297-317.

Herman, P. M. J., 1993. A set of models to investigate the role of benthic suspension feeders in estuarine ecosystems. In: Dame, R.F. (Ed.), Bivalve Filter Feeders in Estuarine and Coastal Ecosystems Processes. Springer-Verlag, Heidelberg, p. 421-454.

Herman, P. M. J., Scholten, H., 1990. Can suspension-feeders stabilise estuarine ecosystems? In: Trophic Relationships in the Marine Environment. Barnes, M., Gibson, R.N. (Eds.) Proceedings 24th Europ. Mar. Biol. Symp., Aberdeen University Press.

Hickman, R. W., 1979., Allometry and growth of the green-lipped mussel *Perna canaliculus* in New Zealand. Mar. Biol., 51: 311-327.

Hicks, D. W., Tunnel, J. W., McMahon, R. F., 2001. Population dynamics of the nonindigenous brown mussel *Perna perna* in the Gulf of Mexico compared to other world-wide populations. Mar. Ecol. Prog. Ser., 211: 181-192.

Iglesias, J. I. P., Urrutia, M. B., Navarro, E., Ibarrola, I., 1998. Measuring feeding and absorption in suspension-feeding bivalves: an appraisal of the biodeposition method. J. Exp. Mar. Biol. Ecol., 219: 71-86.

Incze, L. S.; Lutz, R. A.; True, E., 1981. Modelling carrying capacities for bivalve mollusks in open, suspended-culture systems. J. World Mar. Soc., 12: 143-155.

James, M. R., Ross, A. H., 1996 How many mussels can we farm? Seafood New Zealand, July 1996. p. 50.

James, M. R., Weatherhead, M. A., Ross, A. H., 2001. Size-specific clearance, excretion and respiration rates, and phytoplankton selectivity for the mussel *Perna canaliculus* at low levels of natural food. N. Z. J. Mar. Freshw. Res., 35: 73-86.

Jørgensen, C. B., 1976. Growth efficiencies and factors controlling size in some mytilid bivalves, especially *Mytilus edulis* L.: review and interpretation. Ophelia, 15: 175-192.

Jørgensen, S. E., 1994. Fundamentals of Ecological Modelling. Developments in Environmental Modelling, 19. (2nd Edition). Elsevier. Amsterdam. 628 pp.

Kaiser, M. J.; Laing, I.; Utting, S. D., Burnel, G. M., 1998. Environmental impacts of bivalve mariculture. J. Shellf. Res., 17: 59-66.

Kaspar, H. F., Gillespie, P. A., Boyer, I. C., MacKenzie, A. L., 1985. Effects of mussel aquaculture on the nitrogen cycle and benthic communities in Kenopuru Sound, Marlborough Sounds, New Zealand. Marine Biology, 85: 127-136.

Lasiak, T. A., Barnard, T. C. E., 1995. Recruitment of the brown mussel *Perna perna* onto natural substrata: a refutation of the primary/secondary settlement hypothesis. Mar. Ecol. Prog. Ser., 120: 147-153.

Marin, V. H., 1997. A simple biology, staged-structured population model of the spring dynamics of *Calanus chilensis* at Mejillones del Sur Bay, Chile. Ecol. Model., 105: 65-82.

Marques, H. L. de A., Pereira, R. T. L., Correa, B. C., 1991. Study on reproductive and settlement cycles of *Perna perna* (Bivalvia: Mytilidae) at natural beds in Ubatuba shore – São Paulo State, Brazil. Boletim Instituto Pesca São Paulo. 18: 73-81.

Marques, H. L., Pereira, R. T. L., Correa, B. C., 1998. Seasonal variation in growth and yield of the Brown mussel *Perna perna* (L.) cultured in Ubatuba, Brazil. Aquaculture, 196: 263-273.

Mazouni, N., Gaertner, J. C., Deslous-Paoli, J. M., Landrein, S., d'Oedenberg, M. G., 1996. Nutrient and oxygen exchanges at the water-sediment interface in a shellfish farming lagoon (Thau, France). J. Exp. Mar. Biol. Ecol., 205: 91-113.

Mota, A. N., Machado, J. F. S., 1974. Culture experimental de mexilao *Perna perna* (L.) em Angola. Publ. Mimeogr. Missão Estud. Bioceanol. Pescas, Angola, Ser. Biol. 13: 1-30.

Navarro, E., Iglesias, J. I. P., 1995. Energetics of reproduction related to environmental variability in bivalve mollusks. Haliotis 24: 43-55.

Navarro, E., Iglesias, J. I. P., Pérez Camacho, A., Labarta, U., 1996. The effect of diets of phytoplankton and suspended bottom material on feeding and absorption of raft mussels (*Mytilus galloprovincialis* Lmk.). J. Exp. Mar. Biol. Ecol., 198: 175-189.

Navarro, E., Iglesias, J. I. P., Pérez Camacho, A., Labarta, U., Beiras, R., 1991. The physiological energetics of mussels (*Mytilus galloprovincialis* Lmk) from different cultivation rafts in the Ria de Arosa (Galicia, NW Spain). Aquaculture, 94: 197-212.

Newell, C. R., Campbell, D. E., 1998. MUSMOD©, a production model for bottom culture of the blue mussel, *Mytilus edulis*. J. Exp. Mar. Biol. Ecol., 219: 171-203.

Pérez Camacho, A., Gonzáles, R., 1984. La filtración del mejillón (*Mytilus edulis* L.) en laboratorio. In: Actas do Primeiro Seminario de Ciencias do Mar, As Rías Galegas, Cuadernos da Area de Ciencias Marinas, Seminario de Estudos Galegos, 1: 427-437.

Platt T., Irwin B., 1973. Caloric content of phytoplankton. Limnol. Oceanogr., 18: 306-309.

Pouvreau, S., Bacher, C., Héral, M., 2000. Ecophysiological model of growth and reproduction of the black pearl oyster, *Pinctada margaritifera*: potential applications for pearl farming in French Polynesia. Aquaculture, 186: 117-144.

Powell, E. N., Hoffman, E.E., Klinck, J. M., Ray, S. M., 1992. Modelling oyster populations. I. A commentary on filtration rate. Is faster always better? J. Shellfish Res., 11: 387-398.

Proença, L. A. O., Hama, L. L., Odebrecht, C., 1994. Contribution of microalgae to particulate organic carbon in the shallow area of Lagoa dos Patos estuary, Southern Brazil. Atlântica, 16: 191-199.

Proença, L. A. O., Schettini, C. A. F., 1998. Effect of shellfish culture on phytodetritus vertical fluxes in tropical waters - southern Brazil. Rev. Bras. Oceanogr. 46: 125-133.

Raillard, O., Ménesguen, A., 1994. An ecosystem box model for estimating the carrying capacity of a macrotidal shellfish system. Mar. Ecol. Prog. Ser., 115: 117-130.

Riisgård, H. U., 2001. On measurements of filtration rates in bivalves – the stony road to reliable data: review and interpretation. Mar. Ecol. Prog. Ser., 211: 275-291.

Rodhouse, P. G., Roden, C. M., 1987. Carbon budget for a coastal inlet in relation to intensive cultivation of suspension-feeding bivalve molluscs. Mar. Ecol. Prog. Ser., 36: 225-236.

Rojas, J. C., 1969. Fluctuación mensual de las larvas y crescimento del mejillón *Perna perna* (L.) y las condiciones ambientales de la ensenada de Guatanapare, Edo, Sucre, Venezuela. Bol. Inst. Oceanogr. Univ. Oriente, 8: 13-20.

Ross, A. H., James, M. R., Hadfield, M., Gibbs, M., 1999. Estimating the sustainable production of mussel aquaculture using numerical simulation models. International Conference on Sustainable Management of Coastal Ecosystems, Fernando Pesssoa University, Porto, Portugal, November 1999.

Scarrat, D., 2000. A new invention to stop mussel drop-off. Shellfish World, 1: 13.

Schettini, C. A. F., Daquino, C. A., Carvalho, C. E. V. 2000. Ressuspensão e transporte de sedimentos sob áreas de cultivo de moluscos: caso da Armação do Itapocoroy, SC. Anais da XIII Semana Nacional de Oceanografia . Itajaí (SC), p. 364 -366.

Scholten, H., Small, A. C., 1998. Responses of *Mytilus edulis* L. to varying food concentrations: testing EMMY, an ecophysiological model. J. Exp. Mar. Biol. Ecol., 219: 217-239.

Scholten, H., Small, A. C., 1999. The ecophysiological response of mussels (*Mytilus edulis*) in mesocosms to a range of inorganic nutrient loads: simulations with the model EMMY. Aquat. Ecol., 33: 83-100.

Scholten, H., Klepper, O., Nienhuis, P. H., Knoester, M., 1990. Oosterchelde estuary (S. W. Netherlands): a self-sustaining ecosystem? Hydrobiologia, 195: 201-215.

Slobodkin, L. B., Richman, S., 1961. Calories/gm in species of animals. Nature, 191: 299.

Smaal, A. C., Prins, T. C., Dankers, N., Ball, B., 1998. Minimum requirements for modelling bivalve carrying capacity. Aquat. Ecol., 31: 423-428.

Smaal, A. C., 1991. The ecology and cultivation of mussels: new advances. Aquaculture, 94: 245-261.

Smaal, A. C., Haas, H. A., 1997. Seston dynamics and food availability on mussel and cockle beds. Est. Coast. Shelf. Sci., 45: 247-259.

Smaal, A. C.; Prins, T. C.; Dankers, N., Ball, B., 1998. Minimum requirements for modelling bivalve carrying capacity. Aquatic Ecology, 31: 423-428.

Sobral, P., Widdows, J., 2000. Effects of increasing current velocity, turbidity and particle size selection on the feeding activity and scope for a growth of *Ruditapes*

decussates from Ria Formosa, southern Portugal. J. Exp. Mar. Biol. Ecol., 245: 111-125.

Souchu, P., Vaquer, A., Collos, Y., Landrein, S., Deslous-Paoli, J. M., Bibent, B., 2001. Influence of shellfish farming activities on the biogeochemical composition of the water column in Thau lagoon. Mar. Ecol. Prog. Ser., 218: 141-152.

Stenton-Dozey, J. M. E., Jackson, L. F., Busby, A. J., 1999. Impact of mussel culture on macrobenthic community structure in Saldanha bay, South Africa. Mar. Poll. Bull., 39: 357-366.

Stillman, R. A., McGrorty, S., Goss-Custard, J. D., West, A. D., 2000. Predicting mussel population density and age structure: the relationship between model complexity and predictive power. Mar. Ecol. Prog. Ser., 208: 131-145.

Suplicy, F. M., 2001. Do cultivo de moluscos para a aquaindustria: o momento do Brasil. Panorama da Aqüicultura, 68: 25-38.

Taylor, A. H., Geider, R. J., Gilbert, F. J. H., 1997. Seasonal and latitudinal dependencies of phytoplankton carbon-to-chlorophyll *a* ratios: results of a modelling study. Mar. Ecol. Prog. Ser., 152: 51-66.

Tomalin, B. J., 1995. Growth and mortality rates of the brown mussel *Perna perna* (Linnaeus) in Kwazulu-Natal: a comparison between locations and methods using non-parametric length-based analysis. S. Afr. J. Mar.Sci., 16: 241-254.

Urrutia, M. B., Navarro, E., Ibarrola, I., Iglesias, J. I. P., 2001. Preingestive selection processes in the cockle *Cerastoderma edule*: mucus production related to rejection of pseudofaeces. Mar. Ecol. Prog. Ser. 209: 177-187.

van Erkon Schurink, C., Griffiths, C. L., 1992. Physiological energetics of four South African mussel species in relation to body size, ration and temperature. Comp. Biochem. Physiol., 101: 779-789.

van Erkon Schurink, C., Griffiths, C. L., 1993. Factors affecting relative rates of growth in four South African mussel species. Aquaculture, 109: 257-273.

Van Haren, R. T. F., Kooijman, S. A. L. M., 1993. Application of a dynamic energy budget model to *Mytilus edulis* (L.). Neth. J. Sea. Res., 31: 119-133.

Velez, A., Epifanio, C. E., 1981. Effects of temperature and ration on gametogenesis and growth in the tropical mussel *Perna perna* (L.). Aquaculture, 22: 21-26.

Wainright, S. C., Hopkinson, C.S., 1997. Effects of sediment resuspension on organic matter processing in coastal environments: a simulation model. J. Mar. Sys., 11: 353-368.

Widdows, J., Feith, P., Worral, C. M., 1979. Relationships between seston, available food and feeding activity in the common mussel *Mytilus edulis*. Mar. Biol., 50: 195-207.

Widdows, J., 2001. Bivalve clearance rates: inaccurate measurements or inaccurate reviews and misrepresentation? Mar. Ecol. Prog. Ser., 221: 303-305.

Widdows, J., Fieth, P., Worral, C. M., 1979. Relationships between seston, available food and feeding activity in the common mussel *Mytilus edulis*. Mar. Biol., 50: 195-207.

Wong, W. H., Cheung, S. G., 2001. Feeding rhythms of the green-lipped mussel, *Perna viridis* (Linnaeus, 1758) (Bivalvia: Mytilidae) during spring and neap tidal cycles. J. Exp. Mar. Biol. Ecol., 257: 13-36.